NISEE/COMPUTER APPLICATIONS
DAVIS HALL
UNIVERSITY OF CALIFORNIA
BERKELEY, CALIFORNIA 94720
(415) 642-5113

REPORT NO.
UC SESM 72-6

STRUCTURES AND MATERIALS RESEARCH
DEPARTMENT OF CIVIL ENGINEERING

TIME-DEPENDENT BEHAVIOR OF CONCRETE UNDER SUSTAINED LOAD AND CYCLIC TEMPERATURE

by

HANI M. FAHMI
MILOS POLIVKA
BORIS BRESLER

Report to:
National Science Foundation
Grant GK-3901

APRIL 1972

STRUCTURAL ENGINEERING LABORATORY
UNIVERSITY OF CALIFORNIA
BERKELEY CALIFORNIA

Structures and Materials Research
Department of Civil Engineering
Division of Structural Engineering
and Structural Mechanics

Report No. UC SESM 72-6

TIME-DEPENDENT BEHAVIOR OF CONCRETE UNDER SUSTAINED LOAD AND CYCLIC TEMPERATURE

by

Hani M. Fahmi
Assistant Specialist

Milos Polivka
Professor of Civil Engineering

Boris Bresler
Professor of Civil Engineering

Prepared under the sponsership of
National Science Foundation
Grant GK-3901

Structural Engineering Materials Laboratory
University of California
Berkeley, California

April 1972

ABSTRACT

This investigation was concerned with the time-dependent behavior of concrete under a sustained load at constant or cyclic temperatures. It included experimental and analytical phases. In the experimental phase, creep tests were conducted on micro-concrete hollow cylindrical specimens, 6-in. O.D., 5-in. I.D. and 40-in. long. These specimens were subjected to sustained loading, either compressive or torsional, at a constant relative humidity, 50 or 100 percent. Most of these specimens were stored under load at 73°F for 37 days prior to either raising their temperature and maintaining it at 140°F, or subjecting them to cyclic changes of temperature between 73 and 140°F. Unloaded control specimens were also subjected to the same environmental conditions to determine the deformations due to free shrinkage and thermal changes. Axial deformations of the compression specimens were measured using dial gages as well as electrical strain gages. Angular deformations of the specimens loaded in torsion were measured using dial gages.

The test results obtained showed that creep of concrete is significantly affected by elevated or cyclic temperatures, particularly at 100% R. H.

In the analytical phase of this investigation a mathematical expression was developed, in terms of material parameters and functions determined using the test results, for predicting creep of concrete taking into account temperature, humidity, age and type of load. The expression was based on the thermodynamic equilibrium of the diffusible load-bearing layers in the cement gel. This expression was used, utilizing numerical methods, to predict creep of concrete in torsion or compression at 50 or 100% R. H. and at sustained (73, 140°F) or cyclic temperatures between 73 and 140°F. The predicted creep values were in good agreement with the experimental results.

In addition, a mathematical model based on time-shift principle was developed and used for predicting creep at constant and variable temperatures. Previously published experimental creep data for concrete specimens loaded in compression at constant or variable temperatures were used to compare the predicted creep strains with the experimental results. In both cases good agreement was observed.

ACKNOWLEDGEMENTS

The study reported here was carried out by H. M. Fahmi in partial fulfillment of the requirements for the Ph.D. degree in Civil Engineering at the University of California, Berkeley, under the direct supervision of Professors Milos Polivka and Boris Bresler. The authors are indebted to Professor Frank Hauser for his valuable suggestions concerning this study. In addition, the authors wish to acknowledge the assistance given by the staff of the Structural Engineering Materials Laboratory, by Dr. H. Al-Alusi while he was a graduate student at Berkeley, and by Mr. H. Franco, an engineering student.

During his graduate studies, Dr. Fahmi was sponsored by an Iraqi Government Scholarship to the University of Baghdad.

The financial support for this research was provided by the National Science Foundation under Grant GK-3901.

TABLE OF CONTENTS

LIST OF TABLES

LIST OF FIGURES

NOTATION

b_T = rate constant for macroscopic diffusion which is a function of T

c_h = diffusion parameter which depends on h

e_{ij} = total strain deviator

e'_{ij} = inelastic strain deviator

f_a = effective area factor of the pressure in the fluid per unit area of material

f_d = effective area factor of the diffusible load-bearing layers per unit area of material

h = humidity or relative vapor pressure in the pores

h_{eq} = equivalent humidity, Eq. 1.14

h_s = humidity at self-desiccation of a sealed sample, Eq. B.1

k = sorption resistance of the porous material

s_{ij} = total stress deviator

$s_{d_{ij}}$ = stress deviator in hindered layers

t = time after application of load in days

t_{eq} = equivalent curing time, Eq. 1.17

w = total mass of water per unit volume of porous material

A = a constant, Eq. A.3

C = specific creep function

C' = total specific strain (elastic + creep)

D_T = equivalent thickness for heat transmission

E = modulus of elasticity

G, G_b, G_c, G_d = shear moduli of elasticity of the rheological model and its elements b, c and d, respectively

G_h = a factor which accounts for delayed deviatoric deformation under load due to a change of humidity or temperature

K, K_b, K_c, K_d = volumetric (bulk) moduli of elasticity of the rheological model and of elements b, c, d, respectively

K_h = a factor which accounts for delayed volumetric deformation under load due to a change of humidity or temperature

M = molecular weight of water

R = universal gas constant

T = temperature in ^{o}C (^{o}F in Chapter 5)

T' = absolute temperature in ^{o}K

T'_o = absolute reference temperature in ^{o}K

α = coefficient of thermal dilatation, per ^{o}C

α_o = effective coefficient of instantaneous thermal dilatation, per ^{o}C

α_i, β_i = material constants, Eq. 5.1

$\beta = \beta_h \beta_T$ = relative hydration rate

β_h = function of h only, Eq. 1.18

β_T = function of T only, Eq. 1.18

ε = total volumetric strain (macroscopic)

ε' = inelastic volumetric strain

ε_i = initial elastic strain

ε_v = volumetric strain, Eq. 4.8

ε_{11}, ε_{22}, ε_{33} = principal strains

ϕ = parameter for volumetric creep deformation, or

$= \phi(T) = e^{\psi(T)}$ = shift function for temperature T (Chapter 5)

κ = hygrothermic coefficient

μ = Poisson's ratio

$\nu = \dfrac{K_d}{K_c + K_d}$

ν' = $\frac{G_d}{G_c + G_d}$

ψ = parameter for deviatoric creep deformation, or

= $\psi(T)$ = magnitude of shift for temperature T (Chapter 5)

ρ_o = density of liquid water, 1 g/cm^3

σ = total volumetric stress (macroscopic)

σ_a = pressure in free adsorbed water layers

σ_d = stress resultant in the diffusible load-bearing layers over a unit area of the porous material

σ_v = volumetric stress, Eq. 4.8

σ_{ad} = equilibrium value of σ_d at a given h, T

σ_{ao} = pressure in the fluid

σ_{ah} = parameter which is a function of humidity, Eq. 1.13

σ_{aQ} = parameter which is a function of temperature and accounts for thermal swelling or shrinkage

σ_{11}, σ_{22}, σ_{33} = principal stresses

Δ = increments during time step Δt

$\mathring{A}$ = angstrom = 10^{-8} cm

$\approx$ approximately equals to

1. INTRODUCTION

1.1 General

The fact that creep deformation occurs in concrete has long been recognized. Since practically all concrete members and structures are subjected to some kind of sustained load and since the amount of creep is of the same order of magnitude as the elastic strain, the structural effects of creep are of considerable importance and interest. This is particularly so in concrete structure where the governing factor in the design is deflection, in statically indeterminate structures, and in prestressed concrete structures, where creep and shrinkage foiled all early attempts at using prestressing.

Some experimental investigations (1, 2, 3) have shown that when concrete is subjected to changes of temperature and/or humidity, a considerable increase in creep occurs. These investigations clearly show the significant effects of the environmental conditions on the creep behavior of concrete.

Most of the studies done on the creep and shrinkage of concrete were concerned with constant conditions of temperature and humidity. However, some studies have been made for predicting the effects of various temperatures, humidities, size and shape of specimens, and type and level of stress on the creep of concrete. These studies, however, dealt mainly with the phenomenological point of view of creep and, therefore, are applicable only to a rather limited range of environmental conditions.

A real understanding of the mechanism of creep and shrinkage should be based on a consideration of the internal microstructure of the cement paste.

The load-bearing ability of hindered adsorbed water layers in terms of thermodynamics was first investigated by Powers (4, 5, 6), based on a real understanding of the structure of the cement paste. Bazant (7, 8) then developed macroscopic constitutive equations, based on Powers' work, to predict the creep and shrinkage of concrete under variable conditions of temperature and humidity. These constitutive

equations are related to the thermodynamic equilibrium of the diffusible load-bearing water layers in the cement gel. Furthermore, Bazant proposed a numerical method (9), which for practical purposes is the only feasible one, for the solution of these equations.

In order to be able to use Bazant's constitutive equations for the prediction of creep, some of the parameters and properties of concrete such as the rate of creep parameters, moduli of elasticity, effective area factors, and the hygrothermic coefficient, must be determined experimentally.

This investigation is concerned with the effects of temperature and humidity on the creep behavior of concrete. Since the prediction of the creep of concrete using Bazant's constitutive equations requires the evaluation, from test results, of the various material parameters and coefficients (discussed in Sec. 1.3), the following investigations were carried out:

1. An experimental investigation of creep of concrete, which included compressive and torsional types of load conducted in the temperature range of 73 to 140°F at a constant relative humidity of 50 and 100 percent. Also included was a study of the effects of thermal cycling between 73 and 140°F as well as exposures to sustained temperatures of 73 and 140°F. Only one type of concrete was used, and the sustained stress level was restricted to the so-called linear range of stress-creep strain relationship. The experimental program is presented in detail in Chapters 2 and 3.

2. An analytical study using Bazant's constitutive equations, which is presented in detail in Chapter 4.

   Knowledge of the parameters included in Bazant's constitutive equations will enable the prediction of creep, including the effects of humidity, type of load, and variable temperatures.

3. Also included in this investigation was an analytical study on creep of concrete using the time-temperature shift principle, which is presented in Chapter 5.

1.2 Literature Review

There is a considerable amount of literature concerning the creep behavior of concrete. These papers deal with various aspects of creep, as an observed property of the material, and as a problem in the behavior of structures as well as with the mechanism of creep. Many of these papers describe phenomenological investigations of the influence of properties and composition of concrete on creep.

Excellent reviews on creep of concrete can be found in the papers by Sackman (10), Neville and Meyers (11), Wallo and Kesler (12). The most comprehensive review of creep of concrete appears in a recent publication by Neville (13). In recent years many of the factors influencing creep of concrete have been established with some accuracy; these include: mix proportions, constituents, amount of evaporable water and the extent of drying, age of concrete at time of loading, stress level, temperature and temperature variations. Some of these factors are more significant than others.

A great volume of test results on creep of concrete of different composition is available, but the interpretation of the results requires considerable skill. Thus, it becomes necessary to study the different factors affecting the creep for one type of concrete only.

Since this investigation is concerned with the effect of temperature and temperature variations of concrete under sustained load (creep), only related topics will be reviewed.

Temperature is one of the major environmental factors influencing creep. In recent years, the effect of temperature on creep has received increased attention because of the use of prestressed concrete in nuclear reactor pressure vessels. The problem is also very important for other concrete structures such as bridges which may be exposed to daily or seasonal changes in the environment.

1.2.1. Experimental Studies. -- It is to be noted that experiments dealing with elevated and cyclic or varying temperatures are much more difficult to run and to control, particularly when

dealing with different levels of humidities. Thus, it is not surprising that the results of some of these investigations show different, and in some cases even contradictory conclusions.

One of the early investigations on the importance of temperature on creep was carried out by Theuer (14) in 1937. He reported results of tests carried out on concrete specimens in the temperature range of 26 to 123°F. He found that the higher the temperature, the greater the deformation for a given stress; also, the part of the deformation which occurred within 12 minutes of applying the load increased significantly with temperature rise; and the creep of oven-dry specimens was small and independent of temperature.

In 1938 Kelly (15) reported the results of an investigation on the effects of temperature on mass concrete. The concrete specimens used were subjected to a rather low range of temperatures (60 to 90°F) simulating concrete near the base of a large dam. He found that thermal changes produce appreciable stresses when the deformations are restrained and that these stresses are relieved due to plastic flow. Furthermore, he showed that the direct effect of curing temperature on the plastic flow is small, although the curing temperature may affect flow indirectly through its influence on the rate of hydration.

In 1951 Lee (16) presented results of creep tests in the temperature range of 68 to 104°F which confirmed earlier results that creep increased appreciably with increase in temperature.

In 1960 Serafim and Guerreiro (17) reported that mass-cured concrete specimens, tested at the ages of 3 and 8 days showed that the creep rate at 45°C is higher than at room temperature during the first 4 to 7 days after loading. Then the rate of creep became the same in both cases. They concluded, therefore, that the influence of high constant temperature on creep was slight in that case.

In 1960 Torroja and de la Peña (18) presented some data on tests carried out on cement mortar tubes 100 mm in length, inside diameter 46 mm, and 2 mm wall thickness, and concluded that the creep of the specimens, after being loaded under water for 7 days, was proportional to the temperature in the range of 20 to 50°C.

In 1960 Glucklich and Ishai (19) presented the results of creep tests on sealed, simply supported, slender beams having the dimensions of 0.86 by 0.86 by 32.9 in. These tests were conducted at 16, 30 and 45°C. The sealed beams were cured at 16°C for 21 days and then stored at the specified temperature for 7 more days before the load was applied. The beams were loaded for 38 days, except for one which was loaded for 90 days. They concluded that raising the temperature from 16 to 45°C increased the total deformation, slightly increased the instantaneous elastic deformation, and considerably increased the irrecoverable creep of the hardened cement paste.

In 1960 Hansen (1) reported the results of more extensive creep tests conducted on sealed mortar beams 2 by 5 by 40 cm under sustained bending. The beams were cured in water at 35°C for 6 months and were loaded at temperatures of -15, 0.5, 20, 30, 40 and 60°C after one day storage at the specified temperature. He showed that after 24 days under load the creep of the specimens at 40 and 60°C was two and three times, respectively, the creep of similar specimens at 20°C.

In 1962 England and Ross (20) presented results indicating the predominant influence of high temperatures in the range of 68 to 284°F, where sealed and unsealed concrete specimens loaded for 80 days exhibited increasing creep rates with increase in temperature.

In 1965 Wallo et al (21) found that the effect of temperature on creep of concrete specimens in flexure, stored in water, decreased with time. They also found that temperature variations in the range of 40 to 110°F increase creep whether it is an increase or decrease in temperature.

In 1965 Ruetz (22) reported that the creep rate for 28-day-old sealed concrete specimens increased with increasing temperature up to about 60°C, but a slight decrease was observed with increasing temperature up to 80°C. He attributed the reason for this decrease to the accelerated hydration that took place with the increased temperature, which compensated for the increased creep rate. He also noted that once the accelerated hydration was completed, as for specimens which are completely dry or have been subjected to high temperature before loading, then creep strain increased with temperature.

In 1965 Nasser and Neville (23) reported that creep strain and the rate of creep for mass-cured and wet-cured concrete increase with an increase in temperature up to 160°F and then decrease with further increase in temperature up to 205°F. Also, they reported that there was a linear relationship between creep strain and stress-ultimate strength ratio of up to 70 percent for the different temperatures.

In 1966 Hansen and Eriksson (24) reported that the creep strain of mortar in flexural specimens placed under water was higher for specimens which were first loaded and then heated than that of similar specimens which were first heated and then loaded, that deflections were larger for saturated than for dry specimens, and that rapid rates of heating permanently reduced the modulus of elasticity of cement mortar, indicating internal changes in the material structure. They also reported that thermal cycling lead to excessive deflections.

In 1967 Nasser and Neville (25) reported further results on creep tests on 1- and 50-year old concrete specimens in the temperature range of 70 to 205°F and found that the rate of creep was higher for the 50-year-old concrete.

In 1967 Browne (26) presented some test results for a large number of 6 by 12-in. cylindrical concrete specimens used to evaluate the effects of age and temperature in the range of 68 to 200°F on the elastic and creep behavior for a particular concrete used for the Wylfa nuclear power station vessels. The concrete specimens were sealed at casting and heat was applied one day before loading. The test results obtained confirmed the large effect of temperature on creep rate, particularly in the first 3 days of loading. Also, it was found that the initial elastic deformation increased with increase in temperature, and decreased with age.

In 1967 Hannant (27) reported creep results obtained on sealed concrete specimens tested under uniaxial and multiaxial stresses at temperatures in the range of 27 to 95°C for periods of up to 2 years. He found that there was a linear relationship between creep strain and temperature in the range of 27 to 77°C, that creep strain under uniaxial

stress at 77°C was about 4.0 to 4.8 times the creep strain at 27°C, that there was higher scatter for creep values at high temperatures, and that the modulus of elasticity decreased with higher temperatures. He also showed that the influence of temperature on creep was smaller for pre-dried concrete specimens.

In 1967 Arthanari and Yu (28) reported the results of creep tests on sealed and unsealed 12 by 12 by 4-in. concrete slabs under uniaxial and biaxial stresses in the temperature range of 20 to 100°C. They showed that the creep strain and creep rates increased appreciably with temperature and that creep strain varied linearly with temperature. They also showed that the influence of age at loading upon creep decreased at high temperatures, and that increasing the temperature by steps resulted in higher creep strain values than when the specimens were subjected to the same constant high temperature.

In 1967 Hickey (29) reported results of unsealed 6 by 12-in. concrete cylinders loaded in compression, in the temperature range of 73 to 290°F. The results showed that the creep strain was approximately a linear function of temperature up to 180°F, but increased non-linearly with further increase in temperature up to 290°F. The results also showed a significant increase in the initial creep rates with increasing temperature. In these tests the temperature was raised after application of the load and the relative humidity was different for each temperature condition.

In 1968 Nasser (30) presented some creep results of mass concrete in the temperature range of 35 to 205°F. He showed that creep was enhanced by temperature; that strength, elasticity and creep recovery were independent of temperature; and that the relationship between creep strain and stress-strength ratio in the range of 10 to 70 percent was linear

In 1968 da Silveira and Florentino (31) presented results of creep tests on mass-cured concrete at different ages, at room temperature, and at 45°C. They showed that the temperature rise increased creep and creep recovery and that the creep Poisson's ratio remained constant and approximately equal to the elastic value.

In 1969 Maréchal (32) reported the results of creep tests on unsealed concrete specimens moist-cured for one year at 20°C and then air-cured for 15 days at the respective temperature before application of the load. He found that at the end of a 100-day loading period, creep strain and creep rate were maximum at 50°C, became less at 70°C, reached a minimum at 105°C, and then increased again up to 400°C. Furthermore, he showed that pre-drying the specimens for 30 days before application of the load considerably reduced creep strain at temperatures below 105°C.

In 1969 Browne and Blundell (33) reported creep results of sealed concrete specimens in the temperature range of 68 to 200°F, loaded at ages ranging between 7 and 400 days. They first found a linear relationship between creep strain and the logarithm of time under load, but with further time, a progressive departure from this relationship was observed. However, they showed that total creep strain consistently increased with temperature up to 200°F.

In 1969 Bertero (3) reported results of creep tests in torsion on solid cylindrical concrete specimens 40-in. long, 3 3/4-in. dia. and on similar hollow cylindrical specimens with 3/4-in. wall thickness. Considering his and other results, he concluded that changes in environmental conditions produce an increase in creep, even in cases where concrete was subjected to a stress level below its plastic limit, and that most of the increase in creep due to such changes was irrecoverable. He also concluded that the increase in creep occurring during the first cycle of temperature or hygrometric change is the largest, and that it then diminishes with each additional cycle until it becomes negligible with the third or fourth cycle.

In 1970 McDonald (34) presented some experimental results on creep of concrete under uniaxial, biaxial, and triaxial stresses in the temperature range of 73 to 150°F. He found that the creep was inversely proportional to the modulus of elasticity of concrete; that air-dried specimens exhibited creep similar to, or higher than, sealed specimens; and that creep was higher at 150°F than at 73°F.

1.2.2. Analytical Studies. -- Several attempts have been made over the last sixty years or so, to express creep as a function of such variables as water-cement ratio, cement content, etc. Many of these early studies were contradictory to one another, and even misleading in some cases, for in general it is not possible to change one of the factors influencing the creep of concrete without changing other properties of the concrete which in turn influence creep.

Better methods have been developed in recent years to predict creep behavior of concrete at constant environmental conditions, by using linear viscoelasticity (35), for which a complete treatment and some examples are given by Arutyunyan (36). This theory, however, fails to deal with creep under varying environmental conditions.

In 1962 Bresler (37) proposed that constitutive equations of concrete should take into account time, temperature, and moisture effects.

In 1962 England and Ross (20) introduced a numerical step-by-step method of analysis for reinforced concrete subjected to thermal gradient, including the effects of creep and shrinkage.

In 1963 Sackman (10) presented an excellent review of analytical studies of creep in concrete and reinforced concrete, in which he considered the effects of temperature and humidity. He suggested that concrete behaves as a thermorheologically simple material, and therefore obeys the time-temperature shift principle. Sackman applied this method on Hansen's (1) experimental creep data and replotted it against the logarithm of time, then he attempted to shift the different curves to form a single base curve. The results, as he reported, were encouraging.

In 1964 Bazant (38) presented a general method of analysis for creep and shrinkage effects in concrete and reinforced concrete structures, in which variation of the environment can be accounted for by changing the time scale.

In 1968 Selna (39) reported a review on creep of concrete along with a numerical method for predicting time-dependent behavior of reinforced concrete structures. It should be noted here that numerical methods are particularly suitable for use with digital computers.

In 1969 Mukaddam (40) reported a review of literature on creep of concrete, which particularly considered temperature and age. He also successfully used the time-shift principle to predict the creep behavior of sealed concrete specimens including the effects of temperature, age at loading, and the combined effects of both temperature and age.

A more recent review of simple methods of analyzing the effect of creep and shrinkage of concrete in structural members was reported by Illstone and England (41) in 1970.

In the following section Powers' theory (4, 5, 6) for creep and shrinkage of concrete is briefly presented.

1.3 Powers-Bazant Theory

1.3.1. The Structure of Cement Paste. -- Before going into Powers' theory, it may be appropriate to present a brief description of the structure of hardened portland cement. Hardened portland cement may be considered as a multi-phase porous material, whose solid component consists of unhydrated cement particles and hydrated cement. The completely hydrated cement in its densest form is called cement gel, which is mainly a colloidal system. The structure of the cement gel takes the form of fibers, or bundles of fibers, as well as some sheets which seem to be rolled or folded. The average thickness of these gel particules is about 30 Å and they are separated by pores having an average thickness of 15 Å. Furthermore, the gel has a surface area estimated at about 500 m^2/cc. The extreme narrowness of the pores and the enormous surface area result in a large part of the water in the cement paste being adsorbed. The forces that operate in the binding of the adsorbed water are predominantly van der Waals forces.

The amount of adsorbed water may be considered as a function of vapor pressure or rather, relative vapor pressure (humidity). When in contact with air at a relative humidity of about 17 percent, only one molecular layer of water is adsorbed by the cement gel. At a humidity of 60 percent, only two layers can be adsorbed; at 100 percent

humidity, the thickness of the adsorbed water film is about 5 molecules, which is about 13 Å. Therefore, in a narrow gap thinner than about 26 Å, and above a certain humidity, the two adsorbed layers of the opposite surfaces cannot be freely accomodated, resulting in having adsorbed water molecules filling the pore completely. This case is called hindered adsorption.

These hindered adsorbed layers cause a "disjoining pressure" on the two opposite surfaces, and thus they are load-bearing and considered as structural components of the cement gel. The layers are also referred to as "diffusible load-bearing layers." These adsorbed layers, however, have a high mobility which results in a continuous interchange of molecules between the layers and the contiguous water, as well as continuous interchange between regions of strong and weak adsorption. When the two adsorbed water layers can be accommodated without obstruction, they are referred to as "free adsorbed water layers."

The water contained in the hydrated cement paste can be divided into:

1. Evaporable water, which is all the water that can be evaporated at a given temperature.
2. The so-called non-evaporable water, the amount of which is a function of temperature.

The evaporable water is divided into adsorbed water and capillary water. The adsorbed water in turn is divided, as mentioned earlier, into free adsorbed layers and hindered adsorbed layers. One of the components that may be responsible for short time creep is the water in the central part of the long thin capillaries (thicker than about 25 Å). When a load is applied suddenly the equilibrium of water is destroyed, because water cannot flow immediately out of these capillaries, but diffuses gradually. Thus, such capillaries can be considered part of the diffusible load-bearing layers.

1.3.2. Mechanism of Creep and Shrinkage. -- The thickness of diffusible load-bearing layers is affected by the humidity, temperature, and the pressure acting on the layers according to the laws of thermodynamics. Thus an increase in load, or a decrease in humidity or temperature, will cause the hindered adsorbed layers to be disturbed and lead initially to a transfer of water (diffusion) to the free adsorbed layers. This causes the load-bearing layers to become thinner. Furthermore, the opposite process takes place when there is a decrease in load, or an increase in humidity or temperature; namely, the free adsorbed water from the surrounding pores diffuses into the load-bearing layers, and therefore increases thier thickness.

When drying of concrete takes place, negative film stresses result, which, when added algebraically to the stress in the load-bearing layers will change the disjoining pressure. This in turn results in changing the thickness of the layers.

1.3.3. Constitutive Equations. -- As mentioned before, Bazant (8) further developed this Powers' concept, and derived differential equations for the change of thickness of diffusible load-bearing layers, due to changes of load, temperature or humidity. The interaction of the solid components of the cement paste or concrete with the diffusible load-bearing layers, was introduced according to a rheological model, the simplest form of which is shown in Fig. 1. The effect of hydration on the mechanical properties, as well as the problem of macroscopic water diffusion, were considered. Furthermore, the thermal dilatations and their components are taken into consideration. These components are:

1. Pure thermal dilatation, which is due mainly to the coefficients of thermal expansion of solid and fluid components of the cement paste.
2. Thermal swelling, which is due to the differences in the latent heat of adsorption.

3. Hygrothermic dilatation, which is caused by a change of humidity with temperature, in a sealed specimen. These considerations were used in deriving constitutive equations for the creep of concrete due to any type of stress, varying temperature and humidity. Later, Bazant presented a numerical method for solving these equations (9). In deriving these equations the following assumptions were made:

    1. Concrete is isotropic on a macroscopic scale as well as quasi-homogeneous.
    2. Deformations are considered small so as to fall within the linear part of the stress-strain diagram.
    3. Temperature variations are limited to the range of 32 to 194°F.

Thus, the concrete deformation can be separated into two components, volumetric and deviatoric. Fig. 1 shows a simple form of the rheological model used for the interaction between the diffusible load-bearing layers and the solid part of the material. This model consists of a spring (c) which represents the solid skeleton of the concrete coupled in parallel with a diffusion element (d) which represents the diffusible load-bearing layers. This diffusion unit in turn is connected in series with another spring (b) which reflects the instantaneous deformation. For a wider range of delayed response a model consisting of more than one (n) diffusion unit should be used.

Due to a change of temperature ΔT, at a constant humidity, the constitutive equations take the following form, in which it is implied that $i, j = 1, 2, 3$; and subscript $\mu = 1, \ldots n$.

$$\dot{\varepsilon} = \frac{\dot{\sigma}}{K} + \dot{\varepsilon}'' \tag{1.1}$$

$$\dot{e}_{ij} = \frac{\dot{s}_{ij}}{2G} + \dot{e}''_{ij} \tag{1.2}$$

where

$$\dot{\varepsilon}'' = \sum_{\mu} \dot{\varepsilon}'_{\mu} - \frac{\dot{\sigma}_a}{K} + \alpha_o \dot{T} \tag{1.3}$$

$$\dot{\varepsilon}'_{\mu} = \phi_{\mu} (\sigma_{d_{\mu}} - \sigma_{ad_{\mu}}) - \sigma_{d_{\mu}} \frac{\dot{h}_{eq}}{K_{h_{\mu}}} \tag{1.4}$$

$$\dot{\sigma}_{d_{\mu}} = \nu_{\mu} (\dot{\sigma} - \dot{\sigma}_{a_{\mu}}) - K_{c_{\mu}} (\dot{\varepsilon}'_{\mu} + \alpha_{\mu} \dot{T}) \tag{1.5}$$

$$\dot{e}''_{ij} = \sum_{\mu} \dot{e}'_{ij_{\mu}} = \frac{1}{2} s_{d_{ij_{\mu}}} (\psi_{\mu} - \frac{\dot{h}_{eq}}{G_{h_{\mu}}}) \tag{1.6}$$

$$\dot{s}_{d_{ij_{\mu}}} = \nu'_{\mu} \dot{s}_{ij} - 2G_{c_{\mu}} \dot{e}'_{ij_{\mu}} \tag{1.7}$$

$$K = \frac{1}{\frac{1}{K_b} + \sum_{\mu} \frac{1}{K_{c_{\mu}} + K_{d_{\mu}}}} \tag{1.8}$$

$$G = \frac{1}{\frac{1}{G_b} + \sum_{\mu} \frac{1}{G_{c_{\mu}} + G_{d_{\mu}}}} \tag{1.9}$$

$$\nu_{\mu} = \frac{K_{d_{\mu}}}{K_{c_{\mu}} + K_{d_{\mu}}} \tag{1.10}$$

$$\nu'_{\mu} = \frac{G_{d_{\mu}}}{G_{c_{\mu}} + G_{d_{\mu}}} \tag{1.11}$$

In these equations, the terms subscripted with μ are related to the diffusion units of the model. Since the model used in this investigation (Fig. 1) includes one diffusion unit only, the subscript μ will be omitted from now on for simplicity. The partial derivative with respect to time is denoted by a dot.

ε = total volumetric strain; e_{ij} = total strain deviator

σ = total volumetric stress; s_{ij} = total stress deviator

Thus, $\frac{\dot{\sigma}}{K}$ and $\frac{\dot{s}_{ij}}{G}$ account for the rate of volumetric and deviatoric instantaneous strain.

$\dot{\varepsilon}''$ = rate of inelastic volumetric strain

$\dot{\varepsilon}''_{ij}$ = rate of inelastic deviatoric strain

α_o = instantaneous thermal dilatation coefficient

α_μ accounts for delayed pure thermal dilatation

ϕ, ψ = rate of volumetric and deviatoric deformation parameters, respectively

σ_d = stress resultant over a unit cross section due to diffusible load-bearing layers

σ_{ad} = the value of σ_d required for thermodynamic equilibrium at a given temperature and humidity, which accounts for delayed shrinkage and is given by the expression

$$\frac{T'}{T'_o}\,\sigma'_{ah} + \left(\frac{T'}{T'_o} - 1\right) c_{aQ}, \quad \text{where}$$

$$\sigma'_{ah} = f_d \cdot \frac{RT'}{M}\,\sigma_{ah} \tag{1.12}$$

T' = temperature in °K

T'_o = reference temperature in °K

σ_{aQ} = parameter that accounts for thermal swelling or shrinkage

R = universal gas constant in cc atm/deg/mol

M = molecular weight of water

$\frac{RT'}{M}$ = 1360 at a temperature of 298°K (25°C)

σ_{ah} = a parameter, which was given the following form by Bazant

$$\sigma_{ah} = (h_s - h)\,(1 + h_{eq}) \tag{1.13}$$

h_s = humidity at self-desiccation of a sealed specimen

h_{eq} = the equivalent humidity at a reference temperature T_o and is defined by,

$$dh_{eq} = dh - \kappa\, dT \tag{1.14}$$

T = temperature in °C

κ = hygrothermic coefficient, represents the change of humidity due to a change of 1°C at a fixed total water content

f_d = area factor of diffusible load-bearing layers

f_a = area factor of the stress resultant of the pressure in the fluid

σ_a = volume stress in the fluid, which is given by

$$\sigma_a = \sigma_{ad} \frac{f_a}{f_d} \tag{1.15}$$

K, G = represent the instantaneous volumetric and shear moduli of elasticity, Eqs. 1.8 and 1.9 respectively

K_h = coefficient that accounts for the delayed deformation of concrete under load due to a change in f_d, which occurs as a result of change in humidity h or temperature T.

K_b, K_c, K_d = volumetric elastic moduli for the elements of the model

G_b, G_c, G_d = shear moduli of elasticity of the elements of the model

K_d and G_d are components of K and G which depend on the compressibility of the diffusible load-bearing layers. They are, therefore, functions of humidity.

$$\left.\begin{aligned} K &= \frac{E}{1-2\mu}, \text{ and } E = 2G(1+\mu) \\ \text{Thus, } K &= \frac{2G(1+\mu)}{(1-2\mu)} \end{aligned}\right\} \tag{1.16}$$

μ = Poisson's ratio

E = modulus of elasticity

t_{eq} = equivalent curing time which has the following form:

$$t_{eq} = \int_{t_o}^{t} \beta \, dt' \tag{1.17}$$

β = relative hydration rate

According to Powers' (42), β is less than 1 for $h \leq 0.95$ and is zero when h is less than 0.80; Therefore, β is given by (9):

$$\left.\begin{aligned} \beta &= \beta_h (h) \cdot \beta_T (T) \\ \beta_h &= \frac{1}{1 + (7.5-7.5h)^4} \text{ , and} \\ \beta_T &= \frac{635}{160 - T} - 3.7 \end{aligned}\right\} \qquad (1.18)$$

Furthermore, Keeton (43) showed that there is no increase in the value of the compressive strength and modulus of elasticity with time when the humidity h is less than about 0.80.

A more detailed discussion of the influence of the various terms mentioned above on the time-dependent behavior of concrete will be presented in Chapter 4.

In order to use the above constitutive equations to predict the creep of concrete at varying temperatures and humidities, it is necessary to evaluate the following parameters and coefficients:

1. All volume and shear moduli of elasticity K's and G's.
2. Effective area factor f_d.
3. Rate of volumetric and deviatoric creep parameters ϕ and ψ.
4. Hygrothermic coefficient κ .
5. Humidity at self-desiccation h_s.

The experimental program was planned so that it would provide sufficient data to enable the evaluation of the above parameters and coefficients.

2. EXPERIMENTAL PROGRAM

2.1 Introduction

This chapter includes a description of the fabrication and testing of the concrete specimens.

2.2 Objective

The objective of this part of the investigation was to study the effects of elevated (140°F) and cyclic temperatures (73-140-73°F) at relative humidities of 50 and 100% on the time-dependent behavior of concrete under sustained load.

2.3 Scope

In order to satisfy the aforementioned objective, the following experimental investigations were carried out:

2.3.1. Preliminary Experiments. -- Preliminary investigations were carried out to evaluate the adequacy of the proposed methods of experimentation in obtaining the required test results and to enable an early identification and correction of any problems or difficulties that might arise.

Many of the problems involved in developing equipment and techniques in this experimental work were already detected and solved by Al-Alusi (44)in his previous investigation. It was necessary, however, not only to ensure that these problems would not arise again, but to take care of the additional problems involved in this investigation, particularly those arising from variations in temperature. One of the first problems investigated was the evaluation of the type of instrumentation to be used for measuring deformations in the concrete specimens. It was necessary to look for a method which would permit reliable measurements to be observed from outside the high temperature control rooms. Thus, Linear Voltage Differential Transformers (LVDT's) were used and tested to see if there would be a marked change of readings due to temperature changes and whether there would be any drift of readings with time at constant temperature. A special frame was

built for this purpose to which the LVDT's were affixed, and the whole assemblage was placed in an environmental chamber which was then heated to 140°F. Readings were taken regularly, and the results obtained showed some drift and inconsistency in the readings. The use of LVDT's was therefore considered unsatisfactory for this experimental program.

Another type of instrumentation considered was the use of electrical strain gages. The problem of how to fix these gages to the test specimens had to be solved. Many ideas were considered, and it was finally decided to use strain gages embedded longitudinally mid-way across the section, after increasing the mechanical bond between the concrete and the gage (by a subsequently described method). The use of epoxy for this purpose was avoided, since epoxy will creep with time and thus will change the readings. This method of using embedded strain gages was used by Al-Alusi and found to give good results for compression specimens. However, this method was found to be less adequate for torsion specimens since the average deformation measured by two dial gages was found to be about 2.5 times that observed by four embedded strain gages. Therefore, embedded strain gages were not used for the torsion specimens in this investigation.

In order to check the data obtained from the strain gages in the compression specimens, it was considered advisable to use an additional method of measuring deformations. Thus, the use of dial gages was considered and an evaluation made of how much the dial gage readings would change due to raising the temperature to 140°F. For this purpose a special calibration device made of invar was constructed to which a dial gage was fixed, as shown in Fig. 2. After taking an initial reading the calibration device was placed in a 140°F room, and subsequent readings were regularly recorded. It was found that the dial gage reading increased by about 0.001 in. due to a temperature change from 73 to 140°F. This change in reading due to change of temperature took place within one hour. Then the calibration device was placed back in the 73°F temperature room to see if there was any hysteresis effect, and none was observed. The setting of the dial gage was changed to get a different initial reading on the gage when fixed to the frame, the same thermal cycle was repeated and about the same

changes in dial readings were observed. Every dial gage used in this investigation was similarly calibrated for temperature effect. Results of these calibrations clearly showed that the dial gage would be suitable for use in a constant or cyclic thermal environment

Another problem investigated was how to protect the dial gage from moisture and subsequent rusting, especially in the highly corrosive environment of 100% R. H. and elevated temperature. The method used by Al-Alusi, namely to enclose the gage in a plastic bag, was not considered to be an adequate protection for the gage. A sample gage was therefore sealed by using silicone rubber to close all openings through which moisture might possibly move into the gage. After allowing enough time for the silicone rubber to effect this closing, the sealed gage was placed in an environment of 100% R. H. and 140°F. After two days the gage rusted and therefore did not work properly. Thus, a better method had to be found. Next, a special plexiglass box was made (Figs. 3 and 4) in which a desiccant consisting of activated silica gel was placed to protect the dial gage from moisture. This desiccant would change color when it absorbed a small amount of moisture. The sealed box was then placed in the humid high temperature environment. This method of sealing the gage was found to be satisfactory.

It was also observed that by using the loading system, described in Sec. 2.5.5, it was possible to maintain a constant value of applied compressive load on the specimens even at varying temperatures. This was made possible by placing the pressure accumulator and the pump outside the high temperature room.

Next, the method of instrumentation for the torsion specimens had to be investigated. For this purpose dial gages were considered, and the effect of thermal cycling was studied by fixing an unloaded specimen with the measuring system in the same way as described in Sec. 2.5.2 and then the temperature was raised to 140°F and the changes in the dial gages' readings were observed. After maintaining the high temperature for a sufficient time to permit the readings to stabilize, the temperature was lowered to 73°F and subsequent readings were observed. It was noted that the apparent decrease of readings due to raising the temperature could not be neglected, and therefore a

correction factor had to be applied to the observed readings when varying the temperature even after minimizing these changes as much as possible. Furthermore, it was considered desirable not to use a concrete base for the loading frame, since it may change with temperature, therefore the frame was firmly bolted to two 3 by 4 - in. solid steel sections as shown in Figs. 5 and 6.

Since the environmental conditions of temperature and humidity have a significant effect on the test results, all creep tests were conducted in control rooms maintained at 50% R. H. and operated at either a constant temperature or at varying temperatures. The 100% R. H. specimens were placed in plastic bags in the rooms, as shown in Fig. 15. Two control rooms were used and each had its own system for maintaining or changing temperature and humidity. The temperature and humidity were continuously recorded for each room. Furthermore, copper-constantan thermocouples were placed in the control rooms and near each specimen at 100% R. H. These thermocouples were connected to a recorder. Thus, an additional continuous record of temperature was obtained. The temperature was maintained within ± 3°F, and the humidity was maintained within ± 3%.

Some investigations were also carried out to select an appropriate method of measuring humidity of concrete specimens at 73 and 140°F. For this purpose hygrodynamics' Hygrosensors (Fig. 7) were selected and their adequacy was tested by using standard salt solutions which provided known humidities at varying temperatures. The results of these tests indicated that these moisture gages could be used for measuring the relative humidity in the hygrothermic coefficient and self-desiccation concrete specimens. Since these gages are usable only within a narrow range of humidities, three different hygrosensors had to be used.

2.3.2. Main Test Program. -- All the main specimens were hollow cylinderical concrete specimens with an outside diameter of 6 in., inside diameter of 5 in., and a length of 40 in. The 1/2-in. wall thickness of these specimens was selected so that the concrete would reach hygrothermic equilibrium in a reasonably short time and also to obtain reasonably uniform stresses in the torsion specimens.

A total of thirteen creep specimens were used in this investigation. Four specimens were subjected to sustained compressive load, five to sustained torsional load, and four were used as unloaded controls. The control specimens were subjected to the same hygrothermic treatment as the loaded ones and were used to determine the volumetric changes of concrete at a given environment. These three types of specimens, namely, compression, torsion and control, were used under each of the four environmental conditions investigated.

The four environmental exposures used included a constant relative humidity of 50 or 100% at either a sustained temperature of 140°F or in thermal cycles of 73-140-73°F.

Two compression specimens and two torsion specimens were cast, cured for 21 days at 100% R. H. and 73°F, and tested for strength at the age of 21 days. These values of strength were used to evaluate the magnitude of sustained load to be applied to the test specimens. The sustained compressive stress applied was about 30 percent of the ultimate strength of the specimen. This ratio was selected in order for the creep strain to remain within the linear range of the stress level which is generally assumed to be about 50 percent. Since the torsional deformations were very small, a sustained torsional load of about 40 percent of the torsional strength of the specimen was selected. Measurements of deformation with time for each specimen were recorded at selected time intervals and plotted.

In order to obtain the changes in the values of strength, modulus of elasticity, and shear modulus of elasticity, with time, other tests were conducted using two types of control specimens: 1) hollow cylindrical specimens; and 2) solid 3 by 6 - in. cylindrical specimens to check the changes in the strength of concrete.

2.3.3. Tests to Evaluate the Hygrothermic Coefficient and Self-Desiccation of Concrete. -- As mentioned earlier, one of the coefficients required for this study of concrete at elevated temperatures was the hygrothermic coefficient. To obtain this value two specimens were used having a 1-in. outside diameter, 1/4-in. wall thickness, and 6-in. length with hygrodynamics gage wells fitted at the center of each specimen as shown in Figs. 8 and 9. The 1/4-in. wall thickness

was chosen so that the specimen had the same diffusion path of 1/4 in. as the main specimens. These specimens were cast in special molds, using the same concrete mix as that used in all other specimens. The specimens were demolded after three days and moist-cured for an additional period of 15 days at 73°F, before being transferred to a 50% R. H. and 73°F room to allow the specimen's humidity to decrease to about 50% R. H.

In addition, two prismatic specimens having the dimensions of 1 1/2 by 1 1/2 by 6 in. (Fig. 9) were cast and moist-cured for 240 days. This prolonged curing period was used so that no further hydration would take place during thermal cycling. These specimens were then placed in a 50% R. H. and 73°F environment for about 40 days to allow the specimens to reach 50% R. H.

All of these concrete specimens on reaching about 50% R. H. were completely sealed against moisture loss by using two coats of Armstrong C-7 epoxy resin catalyzed with 8 percent (by weight) of Activator A. Then thermal cycling was started. Humidity measurements of the concrete specimens were taken at regular intervals during storage at 50% R. H. and subsequent thermal cycling.

For tests to determine humidity of self-desiccation, two concrete cylindrical specimens having the dimensions of 1 1/2 in. dia. and 6 in. length (Fig. 9) were cast with the hygrodynamics gage wells fitted at the center in a similar way to that shown in Fig. 8. These specimens were completely sealed by coating them with epoxy C-7 and then enclosing them in a copper jacket.

These tests will be discussed in detail in Appendices A and B.

2.4 Fabrication Of Specimens

2.4.1. Concrete Mix. -- In order to obtain good uniformity and homogeneity of the specimens the concrete selected was "micro-concrete," since the aggregate used was sand only. However, for convenience, it will subsequently be referred to as concrete. The following materials and mix proportions were used:

1. Cement: Santa Cruz Type I portland cement.
2. Aggregate: The aggregate used was a sand (F. M. = 1.55) consisting of a 50-50 blend by weight of Silver Sand grade 65 and Felton Sand No. 2. The mineral composition of this blended sand was about 80 percent quartz and 20 percent feldspar.
3. Mix Proportions: The concrete mix had a cement content of 12 scy and a water-cement ratio of 0.58 by weight. The cement-aggregate ratio was 1:2 by weight.

2.4.2. Casting of Specimens. -- Specially designed molds were used for casting the hollow cylindrical specimens. The mold consisted of two concentric tubes. The outer one was made of two halves of 1/2-in. thick plexiglass, and the inner one was made of three parts of 1/4-in. thick steel, as shown in Fig. 10.

The upper and lower flanges were fixed by using three rods, which were required to assemble the mold. For the torsion mold, a special recess was made on the bottom of the inner and outer shell to accommodate a steel ring to be cast with the torsion specimen. A light film of bond breaker was applied to the inner surfaces. Then after assembling the mold, all circumferential and longitudinal joints were sealed by filling them with Duxseal and covering them with Mylar pressure-sensitive tape. Two specially designed funnels were used to deposit the concrete. The mold was placed on a vibrating table and vibrated at a suitable speed during casting.

2.4.3. Curing. -- The concrete-filled molds were then stored in a 100% R. H. and 73°F room for three days before demolding the specimens and storing them in the same environment up to age 18 days for the 50% R. H. specimens, and up to age 21 days for the 100% R. H. specimens. At this stage the specimens were placed in the control rooms for the creep tests, at the specified temperature and humidity.

2.4.4. Instrumentation for Measuring Deformation. -- The following methods were used to measure deformations:

1. Electrical: Microdot weldable temperature - compensated strain gages (SG 189-6), shown in Fig. 11, were embedded in the specimens during casting. In each compression specimen two gages were placed in the longitudinal direction at the center of the wall thickness, at the mid-height of the specimen, and 180° apart. Only one gage was similarly used for each control specimen. A bridge completion unit (SG 090) was used with each gage in order to obtain accurate long-term strain measurements and to minimize the lead line errors. The flange of the strain gage was pin-holed with an average of 15 holes on each side of the strain tube to improve the bond between the gage and the concrete.

2. Mechanical: Three 1/10,000-in. dial gages placed 120° apart were used for each compression and control specimen, as shown in Figs. 4 and 12. It was considered necessary to use three dial gages for each specimen since three points will define a plane and thus any inhomogeneity and eccentricity of loading would be observed.

   However, there was little loading eccentricity introduced because during loading of each compression specimen a small percentage of the load was applied at first and the resulting deformations were observed. If the difference of the three dial gage deformations was not small, the specimen was unloaded and the loading frame nuts were adjusted to give a more uniform distribution of the load. Furthermore, the loading cell itself acted as a hinge to some extent. The dial gages were supported by the upper ring of three aluminum rings, each ring being fixed to the outside of the specimen with three equally spaced pointed screws. Each dial gage was attached to the ring unit with its tip in contact with a 3/8-in. diameter Quartz bar which was firmly fixed at the bottom ring and passed through a slightly oversize hole in the middle

ring, as shown in Fig. 4. The Quartz bar was selected because it has a very low coefficient of thermal expansion, and this would enable the thermal deformation of the specimens to be accurately measured.

This system was used for the 50% R. H. environment. For the 100% R. H. environment the same system was used, except that specially designed plexiglass boxes were fixed to the ring in order to protect the gages from moisture. The Quartz bar passed through a hole at the bottom of the box. Thus the middle ring became unnecessary and was not used. A suitable thin-walled rubber tube was fixed to the box and the rod to act as a bellows (Fig. 4). Also, blue silica gel in bags made of plastic wire mesh was placed in each box; the gel would change its color to pink when it absorbed moisture, and had to be replaced, indicating that the humidity inside the box was high.

This was made possible without disturbing the system by uncrewing the top cover of the box, replacing the silica gel bags, and fixing the cover again, which had to be done only once or twice since the boxes usually worked satisfactorily as protection against moisture throughout the test.

The average gage length of the compression and control specimens was 33.0 in.

For each torsion specimen two dial gages were used with a 12-in. long arm, and a gage length of about 34 in. The surface of the measuring arm in contact with the dial gage was machined in order to minimize any possible error due to deformations occurring with variations of temperature. In order to protect this part from rusting at 100% R. H. and introducing errors, it was chrome-plated after being machined. Also in this case the dial gages were enclosed in the previously described plexiglass boxes.

3. Optical: An optical method of measuring deformation was employed for the torsion specimens because this method would not be affected by changes of temperature. The system consisted of two aluminum rings each attached to the specimen by using three pointed screws. A 14-in. long, 1/4-in. diameter bronze bar with a 2 by 2-in. plate soldered to its end was firmly fixed to each ring. Special 1 1/2 by 1 1/2-in. targets (K & E 716165) were fixed to the plates. The target had a standard paired-line alignment pattern with an additional bull's eye pattern, as shown in Fig. 5a. A Wild T-2 theodolite was placed a suitable distance in front of each target. This position was fixed for each specimen, and the relative angle between the two targets was observed with the theodolite of one second accuracy. The value of the relative angle was regularly measured and converted into shear strain. The average gage length for this system was 28 in.

2.5 Testing of Specimens

The loading technique used in this investigation was the same as that used by Al-Alusi (44).

2.5.1. Compression Loading System. -- The loading system consisted of two circular plates connected by three rods, and a loading cell, as shown in Figs. 13 and 14. The constant pressure was sustained by using a hydraulic pressure accumulator. The pressure was observed by means of a pressure gage, and any small change in its value, which rarely occurred, was immediately corrected. The loading frame was placed in a metal pan. The specimen was placed on a 2-in. high perforated steel ring having the same cross-section as the specimen, and the ring-supported specimen was then placed on the loading cell. Small fans were fixed to the upper hollow plate to keep air circulating inside the specimen. A more detailed description of the loading system

is presented by Best et al(45). Clear vinyl bags were used in the case of the 100% R. H. specimens (Fig. 15). A water jet at the top of the frame supplied the water necessary for this condition.

2.5.2. Torsional Loading System. -- Details of the loading frame for a torsion specimen are shown in Figs. 5 and 6. This system was also used to obtain the torsional strength of the specimen. A small fan was placed on top of the specimen for air circulation inside the specimen. In the case of 100% R. H. a pan, water jets and a vinyl bag were also used.

2.5.3. Preparation of Specimens . -- When a torsion specimen was 14 days old it was completely sealed by using Saran wrap, and then its upper end was trimmed before using epoxy to fix its loading arms. Within about one hour, the specimen was placed back in the fog room.

When a compression specimen was 14 days old, it was also completely sealed before trimming its ends, by using a rotary type diamond saw. Great care was taken to ensure that the cut was smooth, with the surface perpendicular to the axis of the specimen. This operation took only a few minutes, and then the specimen was brought back to the fog room.

When the compression specimens that were to be tested under constant relative humidity of 50% reached the age of 18 days, the dial gage measuring system was fixed on the compression and control specimens. The specimens were then placed in the control room at 50% R. H. and 73°F temperature, and kept there for 14 days before loading.

As for the specimens that were to be tested under constant relative humidity of 100%, they were removed from the fog room when they were 21 days old, and taken to the control room at 73°F temperature where they were loaded and kept inside the plastic bag. The dial gage measuring system was fixed to the compression specimens, before loading, and to the control specimens.

2.5.4. Hygrothermic Treatment. -- For this purpose there were two groups of specimens, and each group included torsion, compression, and control specimens at 50% and 100% R. H., as summarized in Table 1.

The specimens for each group were cast at different times, so that they were due to be loaded at the same time, namely, at the age of 32 days for the 50% R. H. specimens and at the age of 21 days for the 100% R. H. specimens. The specimens of each group were loaded in a different control room where the temperature was kept constant at 73 ± 3°F and the humidity was kept constant at 50 ± 3% R. H., except for the specimens in the plastic bags where the humidity was 100%. After the specimens had been under this condition for about 37 days (except specimen No. 13 which was heated after 64 days), the temperature of each room was raised to 140°F while maintaining the 50% R. H. This operation took about 2 1/2 hours. This high temperature was kept constant for the whole test of the first group, except at the end when the room was cooled down to 73°F, and the specimens were then unloaded. The temperature of the control room of the second group of specimens was lowered to 73°F after keeping it 14 days at 140°F temperature. Then it was kept at this lower temperature for 14 days. After this the temperature was raised and lowered at 7-day intervals until the end of the test when the specimens were unloaded at 73°F temperature. It took about 2 1/2 hours, to heat or cool the room, by using a special program.

2.5.5. Loading of Specimens. -- Two types of loading were used:

1. Torsional Load: The specimen was placed in the frame and the dial gage and optical measuring systems fixed to the specimen. Initial readings were taken, and then the weights required to produce the necessary torque were placed at the same time on each basket. Immediately, a new set of readings was taken. For each specimen, the latter was considered the zero reading for the creep test.

2. Compression Load: The compression specimen was placed on the loading frame described, with the upper plate just touching the specimen. The valve of the loading cell was closed, and the pressure of the hydraulic accumulator raised to the required value by using a hydraulic pump. The valve of the accumulator was closed, and initial readings were taken for the compression and control

specimens. The loading cell valve was then opened, and the pressure raised to the required value. Thereafter, the accumulator valve was opened and a new set of readings was taken. The load was kept constant during the test.

A deformation-time curve was obtained for each specimen.

3. TEST RESULTS

In this chapter the experimental results are presented with a brief discussion of the various factors that might have affected the results.

3.1 Strength and Elastic Properties

Two types of control specimens were used for the determination of the mechanical properties of the concrete:

1. Solid 3 by 6-in. Cylindrical Specimens : Four of these specimens cured at 100% R. H. and 73°F were tested in compression at the age of 21 days, and the average ultimate strength was 5840 psi. Also average strength values for similar specimens were obtained at the ages of 113, 149 days when cured at 73°F and 100% R. H. Other values were obtained for similar specimens after being subjected to high temperatures and 100% R. H. These values are summarized in Table 2.

2. Hollow Cylindrical Specimens, 6-in. O. D., 5-in I. D. and 40-in. Long : Two tubular specimens (A and B, Table 1) cured at 100% R. H. and 73°F were tested in compression at the age of 21 days. The average compressive strength was 2800 psi and the average modulus of elasticity 3.25×10^6 psi. The lower strength value of these specimens compared to that of the 3 by 6-in. specimens may be attributed to the small wall thickness and to the large size of the tubular specimens as well as to possible bleeding and segregation during casting. The average stress-strain curve for these specimens, using the dial gage measuring system described in Sec. 2.4.4, is shown in Fig. 16a.

   The torsional strength was determined at the age of 21 days by testing to failure two torsion specimens (C and D), using the torsion frame described in Sec. 2.5.2. The average shear

strength was 225 psi and the average shear modulus of elasticity 1.71×10^6 psi. The stress-strain curve for these specimens is shown in Fig. 16b. These values are summarized in Table 2.

In addition to these tests the unloaded hollow control specimens were tested at regular intervals by rapid loading, and unloading immediately after observing the changes in deformations due to load. The results of these tests are shown in Figs. 17, 18 and 19. These results were used to evaluate some of the coefficients required for the analysis as will be discussed in Sec. 4.2.1.

At the end of the creep tests all the specimens were tested for strength. For the compression specimens an extensometer with two LVDT's (Fig. 20) connected to an X-Y-Y recorder was used to give the stress-strain curves. The stress-strain diagrams for the compression specimens are shown in Fig. 21, and for the torsion specimens in Fig. 22.

3.2 Creep Deformations

3.2.1. Creep in Compression . -- The observed axial deformations were converted into strains. The creep strains were obtained by deducting from the strains of the loaded specimens, the free shrinkage and thermal strains measured, at the same time, on the corresponding control specimens. The time-dependent strains of concrete specimens at sustained temperatures up to 140°F and 100% R. H. are shown in Fig. 23, and at 50% R. H. shown in Fig. 24. Furthermore, Figs. 25 and 26 show the time-dependent strains of specimens at cyclic temperatures of 73-140-73°F and 100 and 50% R. H., respectively. These figures also show the free shrinkage and thermal strains with time.

3.2.2. Creep in Torsion. -- Creep deformations for specimens loaded in torsion at sustained temperatures up to 140°F are shown in Figs. 27 and 28 at relative humidities of 100 and 50% , respectively. The results obtained at cyclic temperatures of 73-140-73°F and 100% R. H. are shown in Fig. 29, and for 50% R. H. in Figs. 30 and 31 .

A summary of the creep results is presented in Table 3.

3.3 Discussion Of Test Results

3.3.1. Effect of Moisture Condition on Initial Instantaneous Deformations.

-- The test results obtained show that the instantaneous deformations and thus the modulus of elasticity E and shear modulus G of the concrete specimens at 100 and 50% R. H. were nearly equal when the same load was applied for both compressive and torsional load. This confirms the assumption made that the initial curing used for both the 100% R. H. (21 days) and 50% R. H. (18 days at 100% R. H. and 14 days at 50% R. H.) specimens resulted in having about an equal strength value at the time of loading, i.e. both types of specimens had equivalent curing time t_{eq} = 21 days.

3.3.2. Effect of Moisture Condition on Creep at 73°F

1. Compression: Figs. 23 and 24 show that at the end of 37 days under the same compressive load the creep strain of the 50% R. H. specimen is about 4 times that of the 100% R. H. specimen. These results agree with those obtained in other investigations (1, 4, 44, 46). This behavior can be explained by the fact that the area factor of the diffusible load-bearing layers is smaller, and therefore under higher stresses, for the specimen at 50% R. H. than in a similar specimen at 100% R. H.

2. Torsion: Figs. 27 and 28 show that at the end of 37 days under the same torsional load the creep strain of the 50% R. H. specimen is about 1.8 times that of the 100% R. H. This result also seems to agree with that of other investigations (1, 3, 44, 46) and can be attributed to the same factor mentioned in 1. above.

3.3.3. Effect of Elevated Temperature (140°F) on Creep.

-- After having the specimens under load for about 37 days, the temperature was raised to 140°F while maintaining the constant relative humidities. After studying the test results the following observations can be made:

1. There was a sharp increase of creep strain in all loaded specimens with the first raising of temperature. This agrees with other investigations, particularly Ref. (3).

2. At 50% R. H. the creep strain of the specimens loaded in compression stabilized after about 10 days at 140°F. However, the creep of the specimen loaded in torsion stabilized after about 25 days at 140°F and no appreciable increases in creep was observed after that.

3. At 100% R. H. the creep strain continued to increase with time for both the compression and torsion specimens.

3.3.4. Effect of Thermal Cycling (73-140-73°F) on Creep. -- Effects of cyclic changes of temperature of 73-140-73°F while maintaining constant values of humidities of 50 and 100% were studied and the results obtained are shown in Figs. 25, 26, 29, 30 and 31. A study of these results indicates the following:

1. The first heating to 140°F caused the largest increase in creep for all specimens. This may be attributed to the moisture diffusion within the cement paste which may be responsible for structural decomposition and accelerated deformation.

   Increased deformability with temperature may be an indirect effect of migration of water from one lattice position to another in the water adsorbed between adjacent surfaces of the solid hydrate layer-crystals of the cement gel (24). Migration of water from gel pores to capillary pores has been shown by Helmuth (47) to take place with increasing temperature and thus causes shrinkage. He also showed that the first heating cycle produced irreversible changes in the cement gel, which may explain why deformations are particularly large during the first heating under load.

2. There was very little further increase in creep strain of the 50% R. H. compression specimen with further thermal cycles.

3. For the compression specimen at 100% R. H. creep strain increased with each additional thermal cycle, although this increase was less than that of the first cycle. This increase, however, seemed to be more pronounced during the cooling portion of the cycle.

4. The creep strain of the compression specimen at 100% R. H. and cyclic temperature seemed to be slightly larger than the one obtained under a sustained temperature of 140°F after a loading period of 140 days.

5. Nearly the same magnitude of creep strain was obtained for the 50% of R. H. compression specimens subjected to either the cyclic or the sustained 140°F temperature.

6. The largest increase of creep strain due to cyclic temperature was obtained for the specimen loaded in torsion at 100% R. H. The creep strain under cyclic temperature was about 1.5 times that obtained at sustained temperature of 140°F. The total creep strain at the end of six temperature cycles was about 5 times the initial instantaneous deformation.

3.3.5. Effect of Type of Load on Creep. -- The magnitude of compressive stress applied to the specimens was 910 psi, which is 32% of the specimen's ultimate strength at the time of loading. For torsion specimens this ratio was increased to 42%, or a stress of 95 psi at the outer fiber. These values of stress-strength ratios are considered to be well below the so-called linear limit of creep strain-stress relationship, which is about 50%.

Creep strain in torsion showed a general similarity to creep strain in compression particularly at 73°F. However, it can be observed that the specific creep (creep strain due to a unit stress) in torsion is in general higher than that in compression, as shown in Figs. 32, 33, 34 and 35. The ratio of specific creep in torsion to that in compression after 37 days under load at 73°F was about 1.5 for the specimens at 50% R. H. and 3.2 for the specimens at 100% R. H. Creep strains of the

same order of magnitude have been reported by other investigators (48, 49, 50, 46, 22, 44). However, the ratio of the creep strain after 37 days under load at 73°F to the initial instantaneous strain at time of loading is as follows:

2.28 for the specimen loaded in compression at 50% R. H.

1.51 for the specimen loaded in torsion at 50% R. H.

0.55 for the specimen loaded in compression at 100% R. H.

0.84 for the specimen loaded in torsion at 100% R. H.

These ratios and the ratios of the final creep strain values to the initial instantaneous strains are presented in Table 3.

The fact that creep deformation due to the same value of stress is higher under torsional load than under compressive load may be attributed to the fact that the microcracks due to drying which may have been initiated before application of the load tend to widen due to the tensile component of the torsional loading, whereas in the case of the compressive load the opposite effect takes place, i.e. the cracks normal to direction of loading tend to close with load and creep.

The ratio of total specific creep strain in torsion to that in compression was 1.7 for the specimens subjected to 6 cycles of temperature changes (73-140-73°F) and 50% R. H.; after 6 cycles of temperature changes and 100% R. H., this ratio was about 2.6. For the specimens at sustained 140°F and 50% R. H. this ratio was about 1.60 but at 100% R. H. it was 2.0. All these creep values were obtained after applying the sustained loads for about 140 days.

3.3.6. Effect of Method of Measuring Deformations. -- For the compression specimens each dial gage strain value plotted in the various figures represents the average value obtained from three dial gages. These three gages were equally spaced at 120° around the compression specimen and measured the deformations over an average gage length of 33 in. Each shear strain value shown in the figures represents an average of two dial gages located 180° apart and having a gage length of 34 in.

For the embedded strain gages, the strains shown in the figures represent an average value of two gages spaced at 180° for the compression specimens but only of one gage for the unloaded control specimens. The gage length of these strain gages was only 1 inch. Thus it may be considered that the dial gage values give a more realistic representation of the actual deformations of the specimens. Furthermore, since the embedded strain gages are temperature-compensated, they do not give the true deformations of the specimens at varying temperatures.

In addition to the dial gage measuring system used for the torsion specimens, an attempt was made to use a theodolite to measure angular deformations (Sec. 2.4.4). The accuracy of the results of this method largely depends on the number of readings (repetitions) taken for each value particularly since very small deformations are involved. The 140°F temperature used in these tests did not permit staying in this hot environment long enough to take the number of readings required to give sufficient accuracy. Thus, the deformations obtained using this method showed some scatter and even inconsistencies in a few cases. The deformations observed with the dial gages are therefore considered to be more accurate and quite reliable.

After studying the dial and the strain gage deformations for the compression specimens the following remarks can be made:

1. In general, the strain gage deformations were in good agreement with those obtained using dial gages, although they were slightly lower. This may be attributed to the additional stiffness provided by the gage to the concrete section.

2. The two strain gages in Compression Specimen 10 failed when the temperature was first raised to 140°F. Also, one of the two strain gages in Specimen 4 failed while heating to 140°F and thus the strain gage values for the elevated temperatures shown in Fig. 23 represent only a single gage readings. These were the only failures of strain gages in the test program.

3. It is believed that better strain gage creep deformations at 50% R. H. would have been obtained if two opposite strain gages were used for the control specimens rather than the one gage. A very small change in the strain of the control specimen has a large effect on the creep strain. This is one more reason why the dial gage data are considered to better represent the actual deformations of the specimens.

3.3.7. Effect on Temperature on Modulus of Elasticity and Shear Modulus. -- The results shown in Figs. 17, 18 and in Table 3 indicate about a 25 percent decrease of the modulus of elasticity of the compression specimens at 100% R. H. after being exposed to either a sustained 140°F or a cyclic temperature. Similar results were reported by Hansen and Eriksson (24). Except for these high temperature and humidity compression specimens, all other specimens showed little change of the modulus of elasticity and shear modulus of elasticity with temperature.

3.3.8. Effect of Temperature and Type of Loading on Creep Recovery. -- A study of the results obtained show the following:

1. The irrecoverable component of the creep, defined as the residual strain obtained after loading, in compression at 140°F and 50% R. H. (Specimen 1) is about 97% of the total creep strain defined here as the strain obtained immediately after unloading the specimen. This value is about 95% for the specimen subjected to thermal cycles (Specimen 7). For specimens stored at 100% R. H. the value is 92% at 140°F (Specimen 4) and 91% for thermal cycling (Specimen 10).

2. For creep in torsion the irrecoverable component of creep is 92% of the total creep at 50% R. H. and 140°F (Specimen 3), and 85% after thermal cycling (Specimen 13). In the case of torsion specimens at 100% R. H., the value is about 90% for both the 140°F and the thermally cycled specimens (6 and 12). These results are summarized in Table 3.

3. These results indicate that creep strain caused by either a constant high temperature or by thermal cycling is largely of an irrecoverable nature. This large percentage of irrecoverable creep can be mainly attributed to the irreversible changes in the internal structure of the cement gel which take place during the first heating of the specimens as explained in Sec. 3.3.4. Microcracking of the concrete, as well as aging may also have contributed to the large magnitudes of observed irrecoverable creep strain.

3.3.9. Effect of Carbonation on Creep Results. -- It has been established that concrete is susceptible to shrinkage caused by a chemical reaction of the even relatively low concentration of carbon dioxide (CO_2) in the air with the calcium hydroxide present in the hydrated portland cement. Furthermore, this reaction is dependent on the relative humidity of the environment containing the CO_2 to which the concrete is exposed.

Carbonation occurring at 100% R. H. does not cause any shrinkage, as was shown by Verbeck (51). He also showed that the maximum shrinkage due to carbonation occurs at 55% R. H., and that carbonation may improve the strength and hardness and reduce the permeability of concrete. It was also shown that less carbonation shrinkage results when drying and carbonation occur at the same time, than when the concrete specimen was dried first in a CO_2-free atmosphere and then allowed to carbonate.

Powers (52) proposed a hypothesis which considers carbonation shrinkage to be the result of dissolution of calcium hydroxide crystals while they are under pressure. The carbonation occurring when calcium hydroxide crystals are free from pressure, and the carbonation of other hydration products cause no shrinkage.

An ideal solution to eliminate the effect of carbonation on creep of concrete specimens, therefore, is to conduct the test in a carbon dioxide-free atmosphere. However, the expected small effects of carbonation on the creep results did not justify the additional difficulties and costs involved in conducting the tests in such an atmosphere.

For the test conducted under constant 100% R. H. environment it can be assumed that no shrinkage due to carbonation occurred. As for the tests conducted under 50% R. H. environment, carbonation was minimized by pre-carbonating the specimens. The specimens were first cured at 100% R. H. for 18 days (with no resulting shrinkage due to carbonation) and then stored for 14 days at 50% R. H. in air (permitting carbonation of the thin walled tubular specimens) before applying the load. Additional possible carbonation shrinkage has no effect on the creep of the torsion specimens, because shrinkage, whether caused by carbonation or drying has volumetric effects only. In the case of the compression specimens, additional carbonation shrinkage had no real effect on the creep results since an unloaded control specimen was used for correcting the data of each loaded specimen. Although carbonation of concrete caused a slight increase in strength(53), it can be reasonably assumed that this would have little effect on the creep results of this investigation.

4. ANALYTICAL STUDY AND PREDICTION OF CREEP

4.1 General Outline

As has been mentioned before, in order to develop a mathematical expression to predict creep using the constitutive equations 1.1 and 1.2, it is essential to obtain expressions for the various terms which represent functions and material properties including K's, G's, ϕ, ψ, f_d, G_h and K_h.

As discussed earlier, the most suitable way for solving these constitutive equations is to use a numerical method (9). This method includes subdividing the time into subintervals Δt during which the changes $\Delta\varepsilon$, Δe_{ij}, $\Delta\sigma$, Δs_{ij}, $\Delta\sigma_d$, and Δs_{ij} can be evaluated according to the following finite difference form of the constitutive equations 1.1 and 1.2:

$$\Delta\varepsilon = \frac{\Delta\sigma}{K} + \Delta\varepsilon'' \tag{4.1}$$

$$\Delta e_{ij} = \frac{\Delta s_{ij}}{2G} + \Delta e'_{ij} \qquad (i,j = 1, 2, 3) \tag{4.2}$$

where,

$$\Delta\varepsilon'' = \Delta\varepsilon' - \frac{\Delta\sigma_a}{K} + \alpha_o \Delta T \tag{4.3}$$

$$\Delta\varepsilon' = \Delta t\phi(\sigma_d - \sigma_{ad}) - \sigma_d \frac{\Delta h_{eq}}{K_h} \tag{4.4}$$

$$\Delta\sigma_d = \nu(\Delta\sigma - \Delta\sigma_a) - K_c(\Delta\varepsilon' + \alpha\Delta T) \tag{4.5}$$

$$\Delta s_{d_{ij}} = \nu' \Delta s_{ij} - 2G_c \Delta e'_{ij} \tag{4.6}$$

$$\Delta e'_{ij} = \frac{1}{2} s_{d_{ij}} (\Delta t\, \psi - \frac{\Delta h_{eq}}{G_h}) \tag{4.7}$$

In these equations the terms K, G, ϕ, α_o, ψ, K_h, and G_h represent the material characteristics, and the terms $\Delta\varepsilon$, $\Delta\sigma$, $\Delta\varepsilon''$, Δe_{ij}, Δs_{ij}, $\Delta e'_{ij}$, $\Delta\varepsilon'$ $\Delta\sigma_d$, $\Delta\sigma_a$, ν, ν', and $\Delta s_{d_{ij}}$ can be obtained easily using the constitutive equations. The term Δh_{eq} can be determined by solving the diffusion problem in the concrete during time step Δt.

The following is a brief outline of the procedure used for each time step $(t, t + \Delta t)$;

1. Using the initial values, in time step Δt, of h, T, h_{eq} and t_{eq}, the values of the diffusion coefficient $kb_T c_h$ and the thermal diffusion coefficient C are determined according to their expressions. Then the changes ΔT, Δh, Δt_{eq} and Δh_{eq} (which includes Δh_s and $\kappa \Delta T$) for all nodes are determined by solving the diffusion problem inside the concrete body for time step Δt. A numerical method is used to solve the governing second order partial differential equation.
2. The values of h_{eq}, t_{eq}, h_s are calcualted according to their expressions 1.14, 1.17 and B.1, respectively. Then σ_{ad} is determined from 1.12 and 1.13 as follows:

$$\sigma_{ad} = \frac{T'}{T'_o} \cdot f_d \cdot 1360\ (h_s - h)(1 + h_{eq}) + (\frac{T'}{T'_o} - 1)\ \sigma_{aQ}$$

   The determination of f_d is presented in Sec. 4.2.3 and σ_{aQ} was assumed equal to $0.014\ h_{eq}^2\ (T - 25)$, as was suggested by Bazant (9).
3. If a subinterval smaller than Δt is necessary to get a convergence for the temperature and humidity analysis, then Step 2 is repeated until the values are obtained in time $t + \Delta t$.
4. The mean values of h, T, h_{eq}, t_{eq} in the time interval $(t, t + \Delta t)$ at the center of each element of the body are determined by interpolation.
5. The values of K_b, K_c, K_d, K_h, ν, G_b, G_c, G_d, G_h, ν', K, G (Eqs. 1.8 and 1.9), α_o, α as well as ϕ and ψ are determined according to their respective expressions (to be obtained later).
6. The values of $\Delta\varepsilon'$ and $\Delta e'_{ij}$ are determined using Eqs. 4.4-4.7. Then the value of $\Delta\varepsilon''$ is determined using Eq. 4.3.
7. So far, the values of σ_d, $s_{d_{ij}}$, σ, ε, s_{ij}, e_{ij} as well as $\Delta\varepsilon''$ and $\Delta e'_{ij}$ are determined up to time t. Thus Eqs. 4.1 and 4.2 can be considered as a ficticious incremental elastic stress-strain law with prescribed incremental initial strains $\Delta\varepsilon''$ and $\Delta e'_{ij}$. The determination of the changes $\Delta\sigma$, $\Delta\varepsilon$, Δs_{ij}, Δe_{ij} for given load increments and given boundary displacement increments become, therefore, a problem of elasticity, which is then converted into a problem with equivalent surface and volume loads and therefore with

no initial strains. The solution can easily be carried out using the finite element method.

8. For a creep problem under constant load ($\Delta\sigma = \Delta s_{ij} = 0$), the increase of strain $\Delta\varepsilon$ and Δe_{ij} are determined for time step Δt by the end of step 7 above, i.e., at time $t + \Delta t$, the volumetric strain = $\varepsilon + \Delta\varepsilon$; and the deviatoric strain = $e_{ij} + \Delta e_{ij}$. These values are used as initial values for the next time step repeating the same procedure, and so on. A relaxation problem can similarly be solved, except that the stresses are prescribed instead of strains. Thus for a relaxation problem under constant deformation $\Delta\varepsilon = \Delta e_{ij} = 0$, and the solution is carried out to determine $\Delta\sigma$ and Δs_{ij}.

4.2 Evaluation of Parameters

The objective of this part of the investigation was to evaluate the parameters and functions necessary for the prediction of the time-dependent behavior of concrete under load. These parameters and functions are the moduli of elasticity of the rheological model used, ϕ, ψ, f_d, K_h, G_h, κ, and h_s (determined in Appendix A and B).

Evaluation of the above terms is restricted to the type of concrete used in this investigation. Furthermore, these terms are only valid for the experimental program presented in Chapter 2.

4.2.1. Moduli of Elasticity---The volumetric (bulk) modulus of elasticity K is defined as the ratio of the applied volumetric (hydrostatic) stress σ_v, to the volumetric strain ε_v.

i.e.

$$K = \frac{\sigma_v}{\varepsilon_v} \tag{4.8}$$

where: $\sigma_v = \dfrac{\sigma_{11} + \sigma_{22} + \sigma_{33}}{3}$; σ_{11}, σ_{22}, σ_{33} are principal stresses.

ε_v = change of volume per unit volume

$= \varepsilon_{11} + \varepsilon_{22} + \varepsilon_{33}$; ε_{11}, ε_{22}, ε_{33} are principal strains.

The same definition holds for the bulk moduli of elasticity of spring b(K_b), spring c(K_c), and the diffusion element d(K_d).

The value of K in terms of K_b, K_c and K_d is given by:

$$K = \frac{1}{\dfrac{1}{K_b} + \dfrac{1}{K_c + K_d}} \tag{4.9}$$

and

$$K = \frac{E}{1 - 2\mu} \qquad \text{where } \mu = \text{Poisson's ratio}$$

also

$$K_b = \frac{E_b}{1 - 2\mu_b}$$

$$K_c = \frac{E_c}{1 - 2\mu_c}$$

$$K_d = \frac{E_d}{1 - 2\mu_d} \qquad (4.10)$$

Furthermore, the shear modulus of elasticity G is given by:

$$G = \frac{E}{2(1 + \mu)}$$

also

$$G_b = \frac{E_b}{2(1 + \mu_b)}$$

$$G_c = \frac{E_c}{2(1 + \mu_c)}$$

$$G_d = \frac{E_d}{2(1 + \mu_d)} \qquad (4.11)$$

Solving for μ, μ_b, μ_c and μ_d in Eqs. 4.10 and 4.11, the following is obtained:

$$\mu = \frac{K - 2G}{2(K + G)}$$

$$\mu_b = \frac{K_b - 2G_b}{2(K_b + G_b)}$$

$$\mu_c = \frac{K_c - 2G_c}{2(K_c - G_c)}$$

$$\mu_d = \frac{K_d - 2G_d}{2(K_d - G_d)} \qquad (4.12)$$

also

$$\left.\begin{aligned} \frac{G_b}{K_b} &= \frac{1 - 2\mu_b}{2(1 + \mu_b)} \\ \frac{G_c}{K_c} &= \frac{1 - 2\mu_c}{2(1 + \mu_c)} \\ \frac{G_d}{K_d} &= \frac{1 - 2\mu_d}{2(1 + \mu_d)} \end{aligned}\right\} \qquad (4.13)$$

The experimental values of E with time shown in Fig. 17 are used with an assumed value of Poisson's ratio $\mu = 0.17$(44) to evaluate K according to Eq. 4.10. These results are presented in Fig. 36.

The bulk modulus of elasticity of spring b, K_b, in the model continuously changes with time due to further hydration. Thus K_b may be considered a function of equivalent curing time t_{eq}.

The diffusion unit consists of spring c which represents the solid particles of hydrated and unhydrated cement coupled in parallel with the diffusion element d to provide an elastic restraint on the deformation of the unit. The bulk modulus of the diffusion element, K_d, represents the volume compressibility of the diffusible load-bearing layers, particularly adsorbed water, which depends on humidity.

Thus, $K_b = K_b(t_{eq})$

$K_c = K_c(t_{eq})$

$K_d = K_d(h_{eq})$

The test results of this investigation have shown that at 73°F the value of K is nearly the same for both h = 0.5 and h = 1.0, indicating (Eq. 4.9) that the value of the term $K_c + K_d$ must be rather high in order for h to have such a small effect on the value of K. Thus, $K \approx K_b$ and similarly, $G \approx G_b$. This shows that the instantaneous elastic deformation is essentially represented by K_b and G_b, and is very little affected by K_c, K_d and G_c, G_d, respectively.

It should be pointed out that K_c has a major effect on the volumetric deformations of concrete with time, because the change of thickness of the diffusible load-bearing layers in element d affects the rate of change of

stress in these layers. The effect of K_c on $\dot{\sigma}_d$ is shown in Eq. 1.5. Also, G_c has a similar effect on the deviatoric deformations with time as shown in Eq. 1.7.

The derivation of K_b, K_c, K_d, G_b, G_c and G_d was then carried out according to the following:

1. In light of the above discussion and the work done by Al-Alusi(44), values of K_b, K_c and K_d were selected at t_{eq} = 21 days and 100% R.H. in such a way as to give a value of K nearly equal to the experimental value shown in Fig. 36.
2. With some increase in the values of K_b and K_c, keeping the same value of K_d, another value of K was obtained for t_{eq} = 37 days at 100% R. H. so as to give the same experimental value of K (Fig. 36). Using these two values, expressions for K_b and K_c were obtained.

   The values of K_c directly affect the time-dependent volumetric deformations and therefore the expression for K_c was used to predict creep in compression using the computer program. These predicted creep values were compared with the experimental values at 50 and 100% R.H. and any necessary modification in K_c was made so as to give creep values closer to the experimental values. After obtaining a better value of K_c, it was used to give a better value of K_b.

   After few trials the following expressions for K_b and K_c were obtained:

$$k_b = (6.1 - 17.2/t_{eq} + 50.0/t^2_{eq}) \times 10^6 \text{ psi};$$

$$K_c = (1.4 - 28.2/t_{eq} + 126.8/t^2_{eq}) \times 10^6 \text{ psi}$$

3. As presented in the previous discussion, a very small change in the value of K occurred at lower humidity at time of application of the load. It can, therefore, be assumed that K is a linear function of h. The following expression for K_d was obtained, which gives K values very close to those obtained experimentally for both 50 and 100% R.H. at 73°F:

$$K_d = 1.2\ (3.0 - h_{eq}) \times 10^6 \text{ psi}$$

4. It is expected that no lateral deformation occurs in the diffusible load-bearing layers of element d under uniaxial load. Therefore,

Poisson's ratio μ_d is zero. Thus Eq. 4.13 becomes,

$$G_d = 0.5\ K_d$$

Assuming $\mu_b = 0.17$, $\mu_c = 0.17$ and using these values in Eq. 4.13 the following is obtained:

$$G_b/K_b = 0.28\ ;$$

$$G_c/K_c = 0.28\ .$$

These values were used in Eq. 1.9 to obtain values of G, and some necessary modifications were made to give values of G close to those obtained experimentally. Furthermore, G_c affects creep directly, and the G_c values used gave deviatoric creep strains close to those obtained experimentally.

The final values of G_b and G_c obtained were:

$$G_b = 0.33\ K_b\ ;$$

$$G_c = (0.6 - 20.0/t_{eq} + 62.0/t_{eq}^2) \times 10^6 \text{ psi}\ .$$

4.2.2. Rate of Creep Parameters, ϕ and ψ.--The evaluation of the rate of volumetric and deviatoric creep parameters ϕ and ψ was carried out using experimental creep data for specimens which had no moisture movement, i.e., $\dot{h}_{eq} = 0$, as can be seen from Eqs. 1.4 and 1.6. Furthermore, it should be mentioned that ψ only affects creep in torsion, whereas both ψ and ϕ affect creep in compression.

The parameter ϕ is considered a function of humidity h_{eq} and time after application of the load t. The experimental results obtained showed higher creep strains for specimens at 50% R.H. than those at 100% R.H. Thus, ϕ can be assumed a linear function of h_{eq}.

The following expressions were found to give good results:

$$\phi = 7.0[(0.614 - 0.594\ h_{eq})(\frac{t + 500}{t + 1}) + (T - 25)(1.4\ h_{eq} - 1.0)] \times 10^{-7} \text{ psi/day}$$

$$\psi = 11.36[(1.625 - h_{eq})(\frac{t + 500}{t + 1}) + (T - 25)(4.32\ h_{eq} - 3.16)] \times 10^{-7} \text{ psi/day}$$

Creep strains were calculated for torsional and compressive loadings using the expressions obtained for ϕ and ψ as well as a value of $f_d = 0.05$. The calculation of creep strains was done by the use of a computer program

originally developed by Bazant (9), modified by Al-Alusi (44) and which was further modified to apply to this investigation.

4.2.3. Area Factor f_d.--The area factor f_d is defined as the effective area of diffusible load-bearing layers per unit cross section of the material. The term f_d affects σ_d and σ_{ad}, as was shown in Sec. 1.3, and therefore, it affects the creep behavior, whereas the area factor f_a affects σ_a, which governs the shrinkage of concrete. Thus, f_d is governed by the amount of water in the load-bearing water layers and f_a is governed by the amount of adsorbed water.

As indicated in the previous section, a constant value of $f_d = 0.05$ gave good creep results. A value of $f_a = 0.431$ was found by Al-Alusi to give shrinkage values similar to the experimental results of 100% R.H. concrete specimens when allowed to dry in a 50% R.H. environment at the age of 18 days.

4.2.4. Coefficients K_h and G_h.--The coefficients K_h and G_h account for delayed volumetric and deviatroic deformations, respectively, under load due to a change in the area factor f_d, which occurs as a result of a change in humidity or temperature.

It was observed from the experimental results that the increase in creep was most significant during the first heating.

After few trials to predict creep deformations when the specimens are heated, it was found that approximate values may be adequate. Thus, the following expressions of K_h and G_h, which give good computed creep strains, were developed:

$$\Delta h_{eq}/K_h = \left[312.0 \left(\frac{\Delta h_{eq}}{h_{eq} - 0.2}\right) + 3.65\ \Delta T(1.39\ h_{eq} - 1.00)\right] \times 10^{-6}$$

per psi for heating;

$$= -1.64\ \Delta T \times 10^{-5}\ (1.39\ h_{eq} - 1.00) \text{ per psi for cooling;}$$

$$G_h = 2\ K_h\ .$$

4.3 Prediction of Creep

A mathematical expression was developed using the constitutive equations presented in Sec. 1.3 together with the parameters and coefficients derived in Sec. 4.2 to predict creep deformations of concrete under compressive or

torsional loading when subjected to a constant relative humidity in the range of 50 to 100% at a sustained or cyclic temperature in the range of 73 to 140°F.

A computer program (9,44) was modified and used utilizing the mathematical expression developed to predict creep of concrete in compression and torsion when subjected to the following environmental conditions:

1. Sustained Temperatures (73, 140°F) at 50 and 100% R.H.
2. Cyclic Temperature (73-140-73°F) at 50 and 100% R.H.

The predicted total strains (elastic + creep) as well as the experimental values for the above conditions at sustained and cyclic temperatures in torsion and compression are presented in Figs. 27-30 and 37-40, respectively.

These figures show that good agreement is obtained between the computed and experimental values of total strains (elastic + creep). However, the calculated values of instantaneous recovery of the concrete at 50% R.H. were in good agreement with the experimental results. For the concrete at 100% R.H., however, the calculated values were lower than the experimental values. This is due to a considerable decrease of the modulus of elasticity caused by the sustained or cyclic heating, whereas the assumption made in the analysis was that hydration is accelerated at elevated temperatures and 100% R.H. causing an increase of the modulus of elasticity. It is believed that this can be taken care of, without difficulty, by minor changes in the expression of K_b.

4.4 Remarks on the Mathematical Expression and Its Prediction of Creep

In light of the previous sections the following remarks can be made:

1. A mathematical expression was constructed to give the time-dependent behavior of concrete under sustained load at sustained temperatures and at different humidities. The same expression also gives the time-dependent behavior under sustained load and cyclic temperature.
2. The functions and parameters required for the expression can be evaluated using the experimental results.

3. The predicted total strains (elastic + creep) using the mathematical expression were in good agreement with the experimental results for all the cases considered.

5. PREDICTION OF CREEP USING THE TIME-SHIFT PRINCIPLE

5.1 Introduction

The time-temperature shift principle for dealing with creep at steady temperatures was proposed by Schwarzl and Staverman (54). They suggested that in linear viscoelastic behavior of some materials a change of temperature is equivalent to a shift of the logarithmic time scale. Such materials are called thermorheologically simple.

As mentioned in Chapter 1, the time-shift principle was used by Sackman (10), Mukaddam (40), and Mukaddam and Bresler (55) in predicting creep of concrete including the effect of temperature.

In this chapter, the time-shift principle was first used on some creep data at constant temperatures in order to develop a mathematical model which includes the effect of temperature. Then this model was modified to predict creep at variable temperatures using the principle of superposition for temperature effects. The predicted creep strains using this mathematical model were compared with the experimental results.

5.2 Time-Shift Principle

To illustrate the time-shift principle for a thermorheologically simple material, let C_T and C_{T_o} represent specific creep curves at constant temperatures T and T_o ($< T$), respectively (Fig. 41). If the two curves have the same shape, the C_T curve can be made to coincide with the C_{T_o} curve by shifting it parallel to the logarithmic time-scale by a distance $\psi(T)$. Therefore,

$$C_T(\ln t) = C_{T_o}\,[\ln t + \psi(T)]$$

$$= C_{T_o}\,[\ln t + \ln \phi(T)]$$

$$= C_{T_o}\,\{\ln[t\,\phi(T)]\}$$

$$= C_{T_o}\,(\ln t^*)$$

where $t^* = t\,\phi(T)$;

$\phi(T) = e^{\psi(T)}$ = shift function for temperature T.

Thus the creep strain, as a function of real time t at a constant temperature T, can be obtained from the creep function at T_o, C_{T_o}, by replacing t by the temperature-compensated time $t\,\phi(T)$.

Before the time-shift principle can be applied to concrete, it should be ascertained whether it is thermorheologically simple or not, as will be demonstrated in the following examples using results of published experimental work on the effect of elevated temperature on its creep behavior.

5.3 Effect of Temperature

York et al (56) reported the results of a creep study made on 6 by 16-in. sealed concrete cylinders loaded in compression at age 90 days and temperatures of 75 and 150°F. For the 150°F creep tests, the temperature of the specimens was raised 9 days before application of the load. In order to check whether the concrete can be considered thermorheologically simple or not, the creep data was plotted against logarithmic time and the creep curve for 150°F was then shifted with respect to the creep curve at 75°F to form a single reference curve (Fig. 42a).

The creep test results reported by McDonald (34) and Arthanari and Yu (28), which were briefly described in Chapter 1, were similarly used to obtain the reference creep curves shown in Figs. 42b and 42c, respectively.

Results of the above examples indicate that sealed concrete may be considered as a thermorheologically simple material within the limits of these experiments which were within a temperature range of 68 to 176°F, loading age ranging from 15 to 90 days, and subjected to a stress not exceeding 0.35 of its compressive strength.

5.4 Mathematical Model and Prediction of Creep

5.4.1. Creep Function. -- The function chosen to represent specific creep of concrete at a constant temperature T_o and a given age at loading is of the following form:

$$C(t, T_o) = \sum_{i=1}^{n} \alpha_i (1-e^{-\beta_i t}) \tag{5.1}$$

where, t = time after application of the load.

n = number of terms in the function.

α_i, β_i = material constants.

In this investigation the following two cases were considered:

a. Constant Temperatures: The data for each reference curve obtained above was used to evaluate the constants in the creep function (Eq. 5.1) by the method of least squares. This data was also used to find the magnitude of the shift function, ϕ, necessary for each temperature.

Using this procedure, the results of the three investigations mentioned above would be analyzed.

1. York et al Data - The function representing the reference curve (Fig. 42 a) at a temperature of 75°F and age at loading of 90 days was first obtained. The creep strain at any temperature T is given by replacing the time t by $t\,\phi(T)$ in this function, and the resulting equation is as follows:

$$C(t, T) = 34.09\left[1 - e^{-.25\ t\ \phi(T)}\right] + 65.06\left[1 - e^{-.025\ t\ \phi(T)}\right] + 46.08\left[1 - e^{-.0025\ t\ \phi(T)}\right] + 236.95\left[1 - e^{-.00025\ t\ \phi(T)}\right] \tag{5.2}$$

where: t = time after loading, days

$\phi = 1.00$ at reference temperature $T_o = 75^oF$;

$= 7.03$ at temperature $T = 150^oF$

The creep strains were calculated using Eq. 5.2 at 75 and 150^oF; these as well as the experimental results are presented in Fig. 43a.

2. McDonald's Data - The same procedure gave the creep function for McDonald's data (Fig. 42b) at an age of loading of 90 days and a reference temperature of 73^oF, from which the creep strain at temperature T is given by the following equation:

$$C(t, T) = 43.89\left[1 - e^{-.25\ t\ \phi(T)}\right] + 8.48\left[1 - e^{-.025\ t\ \phi(T)}\right] + 124.52\left[1 - e^{-.0025\ t\ \phi(T)}\right] \quad (5.3)$$

where: $\phi = 1.0$ at reference temperature $T_o = 73^oF$;

$= 5.5$ at $T = 150^oF$

The experimental and calculated creep strains using Eq. 5.3 at 73 and 150^oF are shown in Fig. 43b.

3. Arthanari and Yu's Data - A creep function was obtained, using the same procedure, for Arthanari and Yu's data (Fig. 42c) at an age at loading of 15 days and a temperature of 68^oF. From this function creep strain at temperature T is given by the following equation:

$$C(t, T) = 106.9\left[1 - e^{-.25\ t\ \phi(T)}\right] + 121.5\left[1 - e^{-.025\ t\ \phi(T)}\right] + 362.2\left[1 - e^{-.0025\ t\ \phi(T)}\right] \quad (5.4)$$

where the temperature shift function, $\phi(T)$, determined for the four temperatures is as follows:

Temperature T, °F	Shift Function, $\phi(T)$
68.0	1.00
104.0	2.18
143.6	6.05
176.0	6.69

These results were used to obtain the following expression for the temperature shift function:

$$\phi(T) = 19.95 - 39.51 \left(\frac{T}{68}\right) + 25.74 \left(\frac{T}{68}\right)^2 - 4.78 \left(\frac{T}{68}\right)^3 \qquad (5.5)$$

where: T = temperature, ^{o}F .

The experimental and calculated creep strains using Eq. 5.4 at 68, 104, 143.6, and 176^{o}F are shown in Fig. 43c.

b. Variable Temperature: Arthanari and Yu's data also included a creep test in which the slab was heated from 68 to 138.2^{o}F in two steps (Fig. 44). An attempt was made here to predict the creep of this slab by using Eqs. 5.4 and 5.5. The data show that the instantaneous (elastic) strain increases with temperature due to a decrease in the modulus of elasticity of concrete. Similar observations were made in Chapter 3, by Browne (26), and by Hannant (27). Therefore, the effect of a change in elastic strain caused by a change of temperature should be included. Using Arthanari and Yu's experimental results the following expression for the elastic strain was obtained:

$$\varepsilon_i = \frac{1}{E(T)} = 233 + 1.52\ (T - 68^{o}F)$$

where: the temperature $T \geq 68^{o}F$;

E = modulus of elasticity in ksi.

The total strain C' (elastic + creep) at a variable temperature T is given by:

$$C'(t, T) = 233 + C(t, T_o) + \sum_{i=1}^{n} \{C[(t - t_i), T_i] - C[(t - t_i), T_{i-1}] + 1.52\ \Delta T_i\} \tag{5.6}$$

where: C = specific creep function (Eqs. 5.4, 5.5);

$= 0$, when $t - t_i < 0$

T_o = reference temperature = 68^oF

ΔT_i = increase in temperature = $T_i - T_{i-1}$, ^oF

n = total number of temperature increases

The experimental and calculated total strains using Eq. 5.6 are shown in Fig. 44.

The creep results obtained in Chapter 3 at 100% R. H. (Fig. 23) were used, utilizing the least squares method, to develop the following mathematical model for predicting total strain C' (elastic + creep) at a variable temperature T:

$$C'(t, T) = 288.4 + C(t, T_o) + \sum_{i=1}^{n} \{C[(t - t_i), T_i] - C[(t - t_i), T_{i-1}] + 2.57\ \Delta T_i\} \tag{5.7}$$

where: the specific creep function at constant temperature T is given by:

$$C(t, T) = 92.8\left[1 - e^{-.25\ t\ \phi(T)}\right] - 32.8\left[1 - e^{-.025\ t\ \phi(T)}\right] + 1041.9\left[1 - e^{-.0025\ t\ \phi(T)}\right]$$

$\phi = 1.0$ at reference temperature $T_o = 73^oF$;

$= 3.00$ at 116^oF;

$= 4.35$ at 140^oF.

The calculated total strains using this model (Eq. 5.7) and the experimental results are shown in Fig. 45.

The effect of further aging after application of the load was not considered in predicting creep at variable temperature since no sufficient data was available for its inclusion. However, it is expected that in this case its influence on creep is very small in comparison to that of temperature (28).

The values of $\phi(T)$ for the four sets of experimental data are plotted in Fig. 46. It may be seen that they fall in a relatively narrow band. Thus, it may be possible to estimate the effect of temperature on creep of concrete using an appropriate value of $\phi(T)$ from Fig. 46. The coefficients and exponents for the specific creep function for a particular concrete would need to be determined from experimental data at about $70^{o}F$ and at a limiting higher temperature to cover the temperature range considered.

The mathematical model developed in this chapter for predicting creep of concrete includes the effect of temperature. The creep strains calculated using this mode at constant and variable temperatures are in good agreement with the experimental results.

6. SUMMARY AND CONCLUSIONS

The summary and conclusions presented in this chapter are based on the experimental part of the research program presented in Chapters 2 and 3, and the analytical work presented in Chapters 4 and 5.

6.1 Experimental Investigation

Creep tests were conducted on tubular concrete specimens, 5-in. I. D., 6-in. O. D. and 40-in. long, under compressive and torsional types of loading. Two humidity levels were investigated: 50 and 100% R. H. At the time of loading all specimens had an equivalent curing time of 21 days. These specimens were subjected to different thermal treatments after application of the load: $73^{\circ}F$ temperature for 37 days, which was then raised to $140^{\circ}F$ and maintained at this value until the end of the test, when the temperature was lowered and then the specimens were unloaded. The other group of specimens were subjected to thermal cycling of $73\text{-}140\text{-}73^{\circ}F$.

The following conclusions can be drawn from the results obtained:

1. At $73^{\circ}F$ the creep strain at 50% R. H., in torsion and compression, was higher than that at 100% R. H. This may be attributed to:

   a. The smaller area factor, f_d, of the diffusible load-bearing layers at 50% R. H. results in a higher stress than that at 100% R. H.

   b. Complete hygrometric equilibrium of 50% R. H. in the concrete may not have been completely achieved after the 2 weeks of conditioning at 50% R. H. before load application, resulting in having some "drying creep" effect in addition to the "basic creep."

2. An increase in creep strain and rate of creep, in either compression or torsion, was observed when the concrete was first heated to $140^{\circ}F$. This is in agreement with previous experimental observations, indicating the significance of temperature on creep behavior.

3. After the first thermal cycle, the specimens at 50% R. H. did not show a large increase in creep strain with additional cycles, whereas the specimens at 100% R. H. showed an appreciable increase in creep strain with further thermal cycles, although the increase for each additional cycle was less than that during the first cycle.

4. There was no appreciable increase in creep strain two to three weeks after heating the 50% R. H. specimens, loaded in either compression or torsion, to 140°F. In contrast, however, the creep strain of the specimens at 100% R. H. and 140°F continued to increase with time, until the temperature was lowered to 73°F.

5. The specimens loaded in torsion showed a larger specific creep strain than the corresponding specimens loaded in compression.

6. The effect of cyclic temperature on creep was most pronounced for the specimens at 100% R. H., particularly in torsion.

7. The compression specimens at 100% R. H. showed a decrease in the modulus of elasticity of about 25 percent due to heating to 140°F. For all other compression or torsion specimens, however, no significant changes in the modulus of elasticity and shear modulus were observed with elevated temperatures.

8. Most of the creep strain that occurred at elevated or cyclic temperature was irrecoverable. This may be due to irreversible changes in the structure of the cement gel especially during the first heating.

6.2 Analytical Investigation

6.2.1. Powers-Bazant Theory.--A mathematical expression was developed, based on Bazant's constitutive equations, with the various parameters and coefficients evaluated using the experimental results obtained in Chapter 3. This expression is capable of predicting total strains (elastic + creep) of concrete under compressive or torsional loading, when subjected to a constant humidity in the range of 50 to 100% R. H.

and a constant, variable or cyclic temperature in the range of 73 to 140°F. The mathematical expression developed was used to predict creep strains of concrete at sustained (73 and 140°F) and cyclic (73-140-73°F) temperatures for the following cases:

1. Compression at 50 and 100% R. H..
2. Torsion at 50 and 100% R. H.

The predicted creep strains were in good agreement with the experimental results.

The calculated values of instantaneous recovery of the concrete at 50% R. H. were in good agreement with the experimental results. For the concrete at 100% R. H., however, the calculated values were lower than the experimental values. This is due to a significant decrease in the modulus of elasticity caused by the sustained or cyclic elevated temperatures, whereas the assumption made in the analysis was that hydration is accelerated at elevated tmeperature and 100% R. H., which causes an increase in the modulus of elasticity. However, it is expected that a change in the expressions of the volumetric and shear moduli of elasticity, K_b and G_b, will result in calculating closer values to those obtained experimentally.

It can therefore be concluded from the good correlation between predicted and experimental creep strains that application of the Powers-Bazant theory is adequate and very encouraging for prediction of creep of concrete.

6.2.2. Time-Shift Principle.--The mathematical model developed in Chapter 5 for predicting creep of concrete includes the effect of temperature. The creep calculated according to the model at constant temperatures was in a very good agreement with the experimental results. Also good agreement was obtained in predicting total strains at variable temperatures.

Although a more sophisticated, general expression has been proposed (8) and successfully used (Chapter 4) for predicting creep, taking into account variable temperature and humidity, considerable work is required to obtain the physical parameters and coefficients which have to

be determined experimentally. The model obtained here has the advantage of simplicity as it appears that the values of $\phi(T)$ fall within a narrow band for the different concretes investigated.

6.3 Practical Applications

The type of concrete used in this investigation was a micro-concrete with an aggregate-cement ratio of 2:1 and with a maximum size of aggregate smaller than sieve No. 4. However, structural concrete members in practice are usually made from concrete having larger maximum aggregate size and higher aggregate-cement ratio, which in turn would result in lower creep values than those obtained in this investigation; as was shown by Polivka et al (57), less creep occurs when concrete of higher aggregate-cement ratio is used. Thus, the conclusions presented in Sec. 6.1 are valid only qualitatively to real structural concrete members.

Also, structural concrete members usually have a larger wall thickness than that of the specimens used. This would cause a large portion of the members to remain at a high humidity level for a long period of time, since the diffusion of water in concrete is very slow (58). Therefore, temperature variations will affect creep in a real concrete member in a way closer to the 100% R. H. specimens than the 50% R. H. specimens tested. This would make the consideration of temperature variations a very important factor in such cases.

The prediction of creep strain in practical applications, according to the Powers-Bazant theory and using the computer program developed, is simple and efficient once the various parameters and coefficients are determined.

6.4 Suggestions for Future Research

In light of the experimental and analytical work presented, the following research could be carried out in order to permit a wider application of the Powers-Bazant theory and the time-shift principle for the prediction of creep of concrete:

1. Additional creep studies should be made on specimens at different constant and varying temperatures including different rates of heating.

2. Creep tests should be made on specimens having a large wall thickness, in order to reduce the effect of any microcracking that may take place.

3. Investigate the effect of microcracking on creep, and if required make the necessary modifications in the analysis.

4. Additional analytical investigations should be made using other experimental data. This, however, cannot easily be done since very few investigators have reported full details about their experiments. In the absence of such necessary background information, it becomes very difficult to apply the prediction procedure with any degree of confidence and make any realistic comparisons.

5. Carry out additional experimental work using a wide range of humidity levels in order to study the effect of humidity at constant but different temperatures.

6. Some experimental work is needed on creep behavior of concrete under simultaneous cyclic changes of temperature and humidity before proceeding with the analysis of these cases.

7. Further experimental and analytical work using the time-shift principle on creep of concrete is needed to confirm the validity of this method particularly at variable temperature.

REFERENCES

1. Hansen, T. C., "Creep and Stress Relaxation of Concrete," Proc. No. 31, Swedish Cement and Concrete Research Institute, Royal Institute of Technology, Stockholm, Sept. 1960.

2. L'Hermite, R. G.,"Volume Changes of Concrete," Proc. Fourth International Symposium on the Chemistry of Cement (Washington, D. C., 1960), National Bureau of Standards, Monograph No. 43, V. II, Sept. 1962, pp. 659-694.

3. Bertero, V. V., "Effect of Short-Time Variations in the Environmental Conditions Upon Creep of Concrete," Structures and Materials Research Report No. 69-17, Department of Civil Engineering, University of California, Berkeley, July 1969.

4. Powers, T. C., "Mechanism of Shrinkage and Reversible Creep of Hardened Cement Paste," Proc. International Conference on the Structure of Concrete (London, 1965), Cement and Concrete Association, London, 1968, pp. 319-344.

5. Powers, T. C., "Some Observations on the Interpretation of Creep Data," RILEM Bulletin No. 33, Dec. 1966, pp. 381-391.

6. Powers, T. C., "The Thermodynamics of Volume Change and Creep," Materials and Structures, V. 1, No. 6, Nov.-Dec. 1968, pp. 487-507.

7. Bazant, Z. P., "Constitutive Equation for Concrete Creep and Shrinkage Based on Thermodynamics of Multiphase Systems," Materials and Structures, V. 3, No. 13, Jan.-Feb. 1970, pp. 3-36. (Based on Report 68/1, Department of Civil Engineering, University of Toronto, Toronto, Nov. 1968).

8. Bazant, Z. P., "Thermodynamic Theory of Concrete Deformation at Variable Temperature and Humidity," Structures and Materials Research Report No. 69-11, University of California, Berkeley, Aug. 1969.

9. Bazant, Z. P., "Numerical Analysis of Long-Time Deformations of a Thick-Walled Concrete Cylinder," Structures and Materials Research Report No. 69-12, Department of Civil Engineering, University of California, Berkeley, Aug. 1969.

10. Sackman, J. L., "Creep in Concrete and Concrete Structures," Proc. Princeton University Conference on Solid Mechanics, Princeton, New Jersey, Nov. 1963.

11. Neville, A. M., and Meyers, B. L., "Creep of Concrete: Influencing Factors and Prediction," Symposium on Creep of Concrete, ACI Publication SP-9, 1964, pp. 1-31.

12. Wallo, E., and Kesler, C., "Prediction of Creep in Structural Concrete," T. and A. M. Report No. 670, University of Illinois, Urbana, Illinois, Dec. 1966.

13. Neville, A. M., "Creep of Concrete: Plain, Reinforced and Prestressed," North-Holland Publishing Company, Amsterdam, 1970.

14. Theuer, A., "Effect of Temperature on the Stress-Deformation of Concrete," Journal of Research, National Bureau of Standards, V. 18, No. 2, Feb. 1937, pp. 195-204.

15. Kelly, J. W., "Some Time-Temperature Effects in Mass Concrete," ACI Journal, Proc. V. 34, No. 5, May-June 1938, pp. 573-588.

16. Lee, C. R., "Creep and Shrinkage in Restrained Concrete," Transactions of the Fourth International Congress on Large Dams, V. 3, New Delhi, 1951, pp. 215-230.

17. Serafim, J. L., and Guerreiro, M. Q., "Influence of Temperature on Creep of Mass Concrete," RILEM Bulletin No. 6, Mar. 1960, pp. 23-32.

18. Torroja, E., and de la Peña, C., "Some Results Upon Temperature, Permanent Load and Creep," RILEM Symposium on Concrete and Reinforced Concrete in Hot Countries, Haifa, July 1960.

19. Glucklich, J., and Ishai, O., "The Effect of Temperature on the Deformation of Hardened Cement Paste," RILEM Symposium on Concrete and Reinforced Concrete in Hot Countries, Haifa, July 1960.

20. England, G. L., and Ross, A. D., "Reinforced Concrete Under Thermal Gradients," Magazine of Concrete Research, V. 14, No. 40, Mar. 1962, pp. 5-12.

21. Wallo, E. M., Yuan, R. L., Lott, J. L., and Kesler, C. E., "Prediction of Creep in Structural Concrete for Short-Time Tests," T. and A. M. Report No. 658, University of Illinois, Urbana, Illinois, 1965.

22. Ruetz, W., "A Hypothesis for the Creep of Hardened Cement Paste and the Influence of Simultaneous Shrinkage," Proc. International Conference on the Structure of Concrete (London, 1965), Cement and Concrete Association, London, 1968, pp. 365-387.

23. Nasser, K., and Neville, A. M., "Creep of Concrete at Elevated Temperatures," ACI Journal, Proc. V. 62, No. 12, Dec. 1965, pp. 1567-1579.

24. Hansen, T. C., and Eriksson, L., "Temperature Change Effect on Behavior of Cement Paste, Mortar, and Concrete Under Load," ACI Journal, Proc. V. 63, No. 4, Apr. 1966, pp. 489-504.

25. Nasser, K. W., and Neville, A. M., "Creep of Old Concrete at Normal and Elevated Temperatures," ACI Journal, Proc. V. 64, No. 2, Feb. 1967, pp. 97-103.

26. Browne, R., "Properties of Concrete in Reactor Vessels," Proc. Conference on Prestressed Concrete Pressure Vessels (London, 1967), Institution of Civil Engineers, London, 1968, pp. 131-151.

27. Hannant, D., "Strain Behavior of Concrete Up to 95°C Under Compressive Stresses," Proc. Conference on Prestressed Concrete Pressure Vessels (London, 1967), Institution of Civil Engineers, London, 1968, pp. 177-191.

28. Arthanari, S., and Yu, C. W., "Creep of Concrete Under Uniaxial and Biaxial Stresses at Elevated Temperatures," Magazine of Concrete Research, V. 19, No. 60, Sept. 1967, pp. 149-156.

29. Hickey, K. B., "Creep, Strength, and Elasticity of Concrete at Elevated Temperatures," Report No. C-1257, U.S. Bureau of Reclamation, Denver, Colorado, Dec. 1967.

30. Nasser, K. W., "Creep of Concrete at Low Stress-Strength Ratios and Elevated Temperatures," Symposium on Temperature and Concrete (Memphis, 1968), ACI Publication SP-25, 1971, pp. 137-147.

31. da Silveira, A., and Florentino, C. A., "Influence of Temperature on the Creep of Mass Concrete," Symposium on Temperature and Concrete (Memphis, 1968), ACI Publication SP-25, 1971, pp. 173-190.

32. Maréchal, J. C., "Le Fluage du Béton en Fonction de la Température," Materials and Structures, V. 2, No. 8, Mar.-Apr. 1969, pp. 111-115.

33. Browne, R. D., and Blundell, R., "The Influence of Loading Age and Temperature on the Long Term Creep Behavior of Concrete in a Sealed, Moisture Stable, State," Materials and Structures, V. 2, No. 8, Mar.-Apr. 1969, pp. 133-143.

34. McDonald, J. E., "An Experimental Study of Multiaxial Creep in Concrete," ACI Seminar on Concrete for Nuclear Reactors, Berlin, Sept. 1970.

35. McHenry, D., "A New Aspect of Creep in Concrete and Its Application to Design," Proc. ASTM, V. 43, 1943, pp. 1069-1084.

36. Arutyunyan, N. Kh., "Some Problems in the Theory of Creep," Pergamon Press, New York, 1966.

37. Bresler, B., "Some Factors in the Investigation of Long-Term Behavior of Reinforced Concrete Structures," Road Research Laboratory Report No. LN/150/BB, Department of Scientific and Industrial Research, England, 1962.

38. Bazant, Z. P., "Die Berechung des Kriechens und Schwindens nichthomogener BetonKonstruktionen," Preliminary Publication, Seventh Congress, International Association for Fridge and Structural Engineering, Rio de Janeiro, Aug. 1964, pp. 887-897.

39. Selna, L., "Time-Dependent Behavior of Reinforced Concrete Structures," Structures and Materials Research Report No. 67-19, Department of Civil Engineering, University of California, Berkeley, Aug. 1967.

40. Mukaddam, A. M., "Behavior of Concrete Under Variable Temperature and Loading," Ph.D. Dissertation, Department of Civil Engineering, University of California, Berkeley, Aug. 1969.

41. Illstone, J. M., and England, L., "Creep and Shrinkage of Concrete and Their Influence on Structural Behavior--A Review of Methods of of Analysis," The Structural Engineer, V. 48, No. 7, July 1970, pp. 283-292.

42. Powers, T. C., "A Discussion of Cement Hydration in Relation to the Curing of Concrete," Proc. Highway Research Board, V. 27, 1947. Also, Research Bulletin 25, Portland Cement Association.

43. Keeton, J. E., "Study of Creep in Concrete--Phase I (I-Beam)," Technical Report No. R333-I, U.S. Naval Civil Engineering Laboratory, Port Hueneme, Calif., Jan. 1965.

44. Al-Alusi, H. R., "Effects of Humidity on the Time-Dependent Behavior of Concrete Under Sustained Loading," Ph.D. Dissertation, Department of Civil Engineering, University of California, Berkeley, Nov. 1970.

45. Best, C. H., Pirtz, D., and Polivka, M., "A Loading System for Creep Studies of Concrete," ASTM Bulletin No. 224, Sept. 1957, pp. 44-47.

46. Ali, I., and Kesler, C. E., "Mechanism of Creep in Concrete," Symposium on Creep of Concrete, ACI Publication SP-9, 1964, pp. 35-57.

47. Helmuth, R. A., "Dimensional Changes of Hardened Portland Cement Pastes Caused by Temperature Changes," Proc. Highway Research Board, V. 40, 1961, pp. 315-336. Also, Research Department Bulletin 129, Portland Cement Association.

48. Anderson, P., "Experiments with Concrete in Torsion," Proc. ASCE, V. 60, No. 5, 1934, p. 641; Vol. 61, No. 2, 1935, pp. 247-249.

49. Duke, C. M., and Davis, H. E., "Some Properties of Concrete Under Sustained Combined Stresses," Proc. ASTM, V. 44, 1944, pp. 888-896.

50. Lambotte, H., "Le Fluage du Béton en Torsion," RILEM Bulletin No. 17, Dec. 1962, pp. 3-12.

51. Verbeck, G. J., "Carbonation of Hydrated Portland Cement," ASTM Special Technical Publication No. 205, 1958, pp. 17-36. Also, Research Department Bulletin 87, Portland Cement Association.

52. Powers, T. C., "A Hypothesis on Carbonation Shrinkage," Journal, PCA Research and Development Laboratories, V. 4, No. 2, May 1962, pp. 40-50. Also, Research Department Bulletin 146, Portland Cement Association.

53. Leber, I., and Blakey, F. A., "Some Effects of Carbon Dioxide on Mortar and Concrete," ACI Journal, Proc. V. 53, No. 3, Sept. 1956, pp. 295-308.

54. Schwarzl, F., and Staverman, A. J., "Time-Temperature Dependence of Linear Viscoelastic Behavior," Journal of Applied Physics, V. 23, No. 8, Aug. 1952, pp. 838-843.

55. Mukaddam, M. A., and Bresler, B., "Behavior of Concrete Under Variable Temperature and Loading," ACI Seminar on Concrete for Nuclear Reactors, Berlin, Germany, Oct. 1970.

56. York, G. P., Kennedy, T. W., and Perry, E. S., "Experimental Investigation of Creep in Concrete Subjected to Multiaxial Compressive Stresses and Elevated Temperatures," Research Report 2864-2, Department of Civil Engineering, University of Texas, Austin, June 1970.

57. Polivka, M., Pirtz, D., and Adams, R., "Studies of Creep in Mass Concrete," Symposium on Mass Concrete, ACI Publication SP-6, 1963, pp. 257-283.

58. Carlson, R. W., "Drying Shrinkage of Large Concrete Members," ACI Journal, Proc. V. 33, No. 3, Jan.-Feb. 1937, pp. 327-336.

59. Powers, T. C., and Brownyard, T. L., "Studies of the Physical Properties of Hardened Portland Cement Paste," Research Department Bulletin 22, Portland Cement Association, Mar. 1948.

60. Brunauer, S., "Some Aspects of the Physics and Chemistry of Cement," The Science of Engineering Materials, J. E. Goldman, Editor, John Wiley and Sons, Inc., New York, 1957, pp. 428-468. Also, Research Department Bulletin 80, Portland Cement Association.

APPENDIX A

EVALUATION OF HYGROTHERMIC COEFFICIENT

A1. Introduction.--The solution of Bazant's constitutive equations for creep at varying temperatures requires the determination of the hygrothermic coefficient κ which is defined as the change of humidity h with temperature T at a constant water content w.

Humidity h is assumed to be a function of water content w, equivalent curing time t_{eq}, and temperature T.

Thus $$h = h(w, t_{eq}, T) \tag{A.1}$$

and $$dh = (k/\rho_o)dw + dh_s + \kappa dT \tag{A.2}$$

The coefficient k represents the dependence of h on w at constant t_{eq} and T. The value of k can be obtained from adsorption-desorption isotherms (59,60). The term kdw is zero for a constant water content. The term dh_s represents the change of humidity h, due to hydration, in a sealed specimen at constant temperature. Thus, the self-desiccation function h_s is a function of t_{eq}. It can be determined experimentally, as will be shown in the following section, or for a well aged concrete $dh_s = 0$.

A2. Experimental Procedure.--Two concrete specimens were used for the determination of the hygrothermic coefficient κ, as explained in Sec. 2.3.3. The cylindrical specimens used were of 1-in. diameter and 6-in. length, as shown in Fig. 8. These specimens were demolded at the age of 3 days and then cured at 100% R. H. and 73°F for a total period of 18 days before being placed in a 50% R. H. room when humidity measurements of the interior of the concrete were taken at regular time intervals.

These specimens were completely sealed against moisture movement by using two coats of epoxy C-7 before the thermal treatment began at the age of 67 days. The age of 67 days was selected since it was the age at which the main test specimens were first heated.

In addition, two prismatic specimens, about 9 months old, having the dimensions of 1 1/2 by 1 1/2 by 6-in. were similarly used in order to eliminate the effect of further hydration during the thermal treatment.

A3. Test Results.--The results obtained from these tests are shown in Fig. 47 for the cylinder specimens, and in Fig. 48 for the prismatic specimens. Each data point shown in these figures represent an average value of two specimens. The values of κ were computed and are presented in Table 4.

The results obtained indicated that the value of κ is positive and that the first heating produced the largest value of κ, which may offer an explanation of why no appreciable increase in creep strain was observed when heating the 50% R. H. concrete specimens after the first thermal cycle.

The following expression for κ was derived and used in the analysis (Chapter 4):

$$\kappa = \frac{A.h\ (1.00-h)}{(1.32-h)} \qquad (A.3)$$

where $A = 0.021$ for the first heating;

$= 0.0002$ for subsequent thermal cycles.

APPENDIX B

EVALUATION OF SELF-DESICCATION FUNCTION

B1. Introduction.--The term dh_s represents the change of internal humidity of concrete, h, due to hydration at a constant water content, i.e. in a sealed concrete specimen. Self-desiccation is considered a function of equivalent curing time t_{eq}. In order to obtain an expression for this function in terms of t_{eq}, an experiment was carried out as described in the following section.

B2. Experimental Procedure.--Two concrete cylinders having the dimensions of 1 1/2-in. dia. and 6-in. length were cast using the same concrete mix as that used in the creep study. These specimens were demolded at the age of 3 days and then cured at 73°F and 100% R. H. up to the age of 21 days when they were completely sealed by using two coats of epoxy C-7 and then enclosing them in a copper jacket, as shown in Fig. 9. Humidity measurements of the interior of the concrete were taken at regular intervals.

The specimens were kept at 73°F until age of 58 days when they were heated to 140°F and kept at this temperature until the end of the test.

B3. Test Results.--The results obtained from these tests are shown in Fig. 49 (average of two specimens). These results indicated that the change of internal humidity h_s due to hydration was very small. This may be attributed to the high water-cement ratio (0.58 by wt.) of the concrete mix.

Using these test results the following expression was derived:

$$h_s = \frac{0.98\ t_{eq} + 20}{t_{eq} + 20} \qquad \text{(B.1)}$$

Fig. 49 also shows the values of h_s calculated according to the above expression.

TABLE 1

LOADING AND ENVIRONMENTAL CONDITIONS OF CREEP TESTS

Specimen	Type of Specimen	Loading		Relative Humidity, %	Temperature, ^{o}F
		Age, days	Stress-Strength Ratio		
Strength Specimens					
A, B C, D	Compression Torsion	21	-	100	73
Creep Specimens					
1	Compression	32	0.32	50	Sustained (73, 140)
2	Control	32	-	50	
3	Torsion	32	0.42	50	
4	Compression	21	0.32	100	
5	Control	21	-	100	
6	Torsion	21	0.42	100	
7	Compression	32	0.32	50	Cyclic (73-140-73)
8	Control	32	-	50	
9	Torsion*	32	0.42	50	
10	Compression	21	0.32	100	
11	Control	21	-	100	
12	Torsion	21	0.42	100	
13	Torsion	32	0.42	50	
14	Torsion	65	0.42	50	

* Failed during the first heating.

TABLE 2

STRENGTH AND ELASTIC PROPERTIES OF CONCRETE

A. 3 by 6-in. cylinders cured at 100% R. H.

Age, days	Temperature, °F	No. of specimens tested	Compressive Strength, psi
21	73	4	5840
113	73	3	6400
149	73	4	6340
164	cyclic (73-140-73)	2	5650
205	sustained (73, 140)	2	5410

B. Hollow cylinderical specimens - 6-in. O.D., 5-in. I.D., 40-in. long, cured at 100% R. H. and 73°F for 21 days. The values are average of two specimens.

	Strength, psi	Modulus of Elasticity, 10^6 psi	Shear Modulus, 10^6 psi
Compression	2800	3.25	-
Torsion	225	-	1.71

TABLE 3

SUMMARY OF CREEP TEST RESULTS

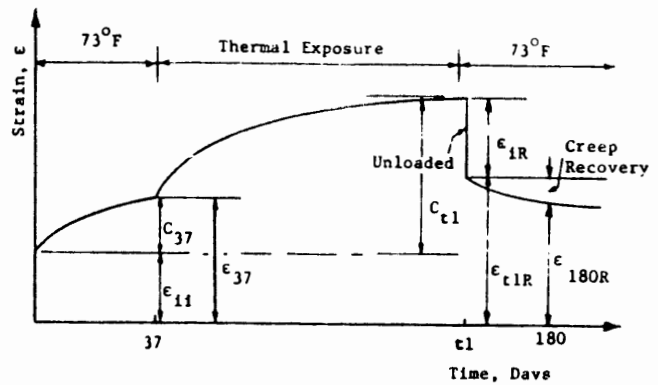

Specimen No.	Storage Condition		Sustained Stress			Strain, 10^{-6}								Ratio		
							Instantaneous + Creep				Creep					
	Temperature, °F	Relative Humidity, %	Type	psi	Period, Days t1	Initial Instantaneous ε_{ii}	After 37 Days ε_{37}	After t1 Days ε_{t1}	Instantaneous Recovery ε_{1R}	Residual at End of Test ε_{180R}	After 37 Days C_{37}	After t1 Days C_{t1}	Residual on Unloading ε_{t1R}	$\frac{C_{37}}{\varepsilon_{ii}}$	$\frac{C_{t1}}{\varepsilon_{ii}}$	$\frac{\varepsilon_{180R}}{\varepsilon_{t1R}}$
1	Sustained** (73,140)	50	Compression*	910	155	249	820	1250	260	962	571	1000	990	2.28	4.00	0.97
3			Torsion	95	155	57	143	221	62	146	86	164	159	1.51	2.90	0.92
4		100	Compression*	910	154	263	409	1238	388	780	146	975	850	0.55	3.70	0.92
6			Torsion	95	147	57	105	258	65	174	48	201	193	0.84	3.53	0.90
7	Cyclic** (73-140-73)	50	Compression*	910	138	254	814	1192	256	892	560	938	936	2.20	3.70	0.95
13			Torsion†	95	136	70	148	239	67	145	77	170	172	1.10	2.43	0.84
14			Torsion	95	95	55	112	18[illegible]	55	125	57	130	128	1.03	2.36	0.97
10		100	Compression*	910	138	243	383	1344	324	929	140	1100	1020	0.58	4.53	0.91
12			Torsion	95	138	59	110	354	57	268	50	295	297	0.85	5.0	0.90

* Compressive strains are corrected for shrinkage and thermal strains as observed on unloaded control specimens.

** Maintained at 73°F for 37 days before thermal exposure.

† Maintained at 73°F for 64 days before thermal cycling.

TABLE 4

HYGROTHERMIC COEFFICIENT κ PER ^{o}C

Heating Cycle No. (73-140°F)	Cylindrical Specimens (1-in. Dia., 6-in. long)	Prismatic Specimens (1 1/2 by 1 1/2 by 6 in.)
1	0.0062	0.0070
2	0.0012	0.0012
3	0.0012	0.0016
4	0.0012	0.0015

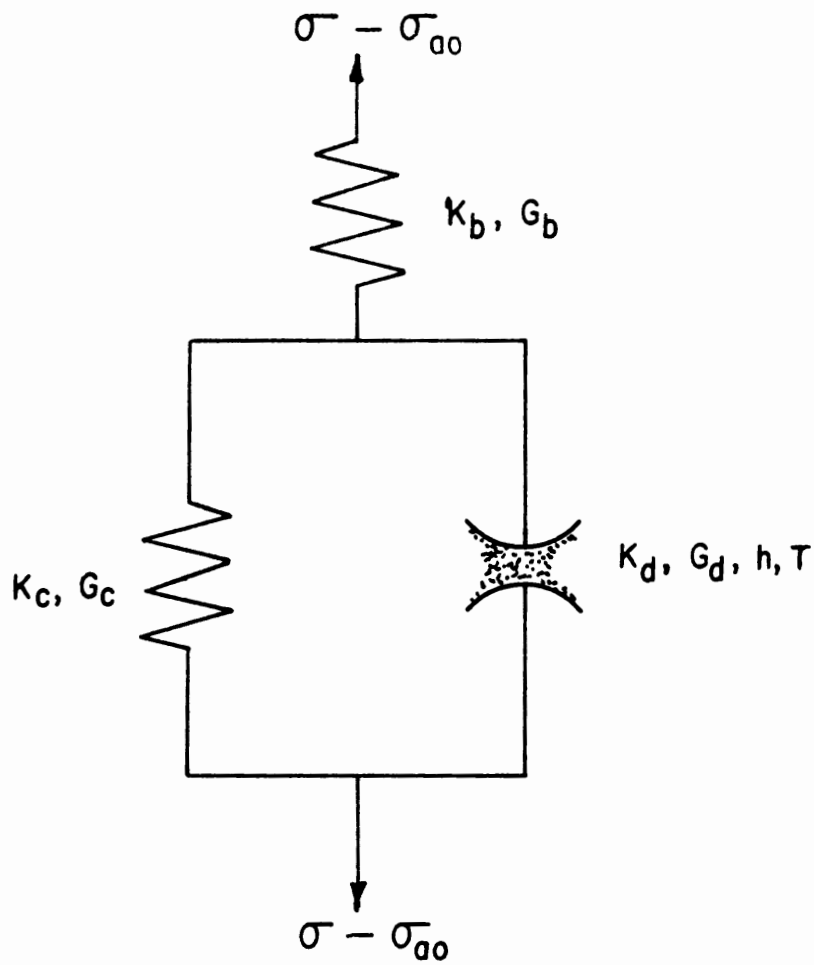

FIG. 1 RHEOLOGICAL MODEL FOR THE INTERACTION OF THE ELASTIC SOLID PARTICLES OF CEMENT PASTE OR CONCRETE WITH THE DIFFUSIBLE LOAD-BEARING LAYERS

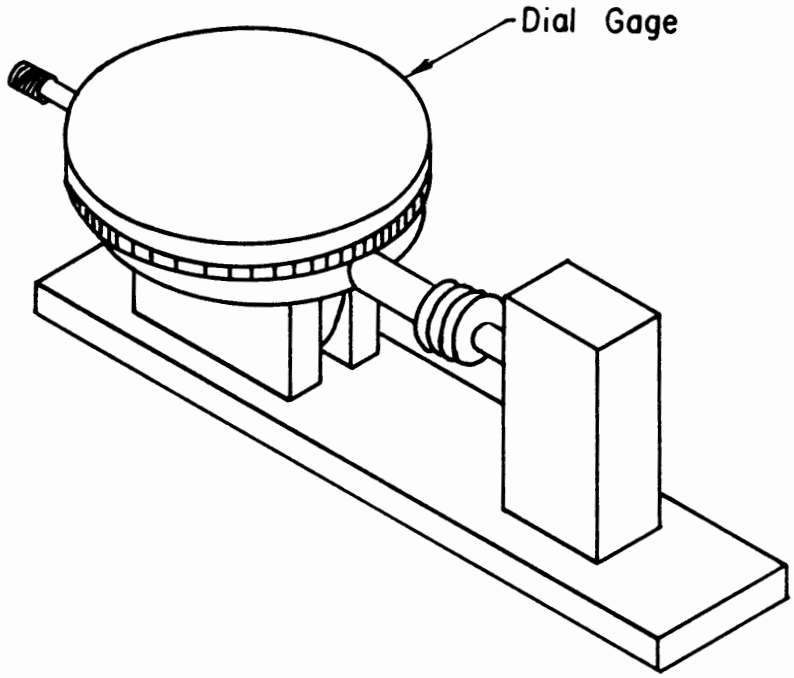

FIG. 2 DIAL GAGE CALIBRATNG DEVICE

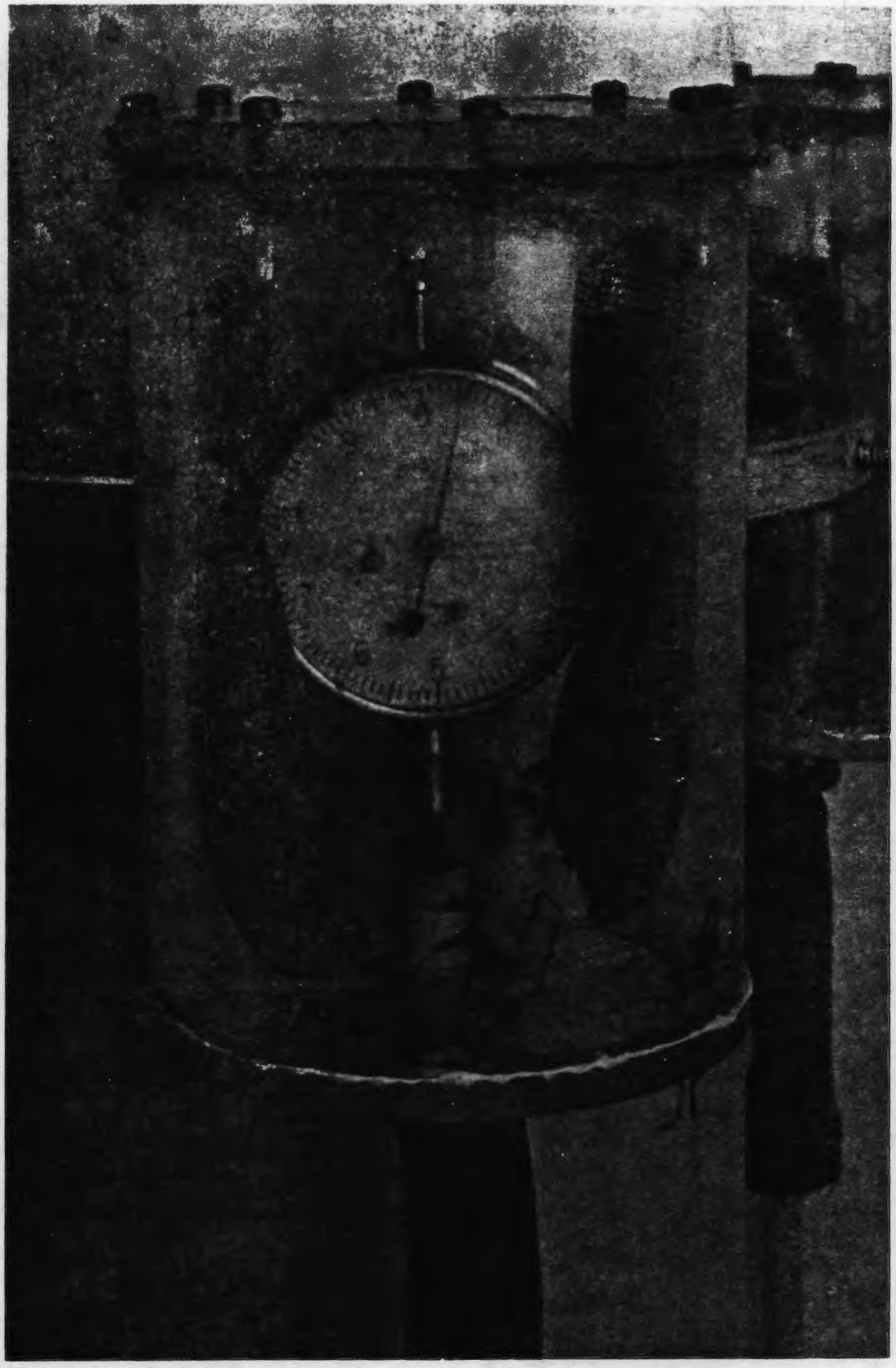

FIG. 3 DIAL GAGE PROTECTIVE PLASTC BOX

a) AT 50 % R.H. b) AT 100 % R.H.

FIG. 4 CONCRETE SPECIMENS WITH DIAL GAGE MEASURING SYSTEM

(a)

FIG. 5 TORSION LOADING FRAME

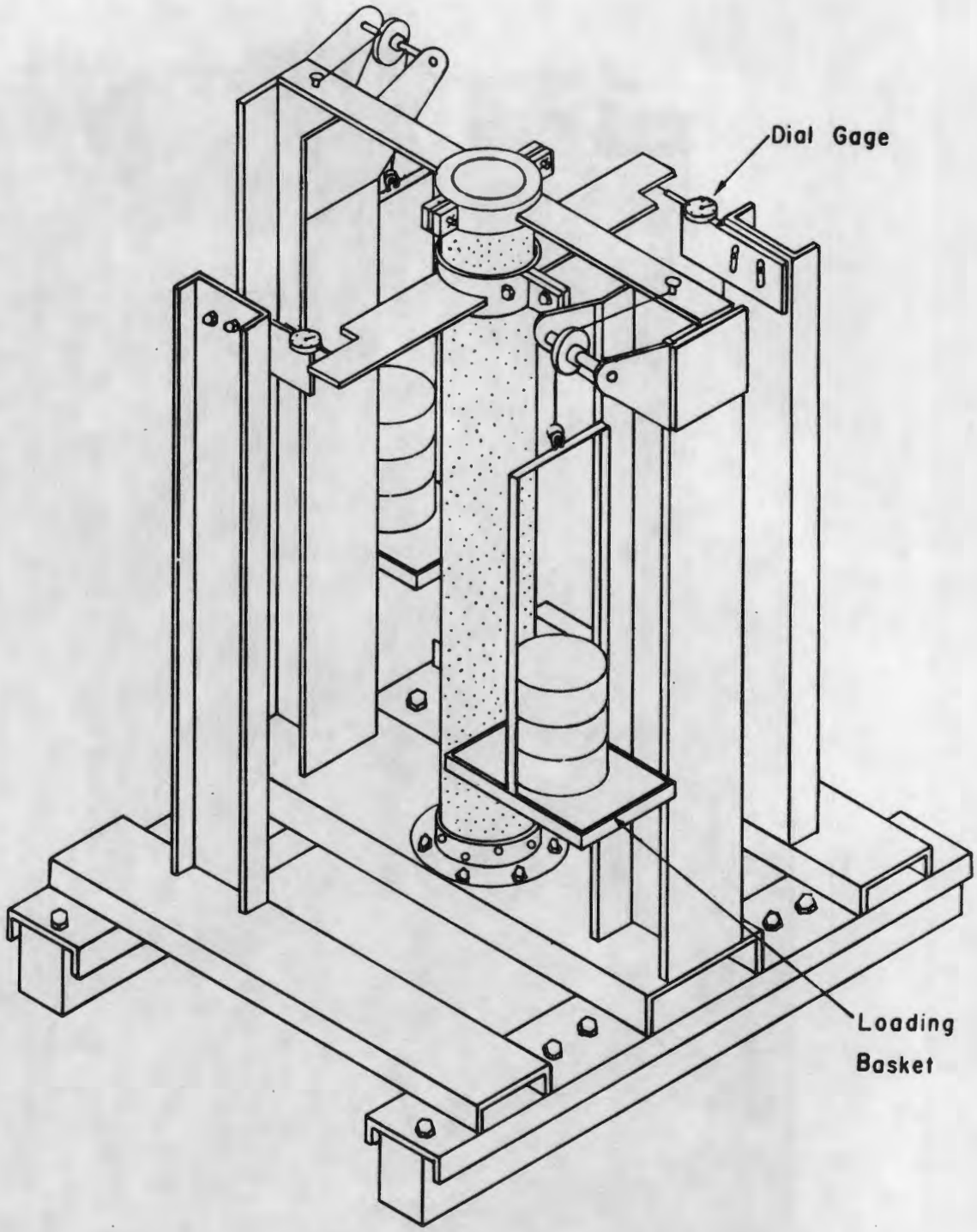

(b)

FIG. 5 (CONTINUED)

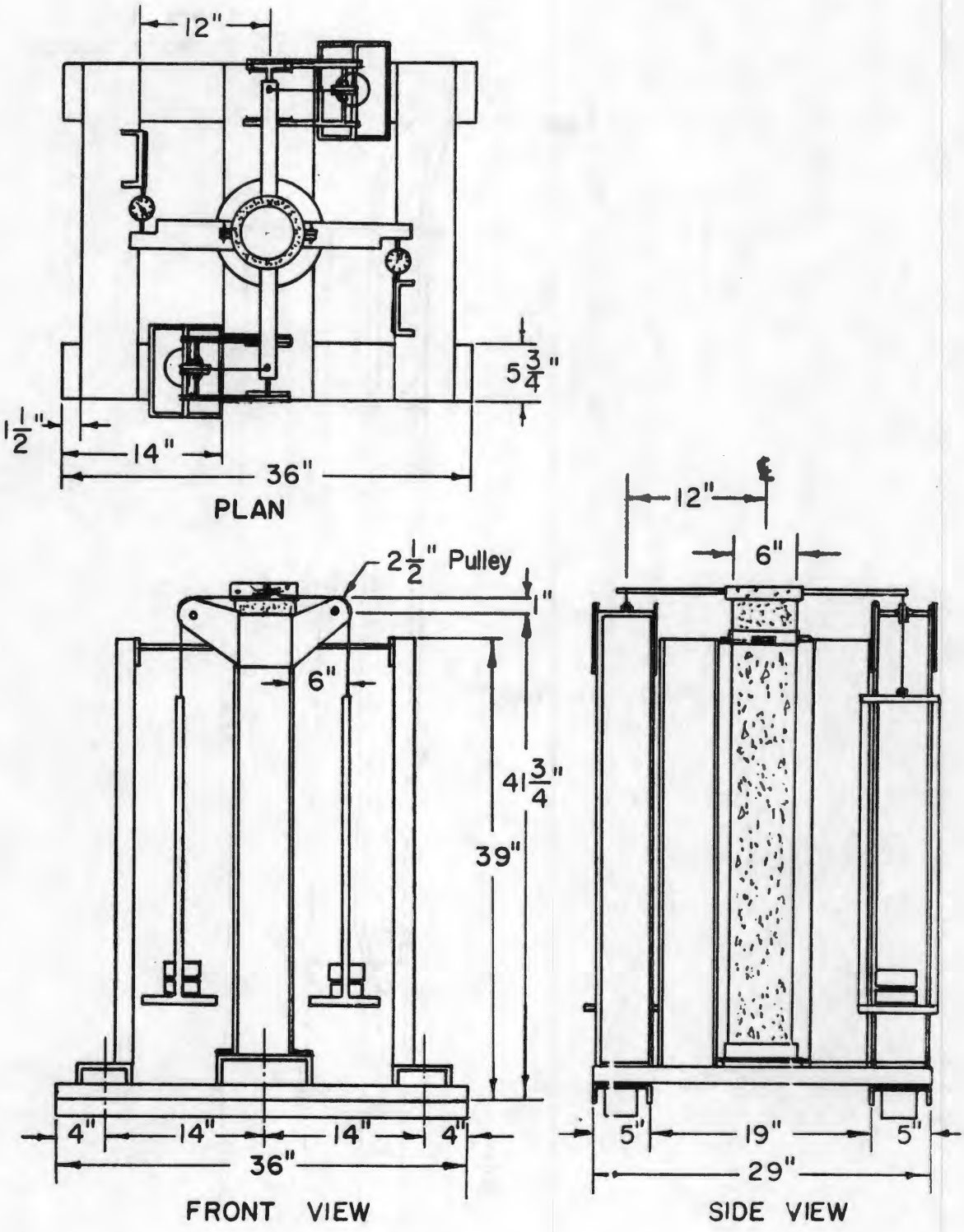

FIG. 6 DETAILS OF TORSION FRAME

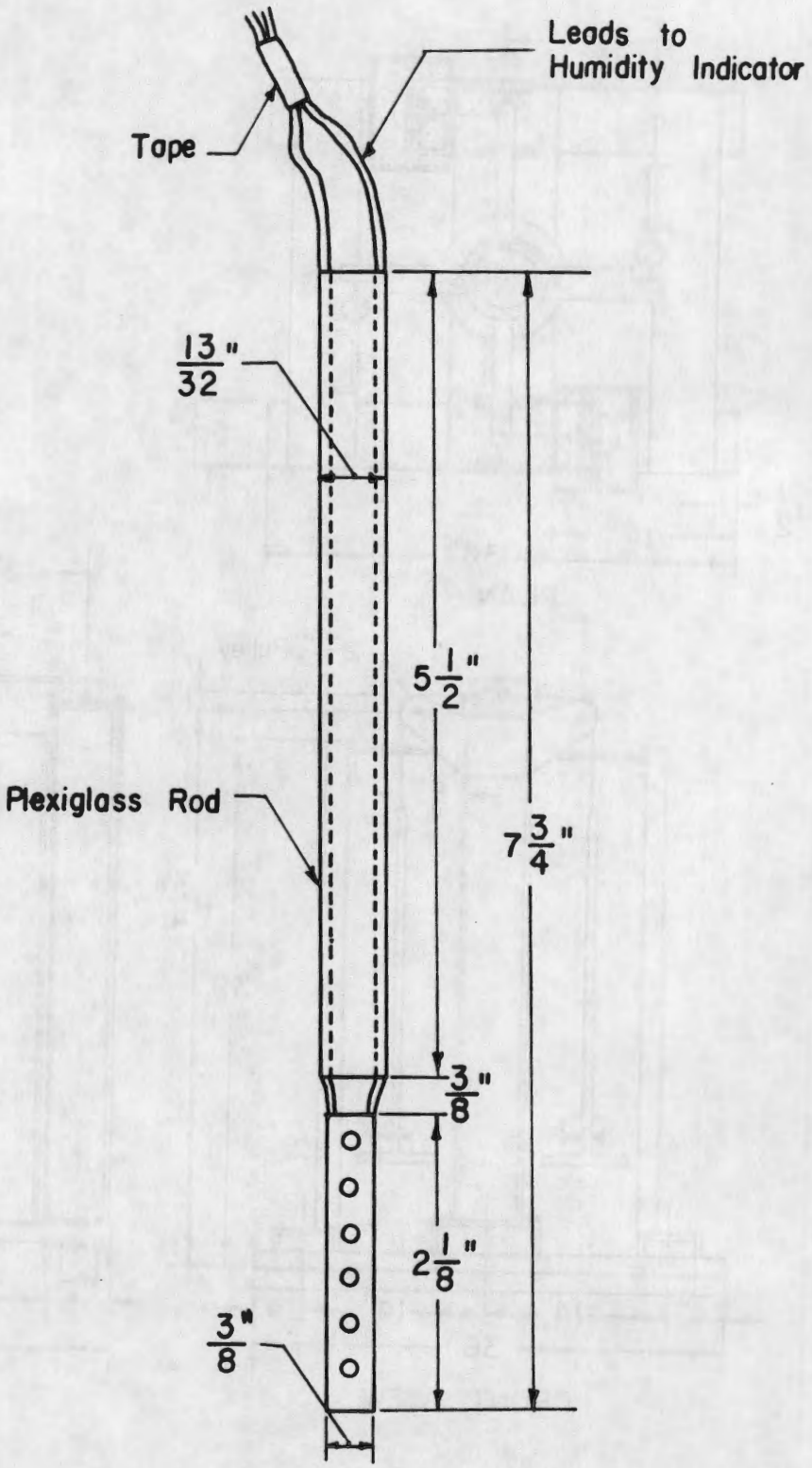

FIG. 7 DETAILS OF RELATIVE HUMIDITY GAGE

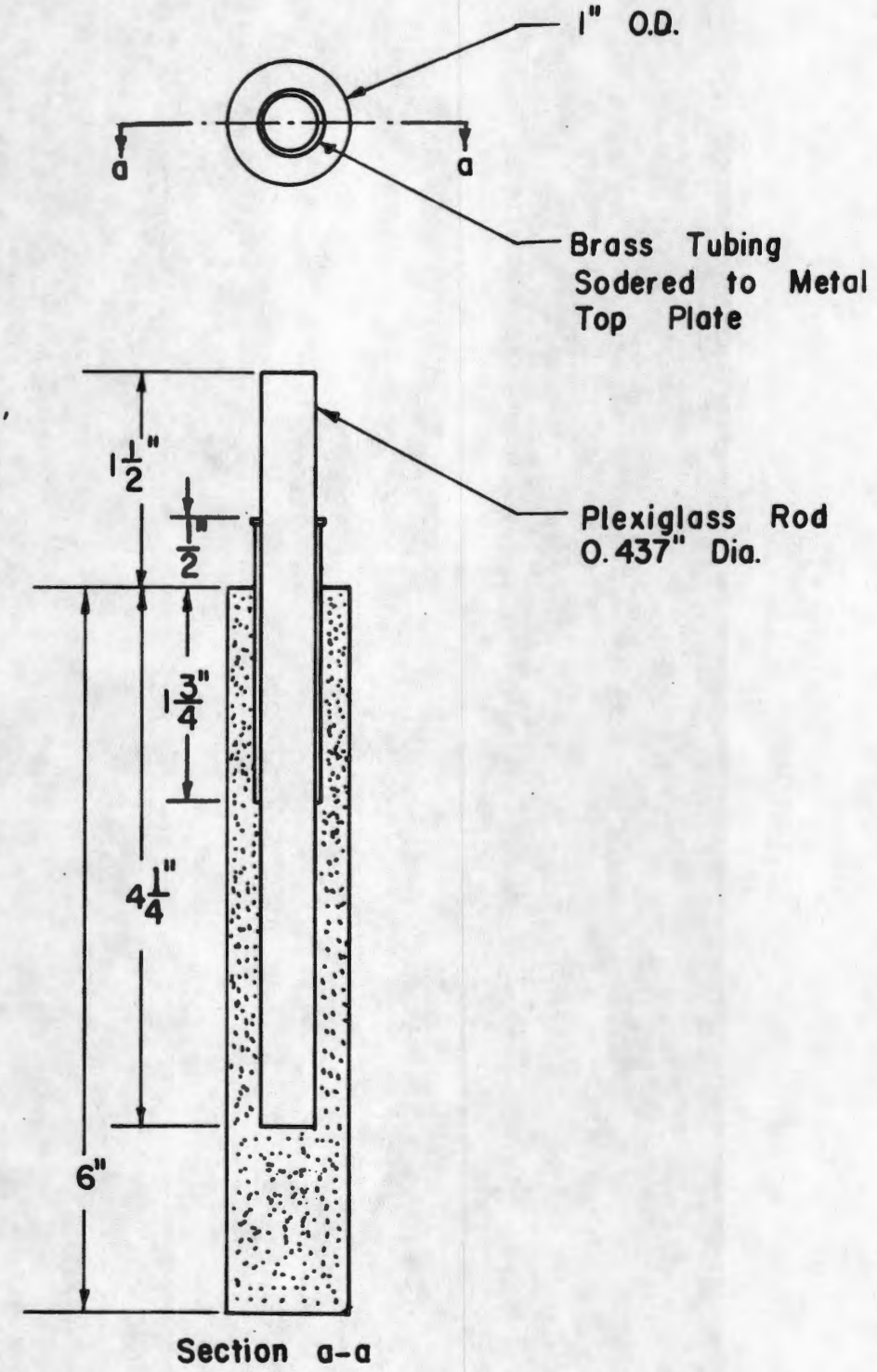

FIG. 8 DETAILS OF SPECIMEN FOR HYGROTHERMIC COEFFICIENT

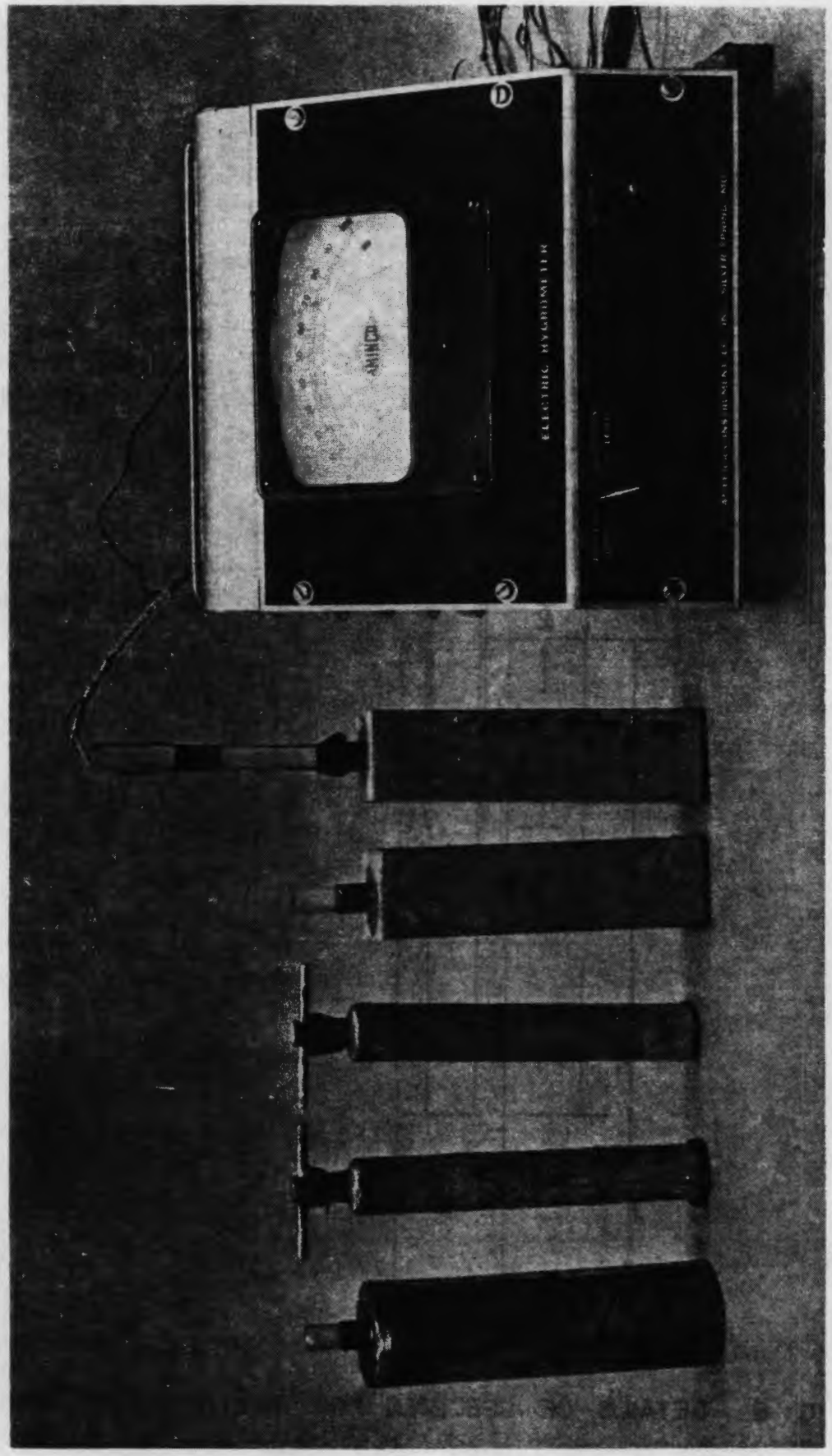

FIG. 9 HYGROTHERMIC COEFFICIENT AND SELF-DESICCATION SPECIMENS

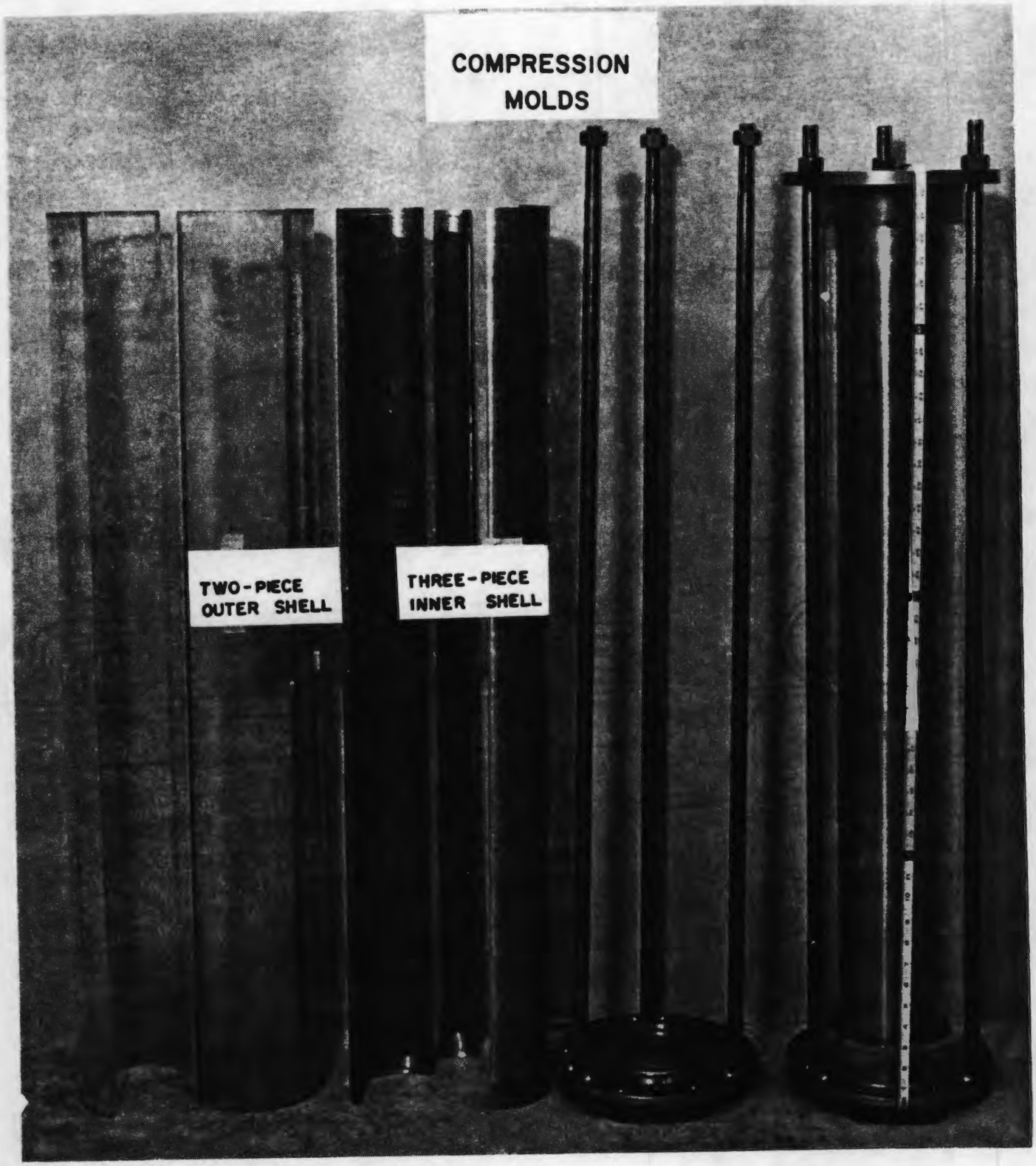

FIG. 10 DETAILS OF CASTING MOLDS

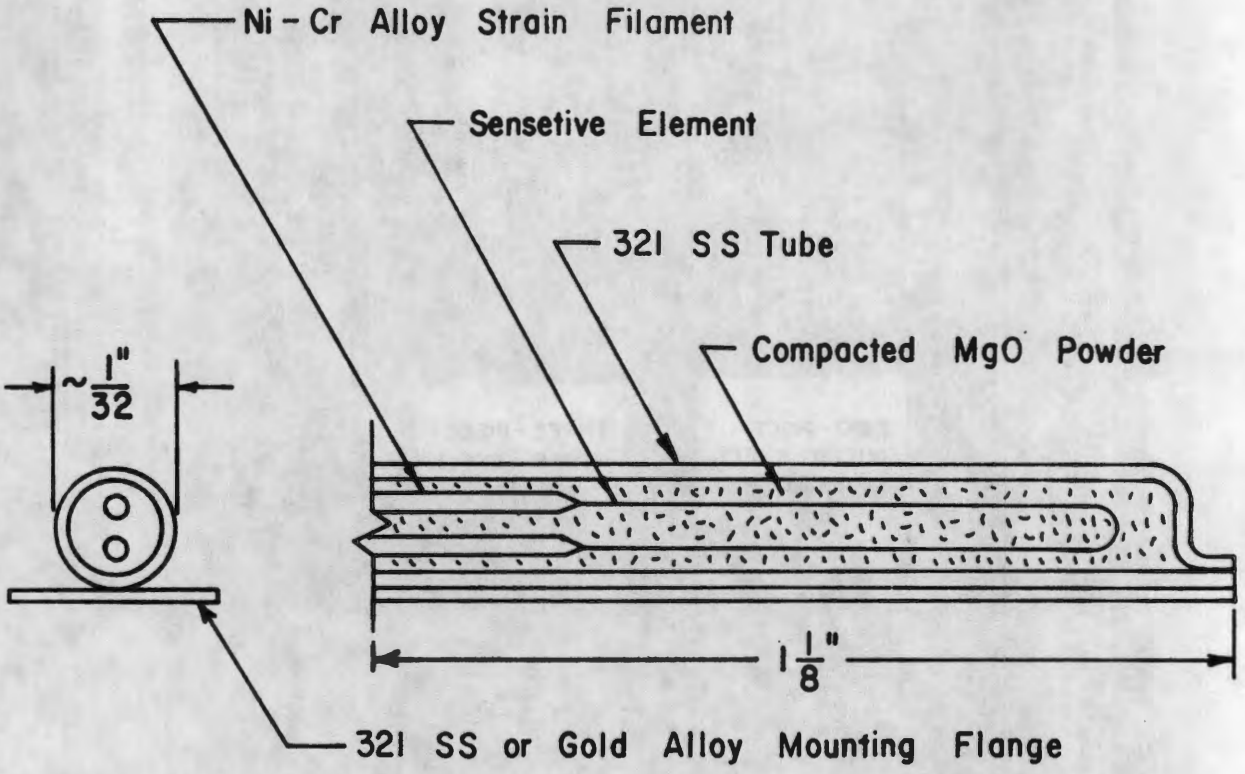

FIG. 11 DETAILS OF MICRODOT STRAIN GAGE (SG 189)

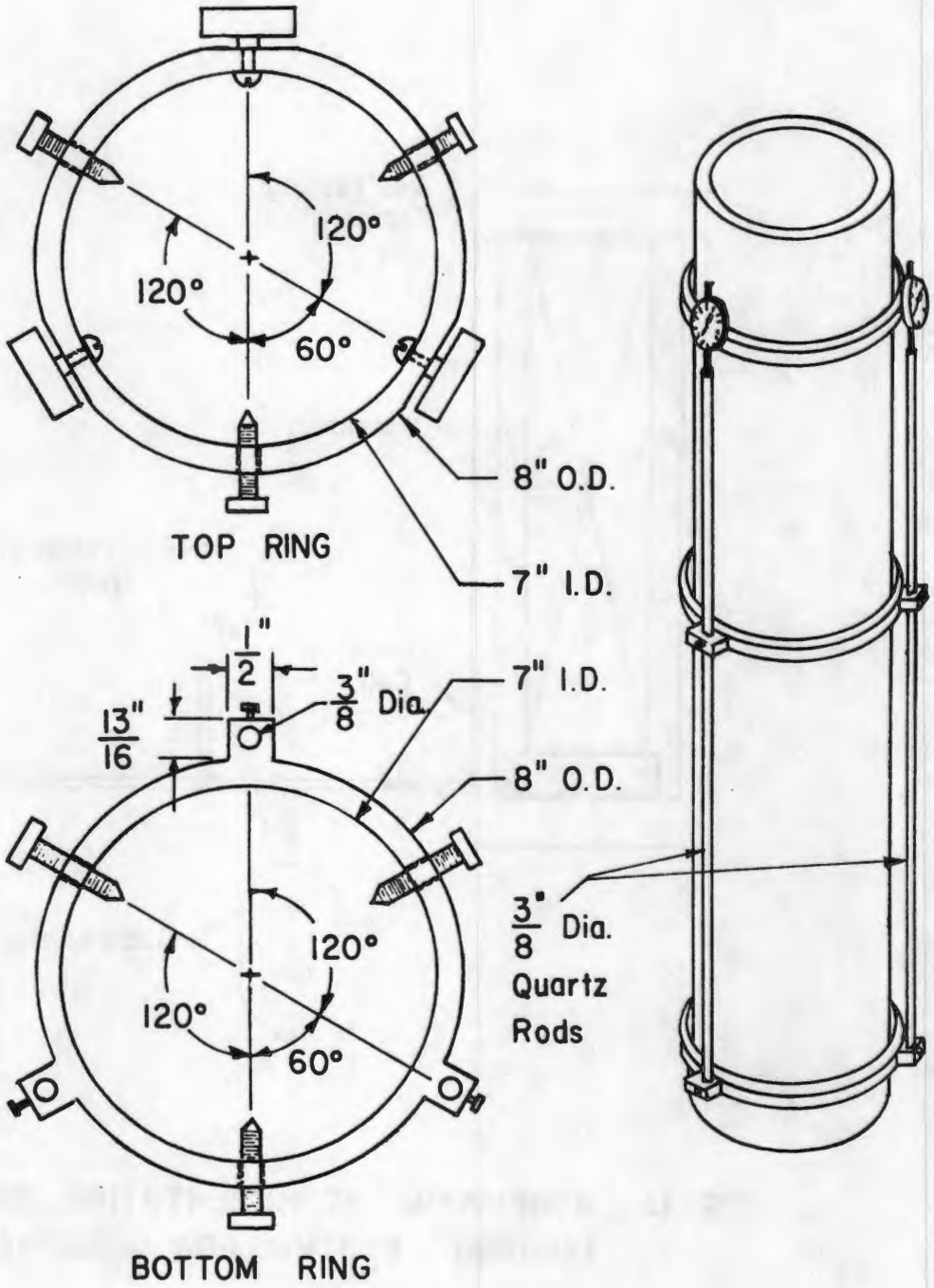

FIG. 12 DETAILS OF MECHANICAL MEASURING SYSTEM FOR COMPRESSION SPECIMEN

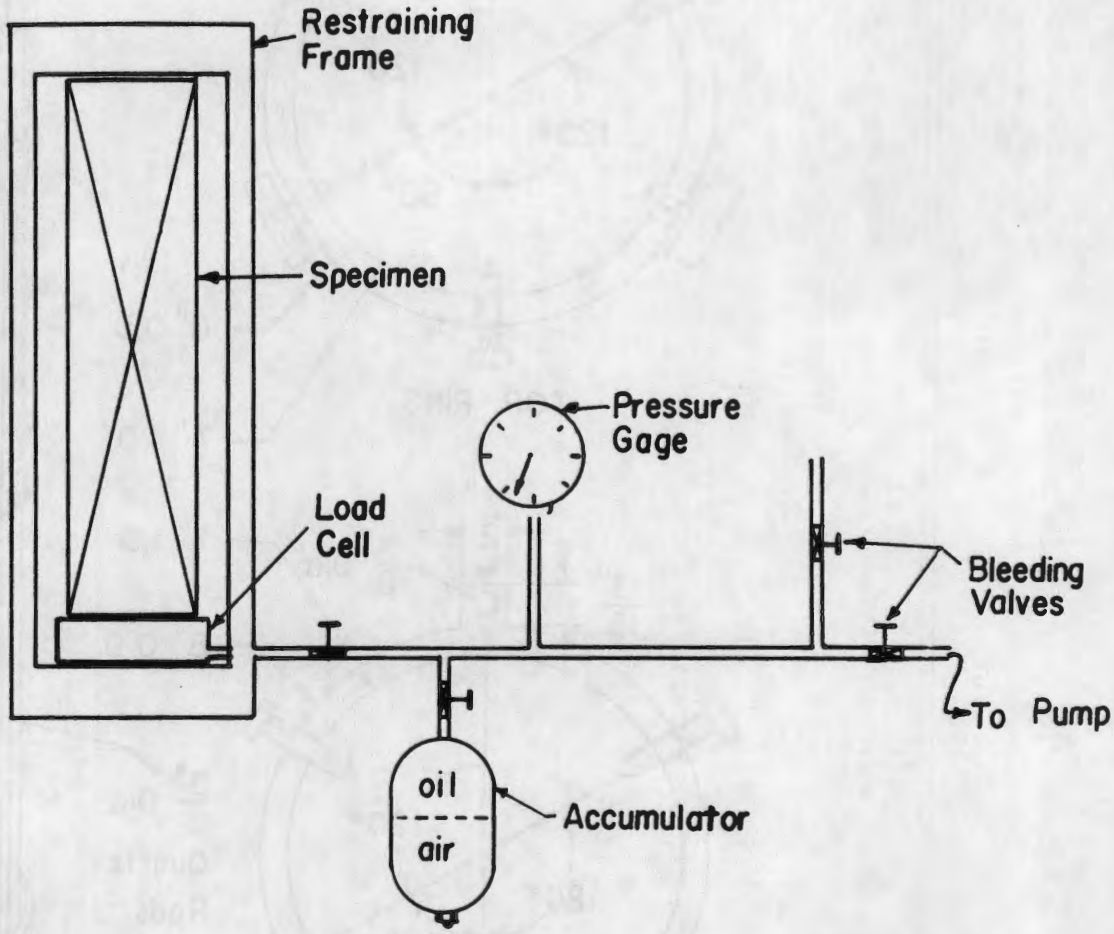

FIG. 13 SCHEMATIC REPRESENTATION OF THE HYDRAULIC LOADING SYSTEM FOR COMPRESSION SPECIMEN

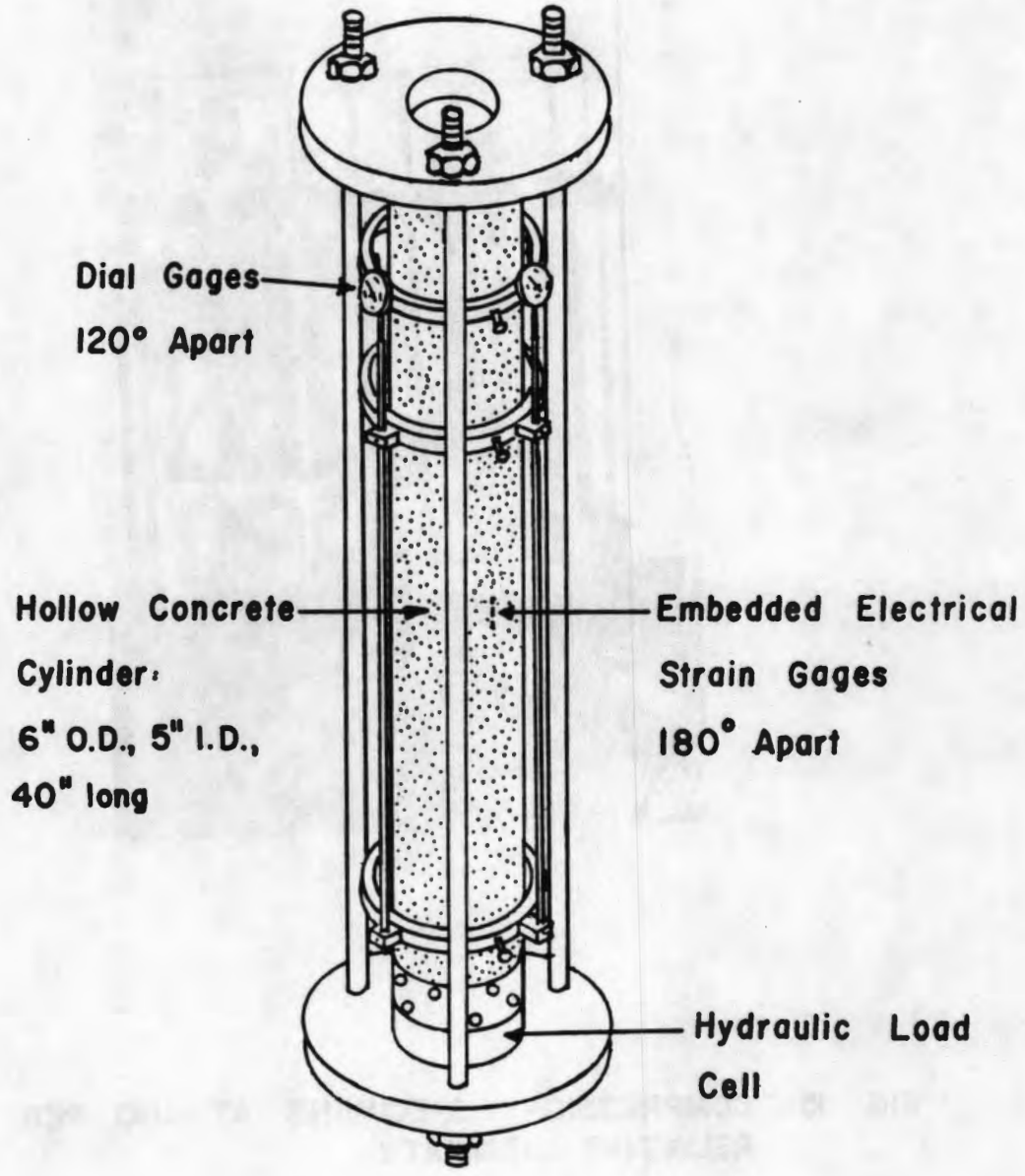

FIG. 14 LOADING FRAME OF COMPRESSION SPECIMEN

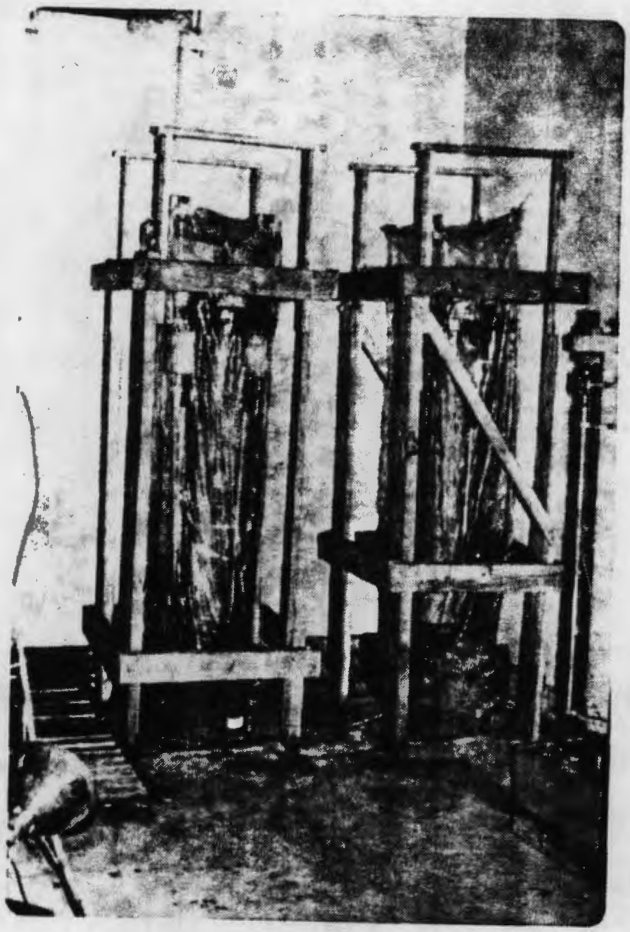

FIG. 15 COMPRESSION SPECIMENS AT 100 PER CENT RELATIVE HUMIDITY

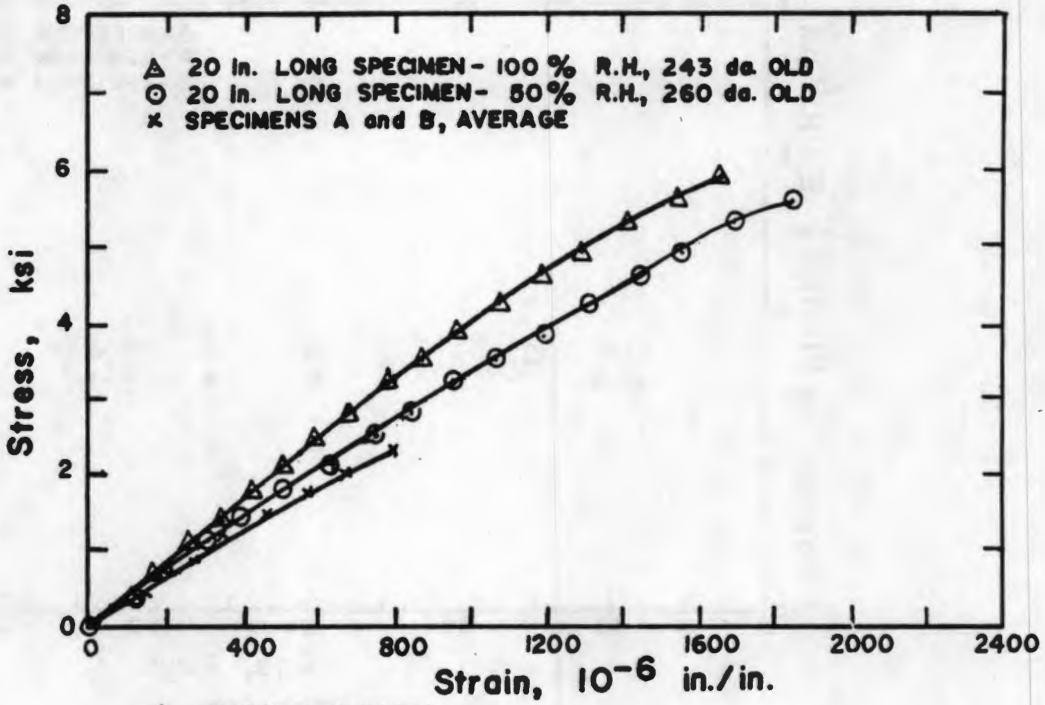

a) COMPRESSION

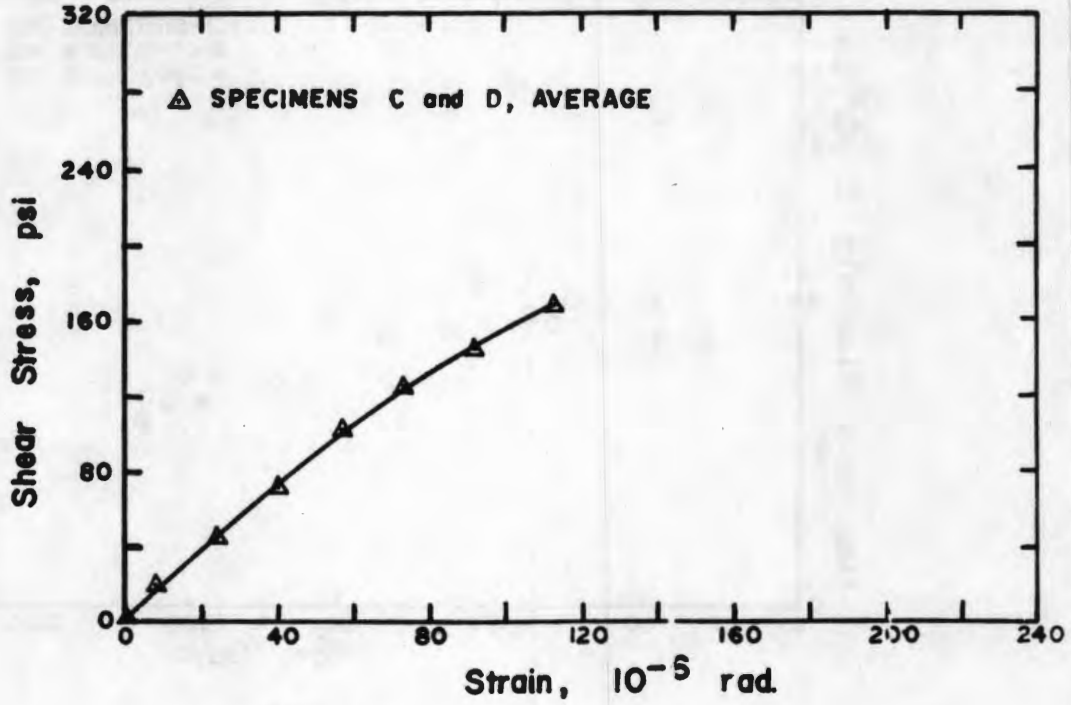

b) TORSION

FIG. 16 STRESS-STRAIN RELATIONSHIP FOR 21-DAY OLD CONCRETE SPECIMENS

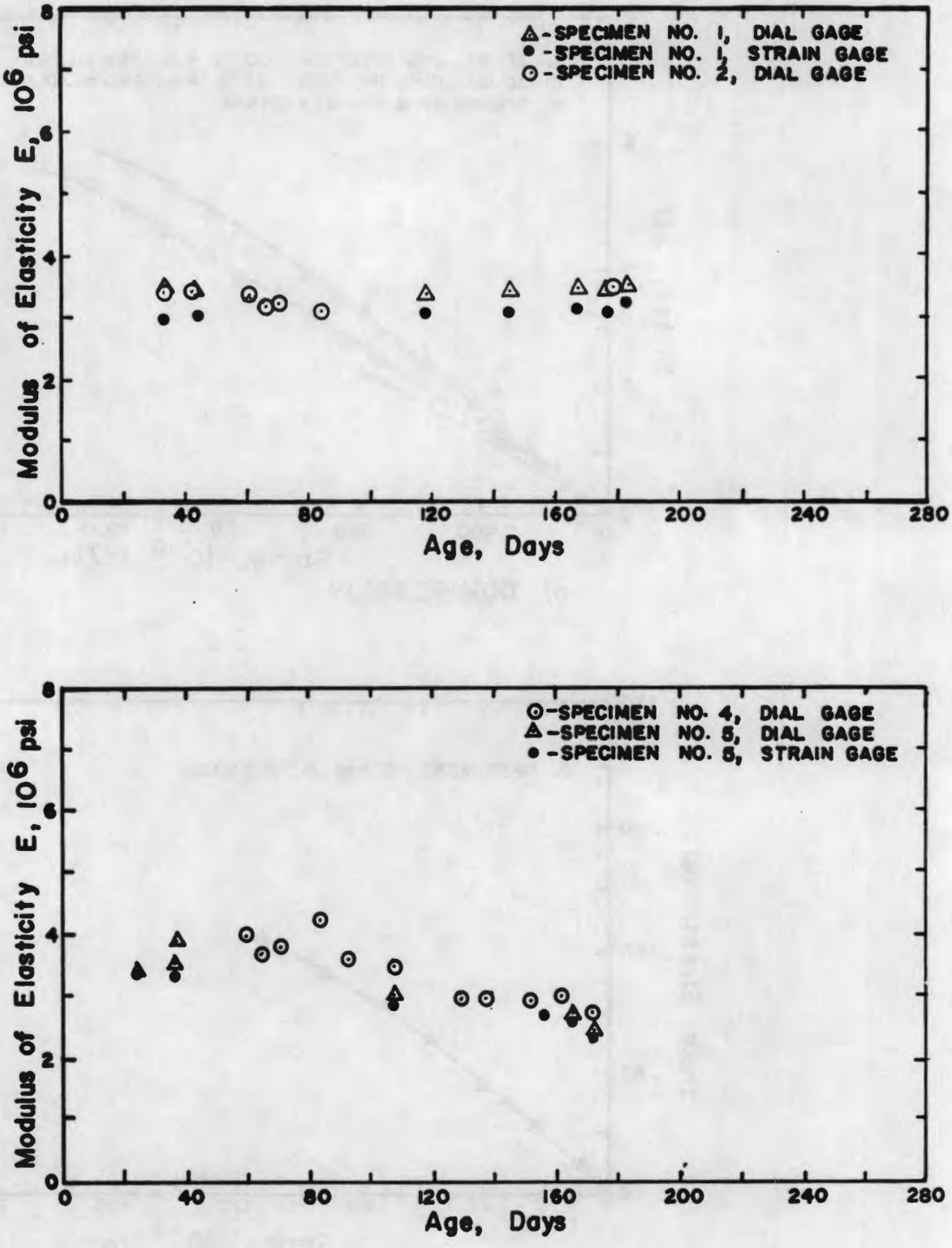

FIG. 17 MODULUS OF ELASTICITY-TIME RELATIONSHIP FOR COMPRESSION SPECIMENS AT SUSTAINED TEMPERATURES

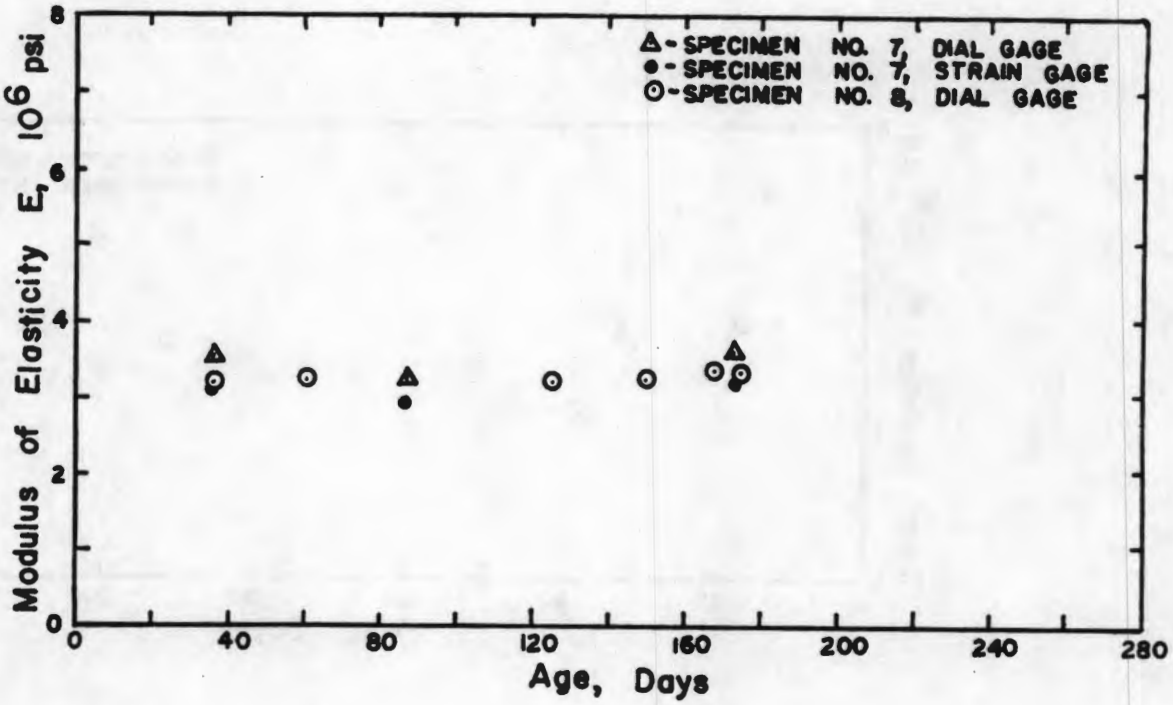

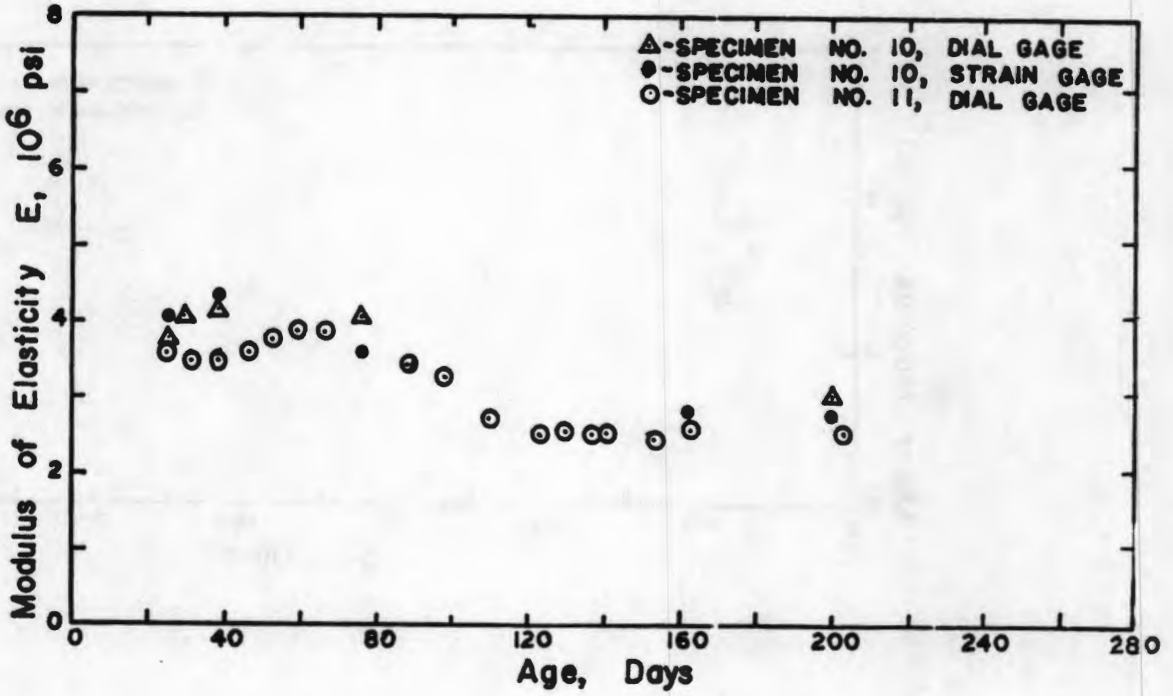

FIG. 18 MODULUS OF ELASTICITY-TIME RELATIONSHIP FOR COMPRESSION SPECIMENS AT CYCLIC TEMPERATURE

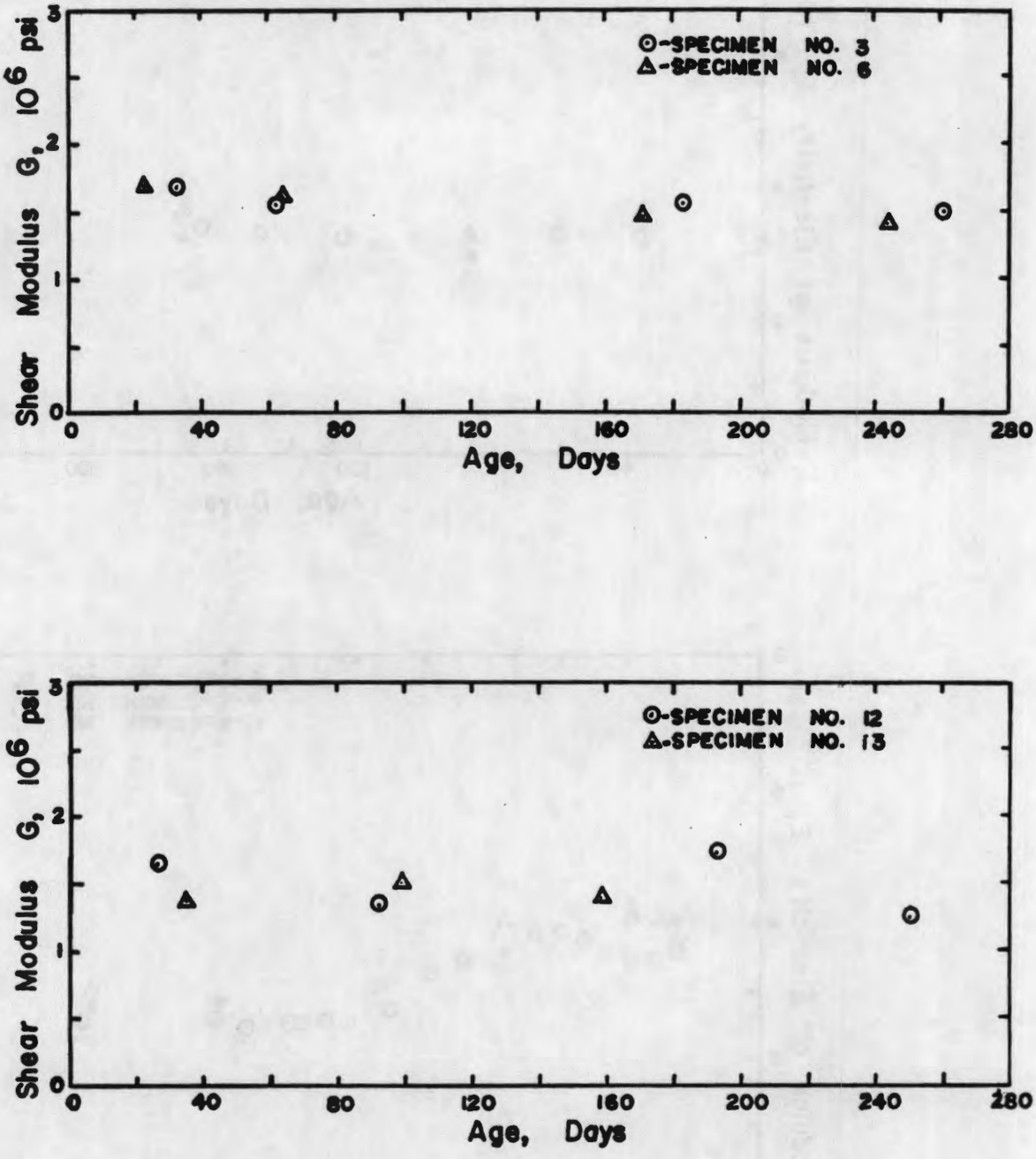

FIG. 19 SHEAR MODULUS OF ELASTICITY-TIME RELATIONSHIP FOR CONCRETE SPECIMENS

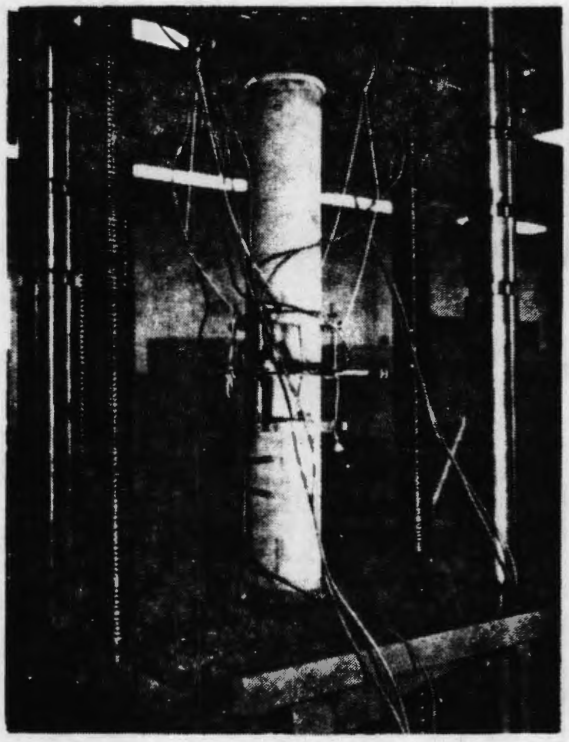

FIG. 20 COMPRESSION TEST OF HOLLOW CYLNDRICAL SPECIMEN

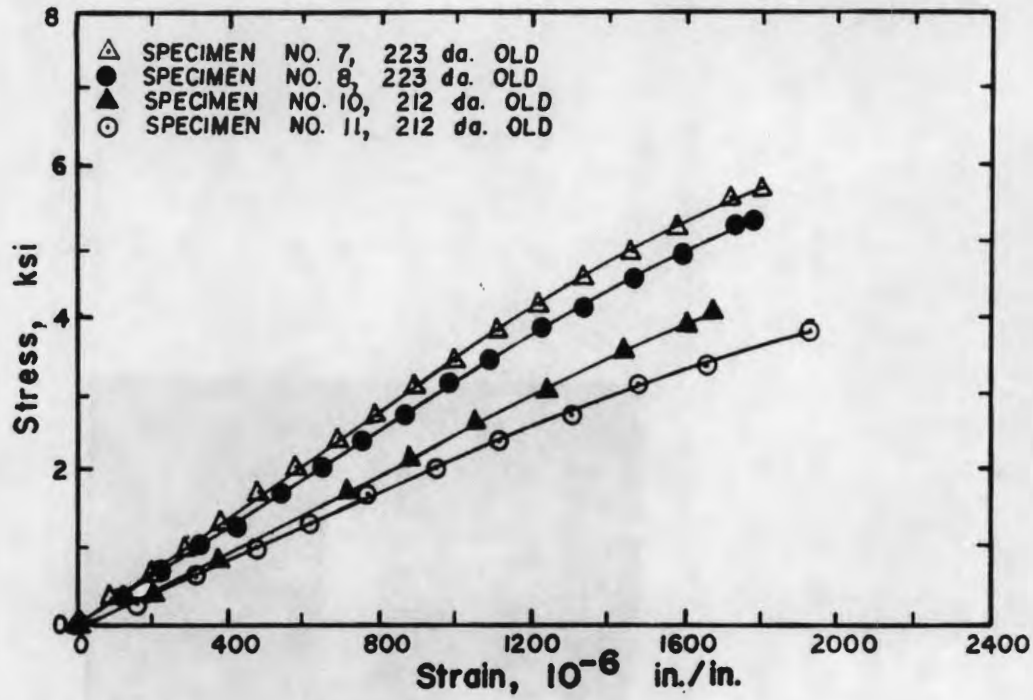

a) CYCLIC TEMPERATURE

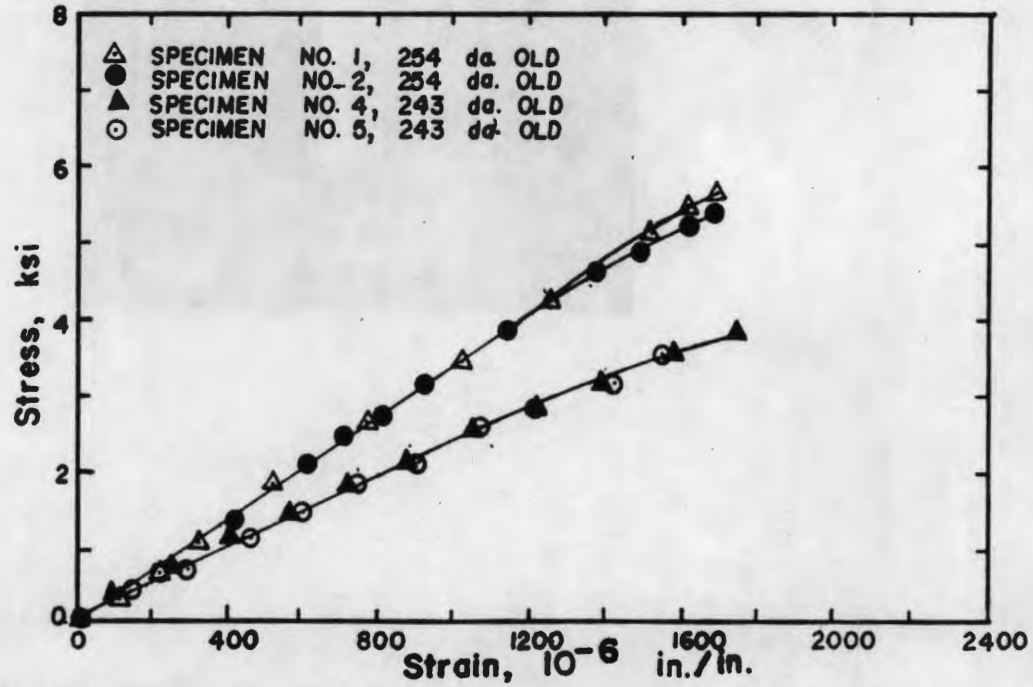

b) SUSTAINED TEMPERATURE

FIG. 21 STRESS-STRAIN DIAGRAMS FOR CONCRETE SPECIMENS IN COMPRESSION

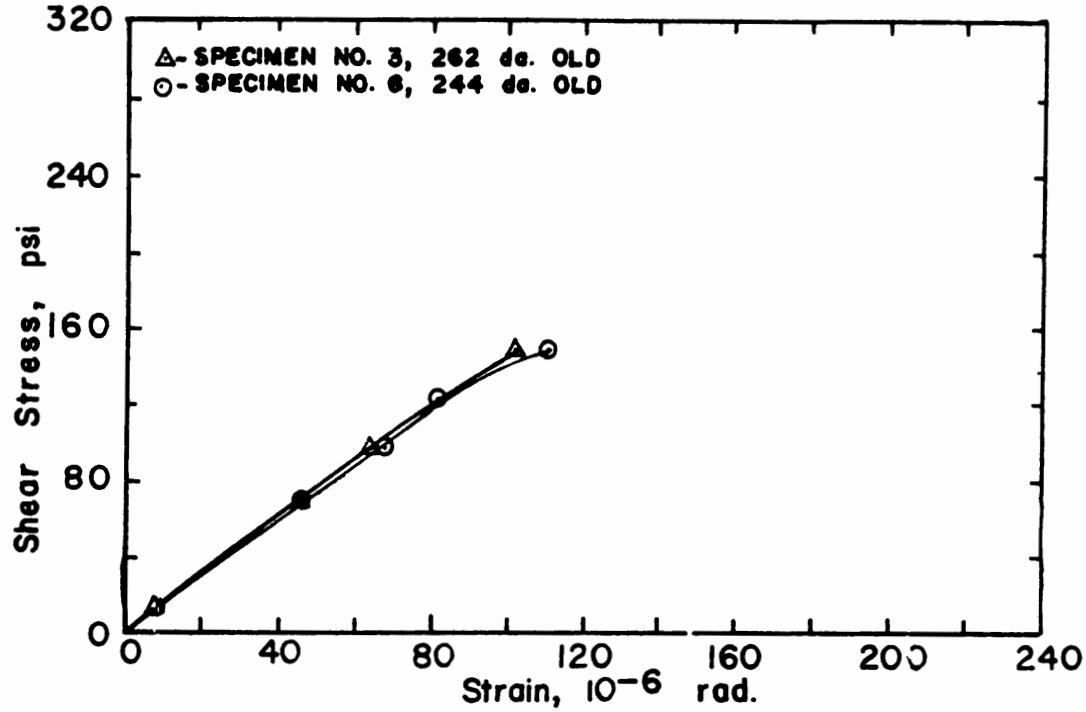

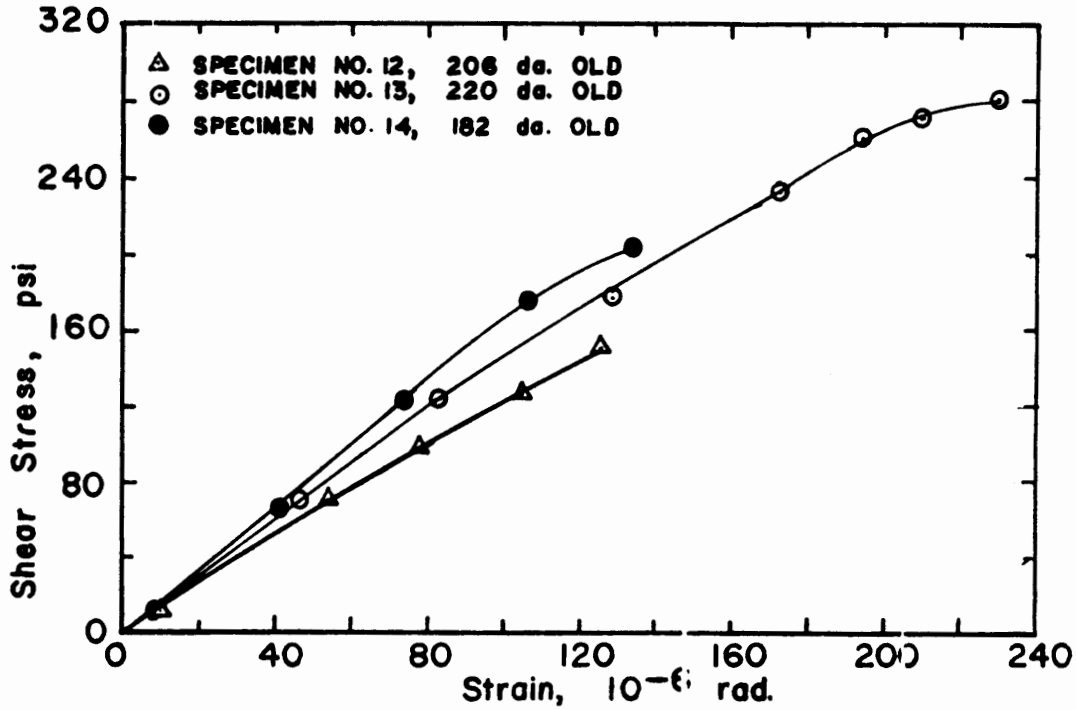

FIG. 22 STRESS STRAIN RELATIONSHIP FOR CONCRETE SPECIMENS IN TORSION

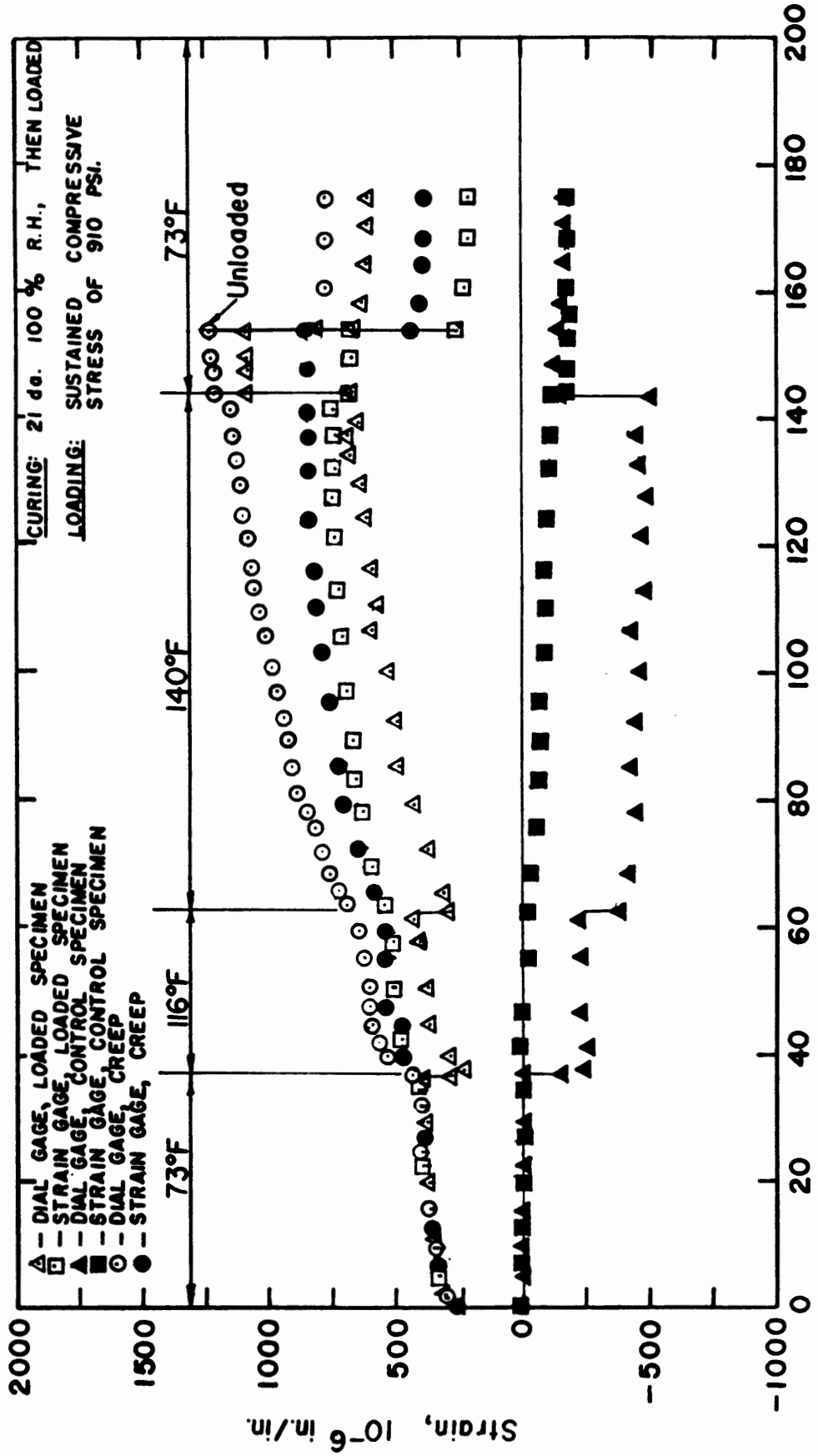

FIG. 23 EFFECT OF 140°F TEMPERATURE AT 100 PER CENT RELATIVE HUMIDITY ON CREEP IN COMPRESSION

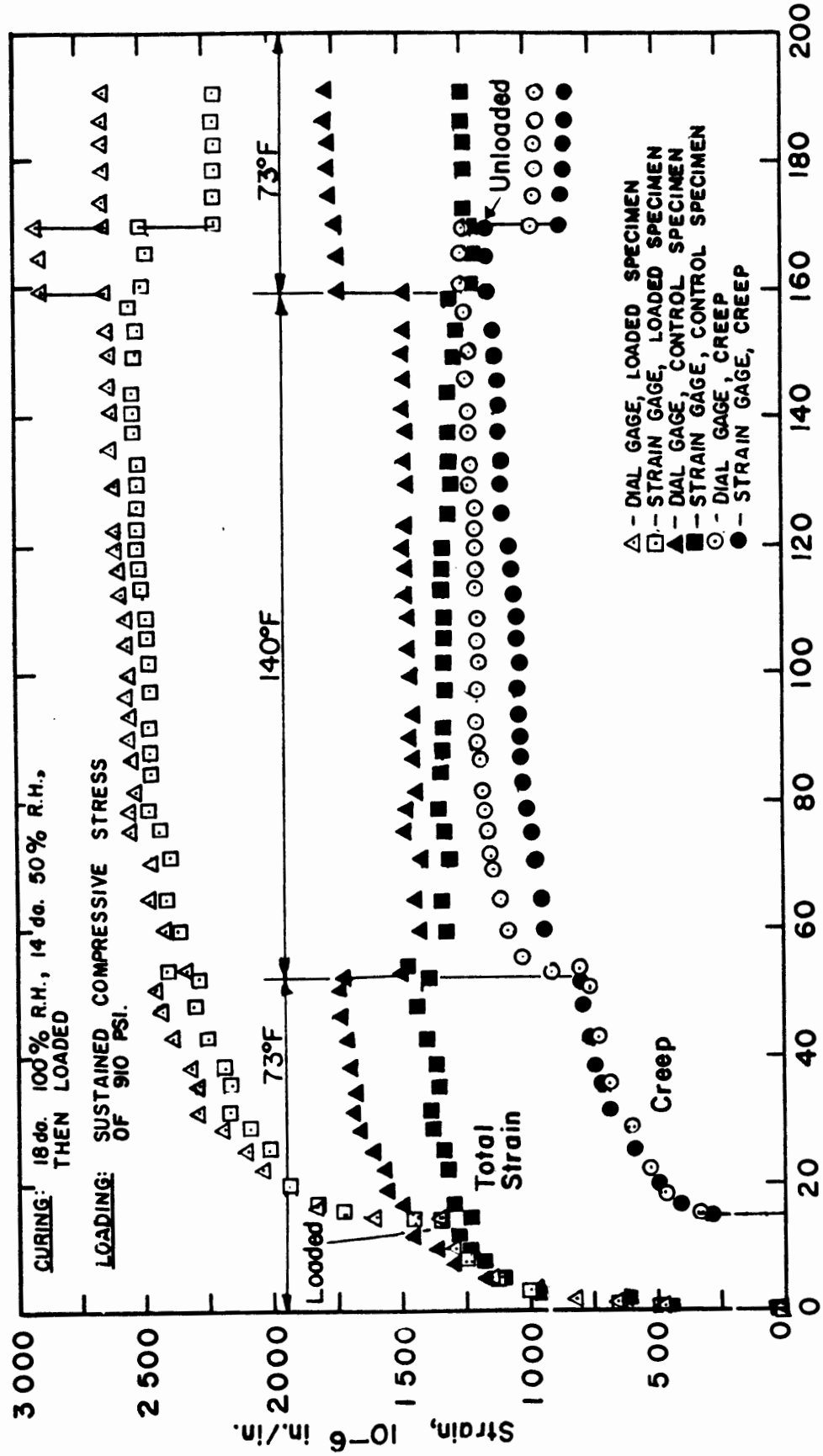

FIG. 24 EFFECT OF 140° F TEMPERATURE AT 50 PER CENT RELATIVE HUMIDITY ON CREEP IN COMPRESSION

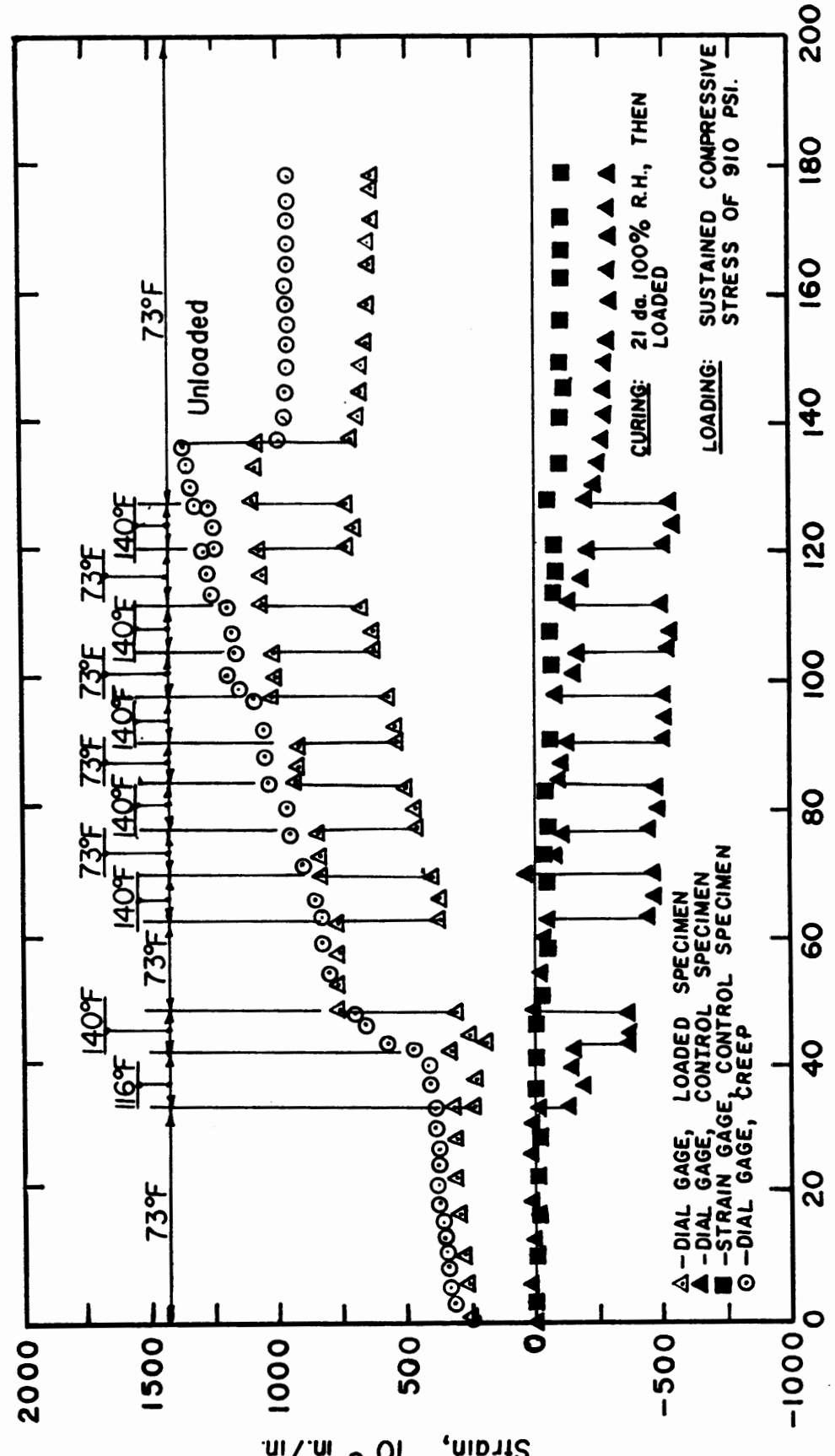

FIG. 25 EFFECT OF CYCLIC TEMPERATURE AT 100 PER CENT RELATIVE HUMIDITY ON CREEP IN COMPRESSION

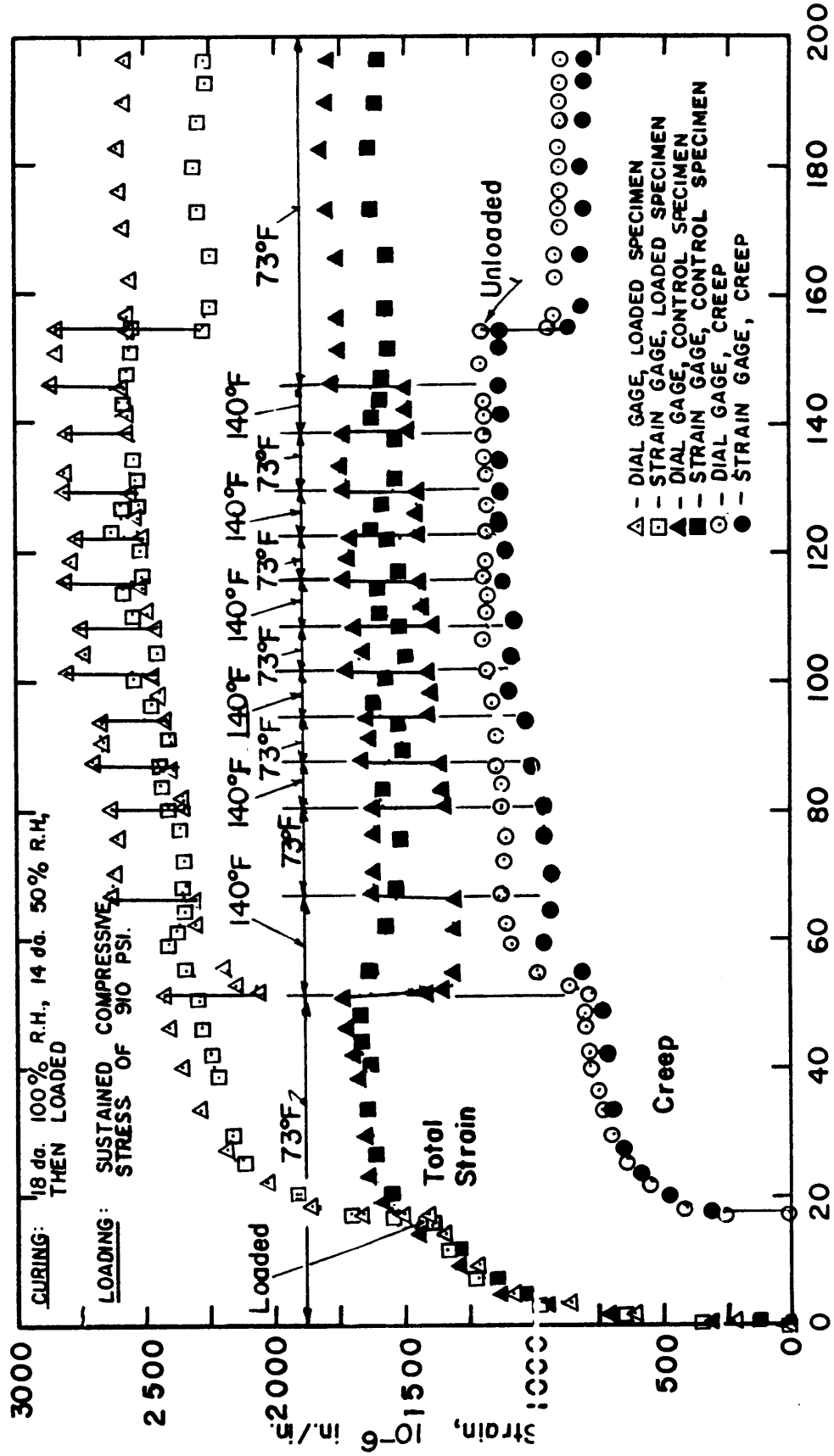

FIG. 26 EFFECT OF CYCLIC TEMPERATURE AT 50 PER CENT RELATIVE HUMIDITY ON CREEP IN COMPRESSION

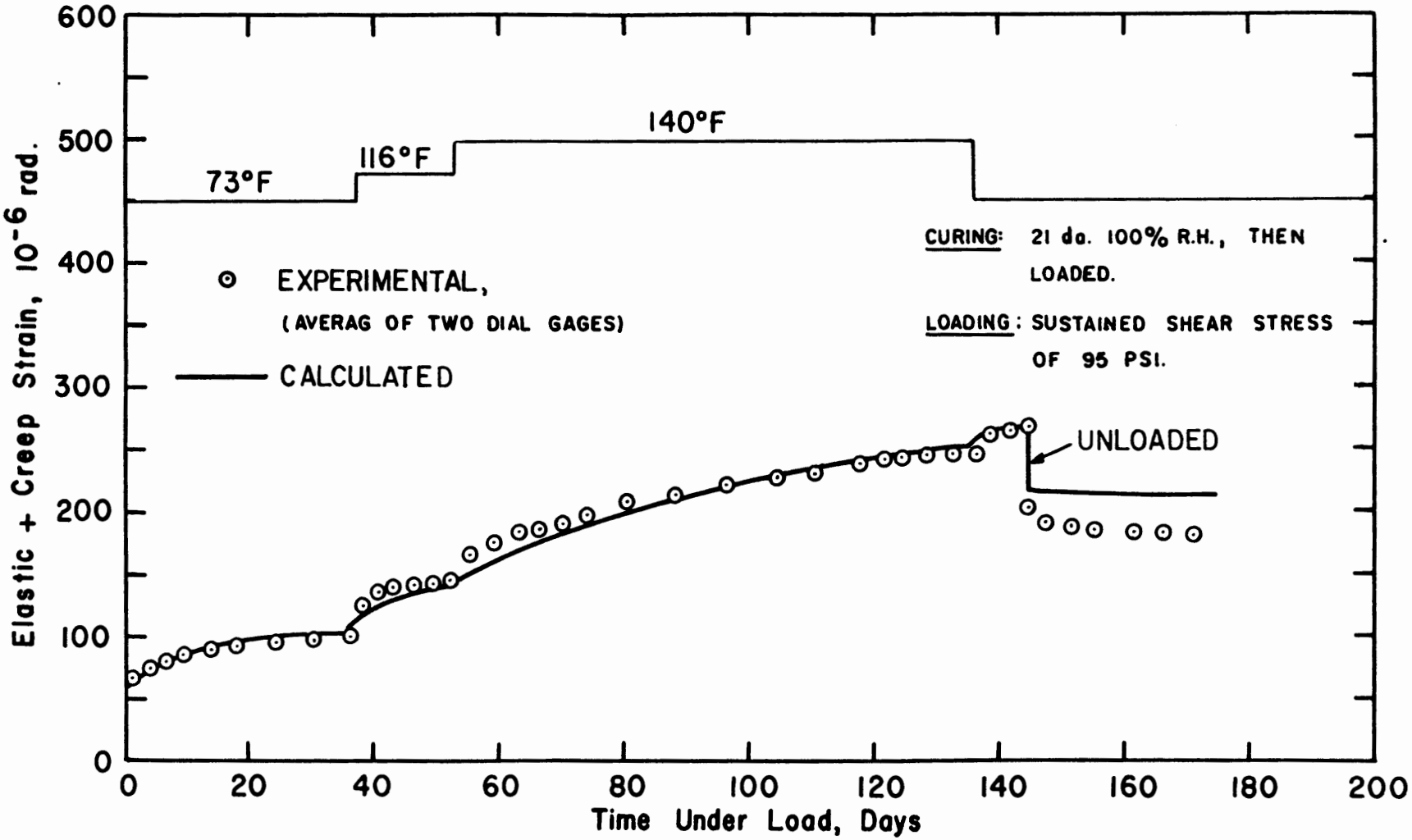

FIG. 27 COMPARISON OF CALCULATED AND EXPERIMENTAL CREEP IN TORSION AT SUSTAINED TEMPERATURES AND 100 PERCENT RELATIVE HUMIDITY

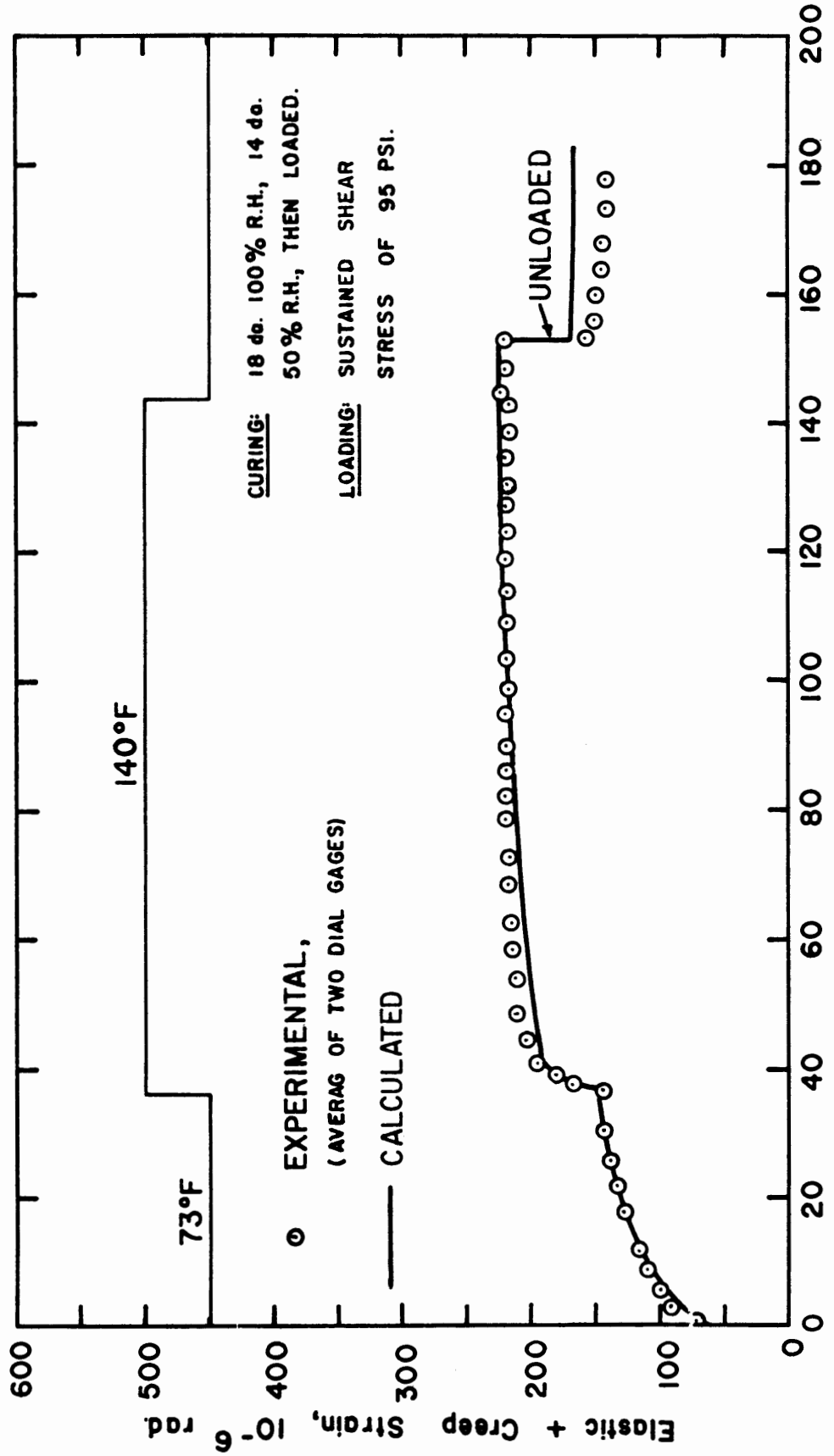

FIG. 28 COMPARISON OF CALCULATED AND EXPERIMENTAL CREEP IN TORSION AT SUSTAINED TEMPERATURES AND 50 PERCENT RELATIVE HUMIDITY

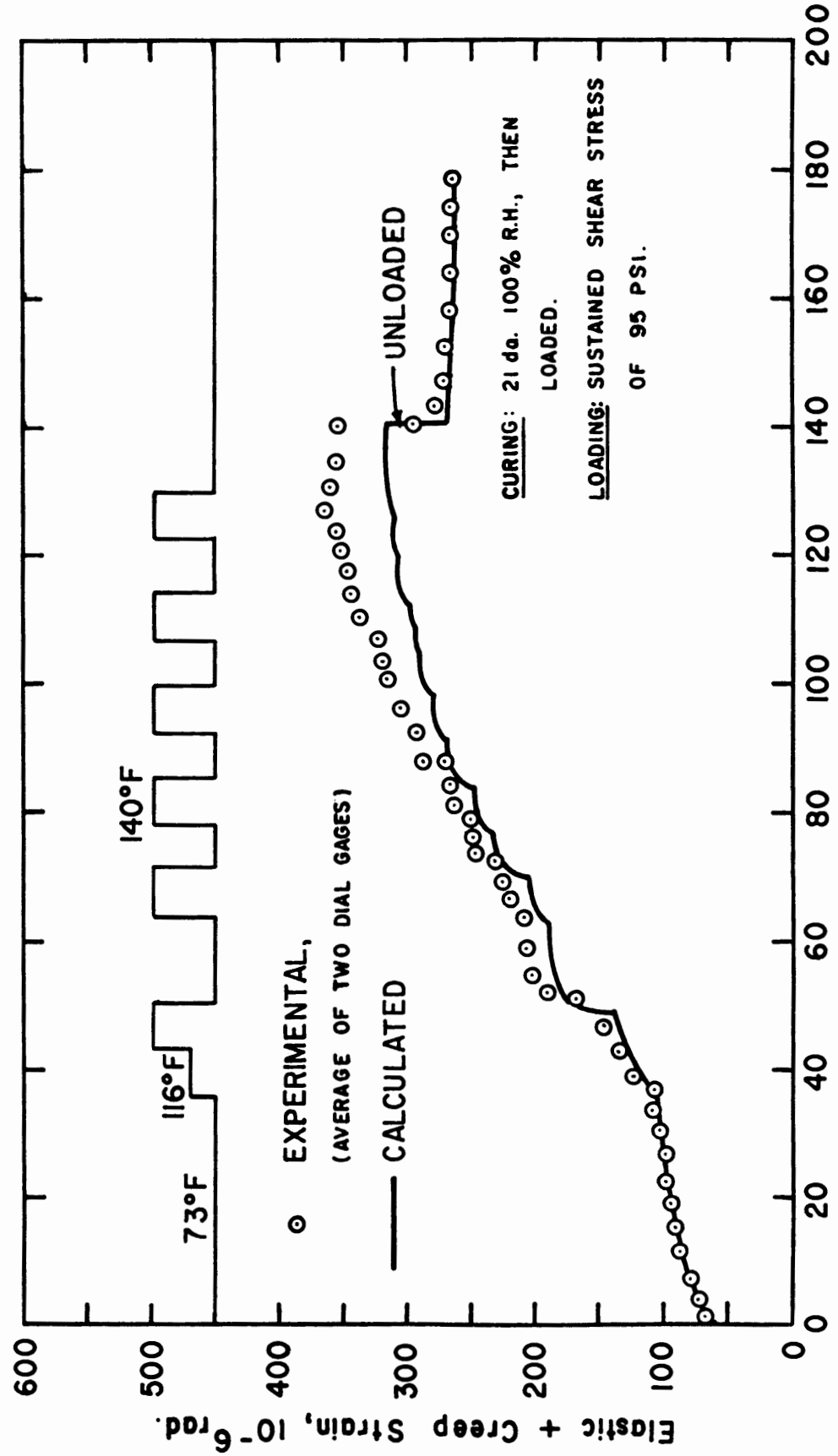

FIG. 29 COMPARISON OF CALCULATED AND EXPERIMENTAL CREEP IN TORSION AT CYCLIC TEMPERATURE AND 100 PERCENT RELATIVE HUMIDITY

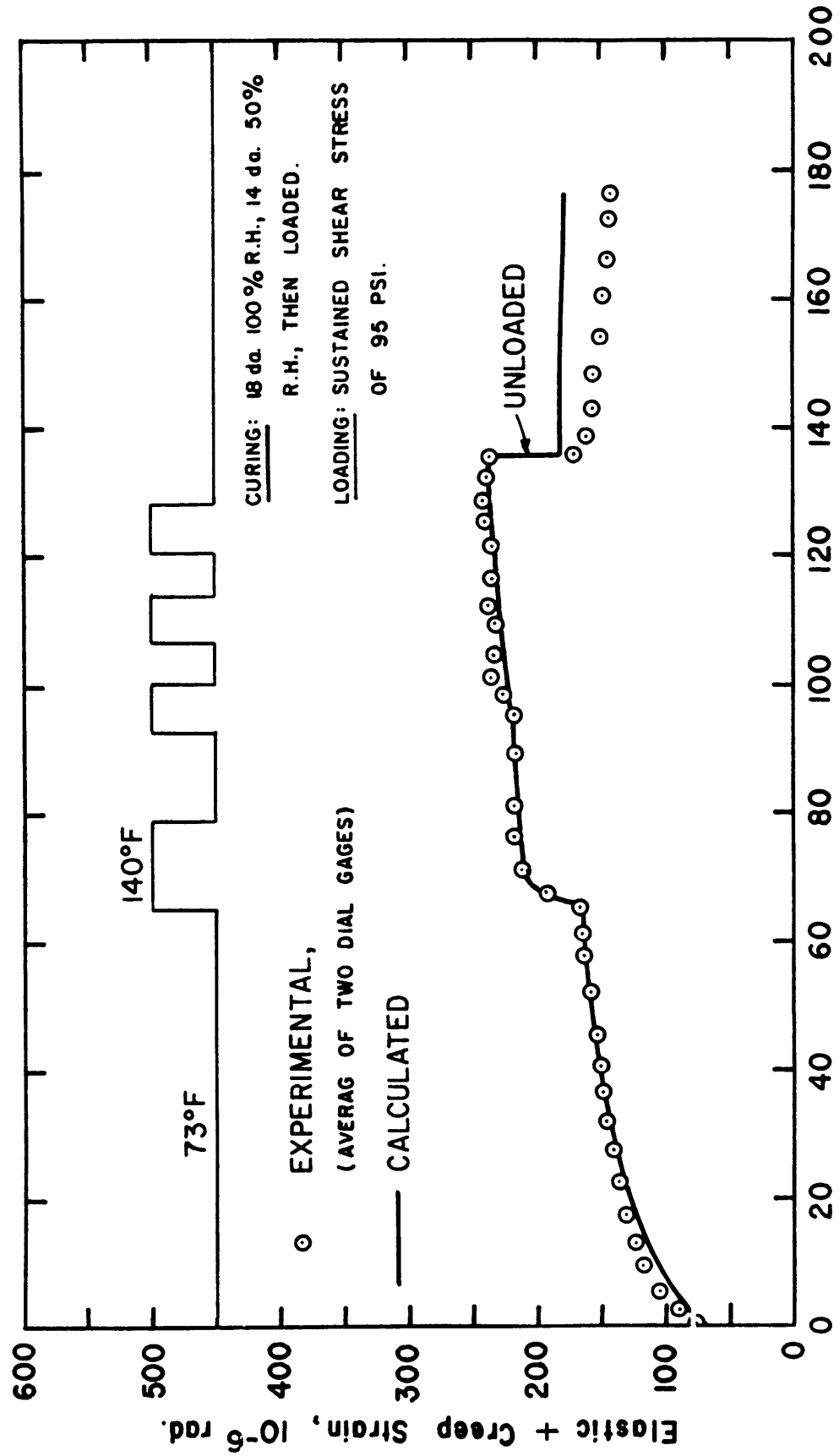

FIG. 30 COMPARISON OF CALCULATED AND EXPERIMENTAL CREEP IN TORSION AT CYCLIC TEMPERATURE AND 50 PERCENT RELATIVE HUMIDITY

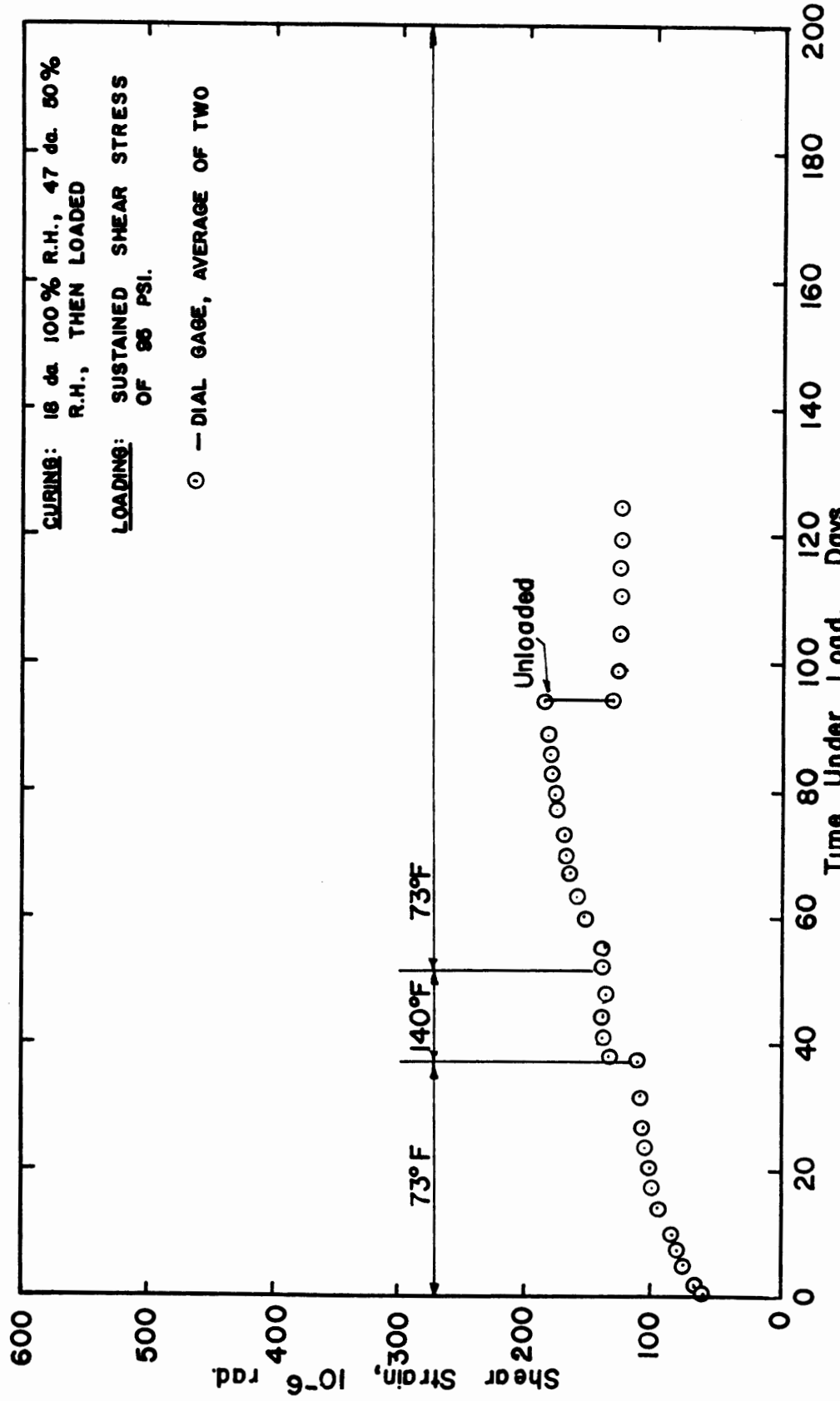

FIG. 31 EFFECT OF CYCLIC TEMPERATURE AT 50 PER CENT RELATIVE HUMIDITY ON CREEP IN TORSION

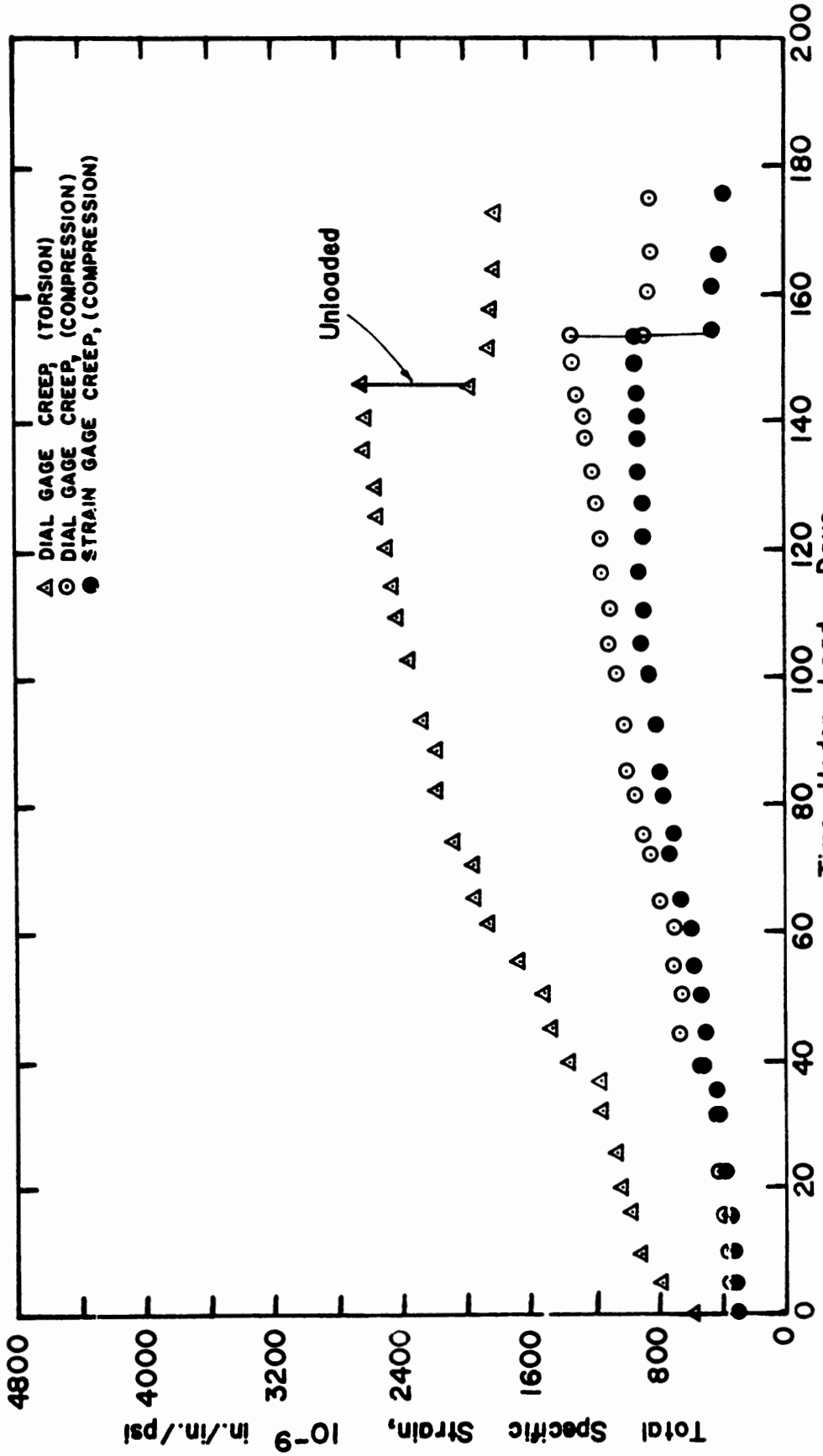

FIG. 32 EFFECT OF 140°F TEMPERATURE AT 100 PER CENT RELATIVE HUMIDITY ON SPECIFIC CREEP OF CONCRETE IN COMPRESSION AND TORSION

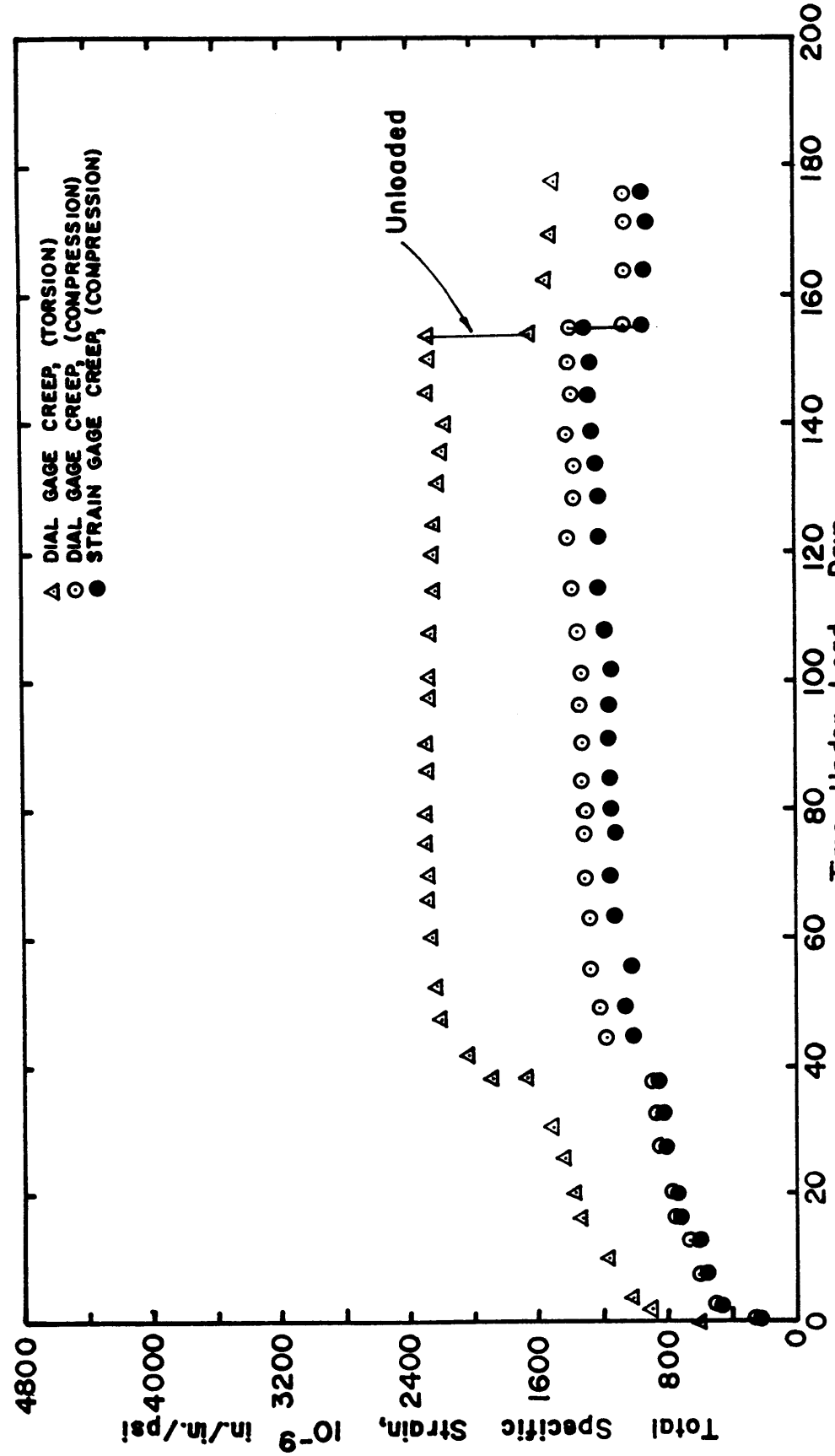

FIG. 33 EFFECT OF 140°F TEMPERATURE AT 50 PER CENT RELATIVE HUMIDITY ON SPECIFIC CREEP OF CONCRETE IN COMPRESSION AND TORSION

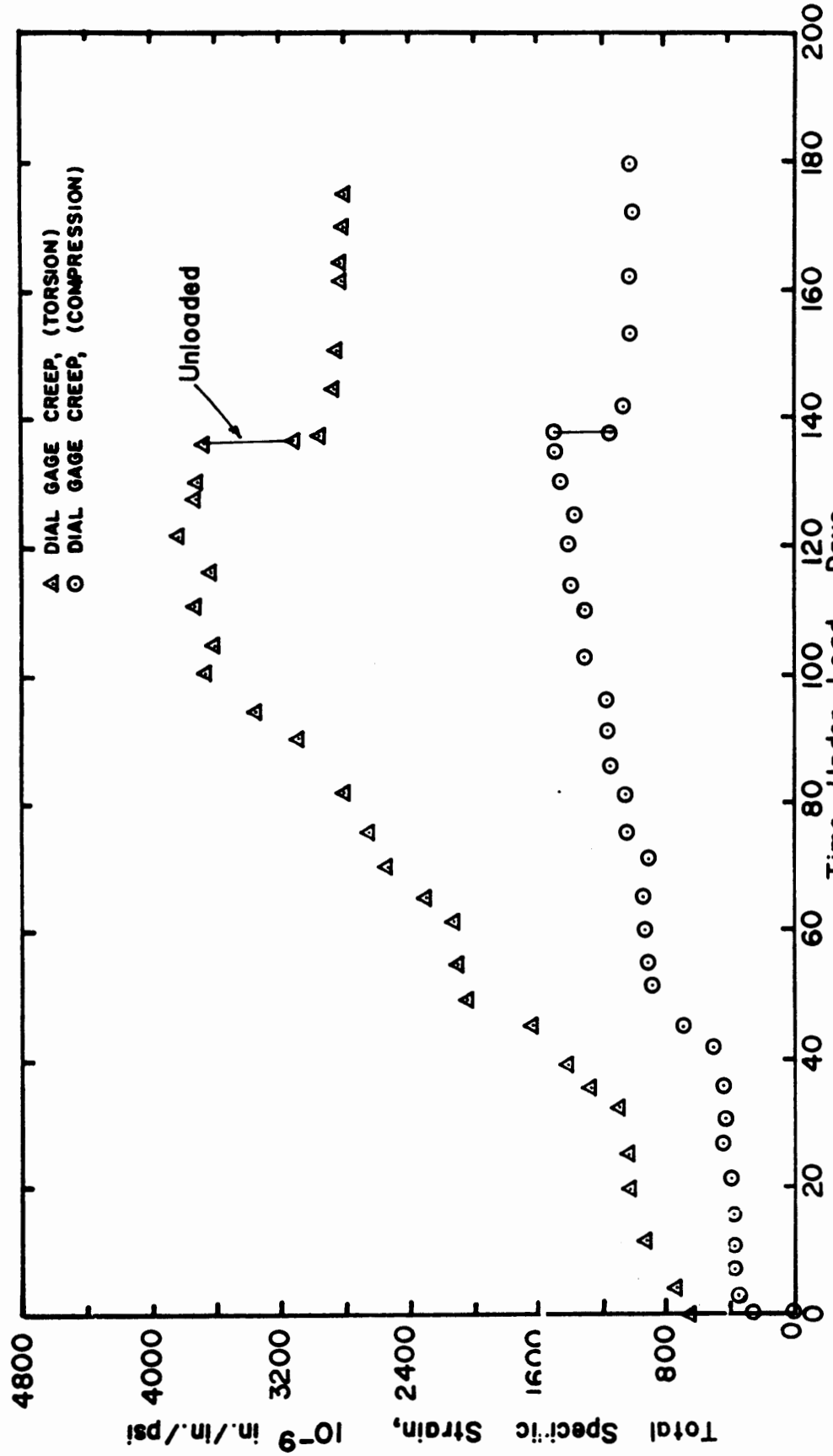

FIG. 34 EFFECT OF CYCLIC TEMPERATURE AT 100 PER CENT RELATIVE HUMIDITY ON SPECIFIC CREEP OF CONCRETE IN COMPRESSION AND TORSION

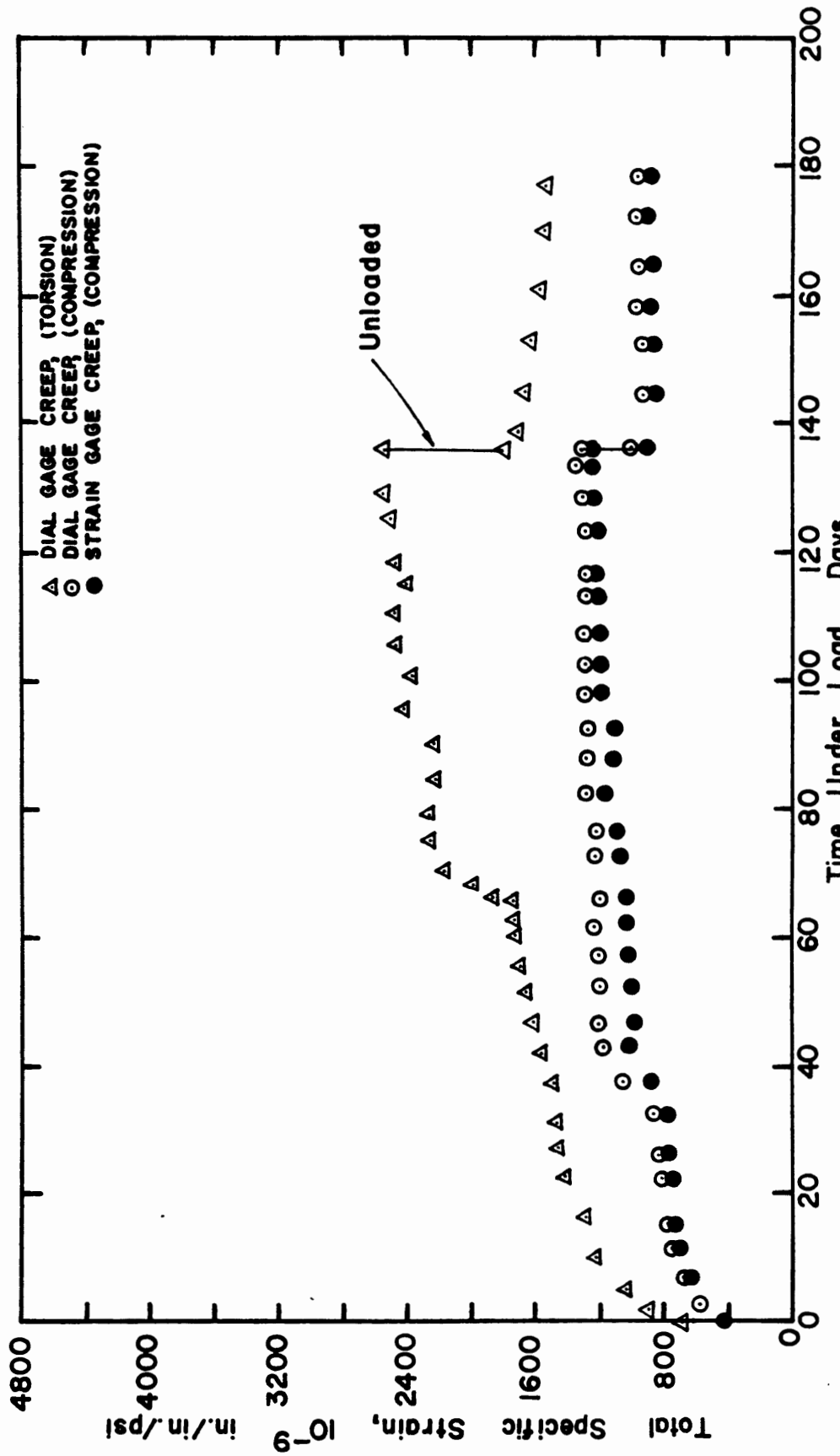

FIG. 35 EFFECT OF CYCLIC TEMPERATURE AT 50 PER CENT RELATIVE HUMIDITY ON SPECIFIC CREEP OF CONCRETE IN COMPRESSION AND TORSION

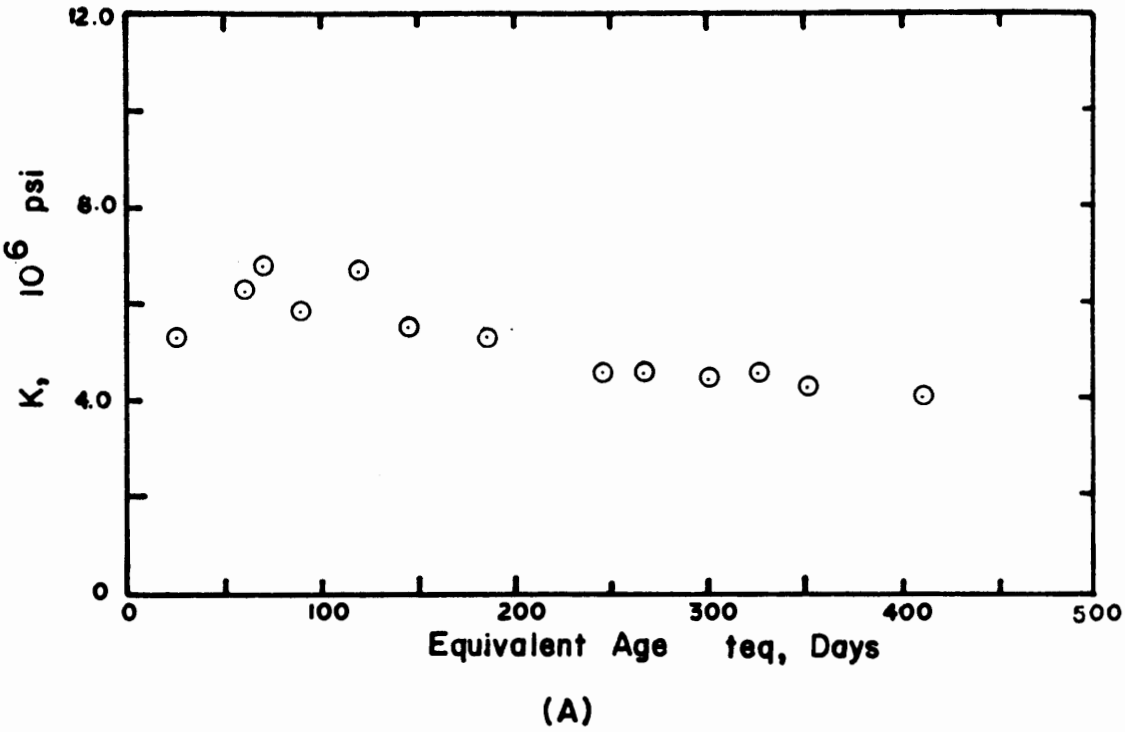

(A)

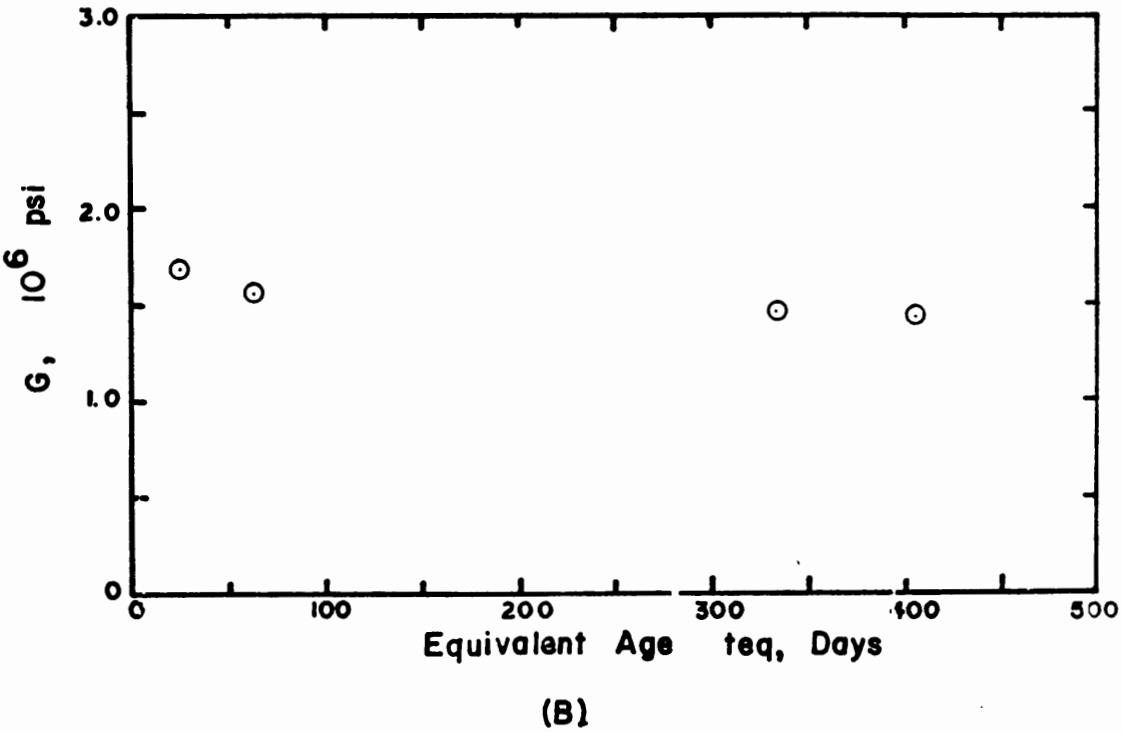

(B)

FIG. 36 EFFECT OF EQUIVALENT CURING TIME ON K AND G AT 100 PER CENT RELATIVE HUMIDITY

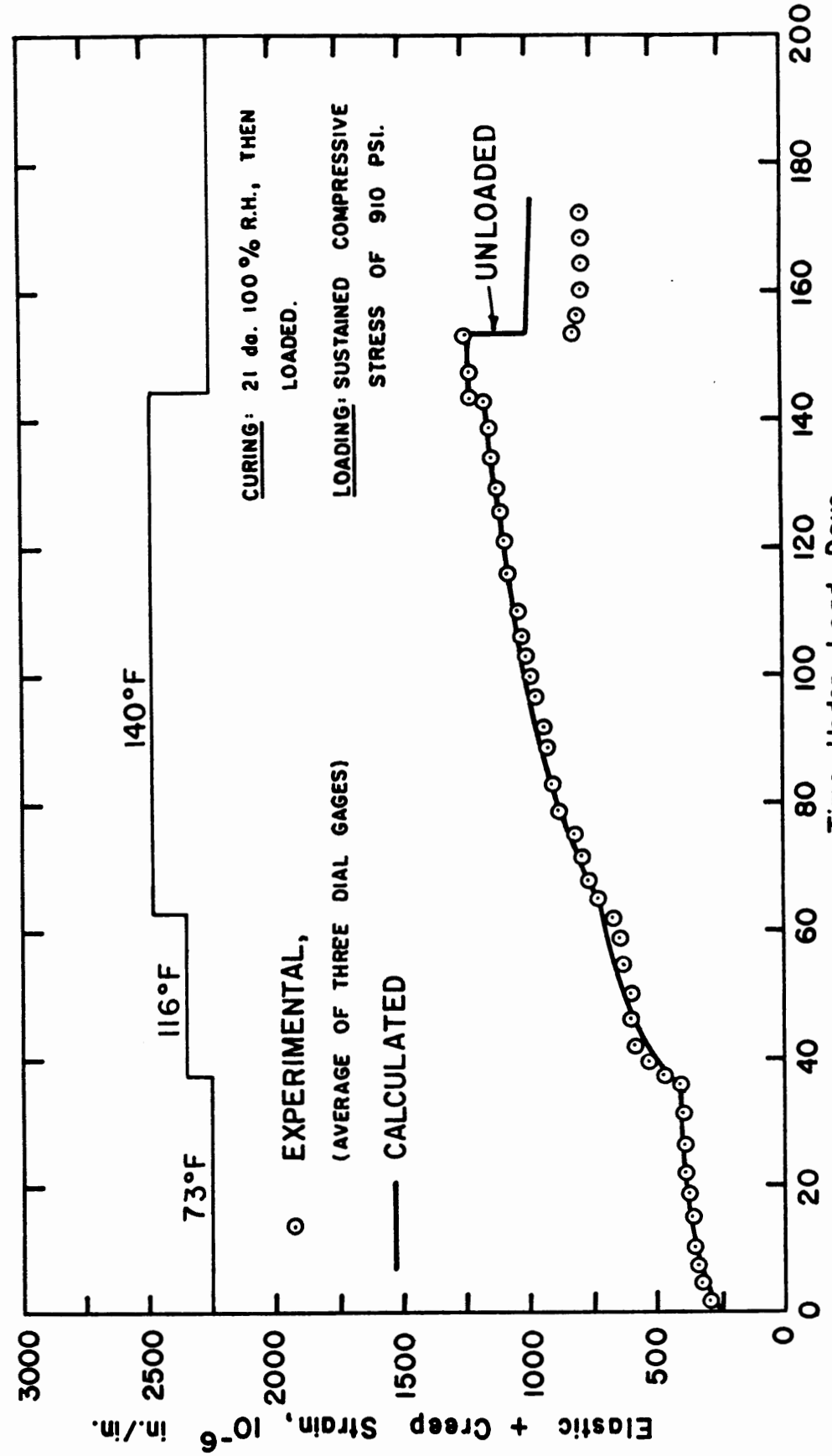

FIG. 37 COMPARISON OF CALCULATED AND EXPERIMENTAL CREEP IN COMPRESSION AT SUSTAINED TEMPERATURES AND 100 PERCENT RELATIVE HUMIDITY

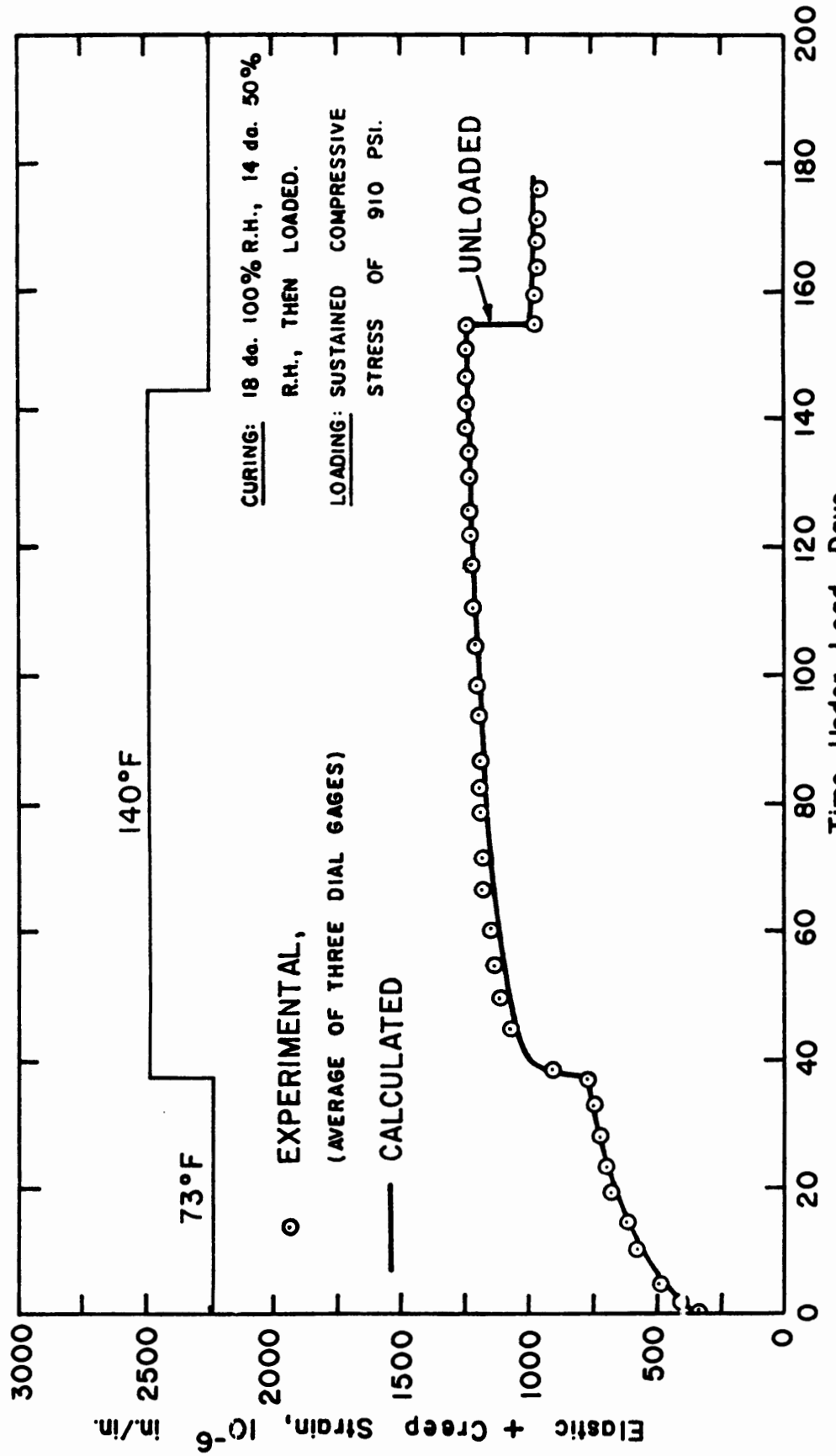

FIG. 38 COMPARISON OF CALCULATED AND EXPERIMENTAL CREEP IN COMPRESSION AT SUSTAINED TEMPERATURES AND 50 PERCENT RELATIVE HUMIDITY

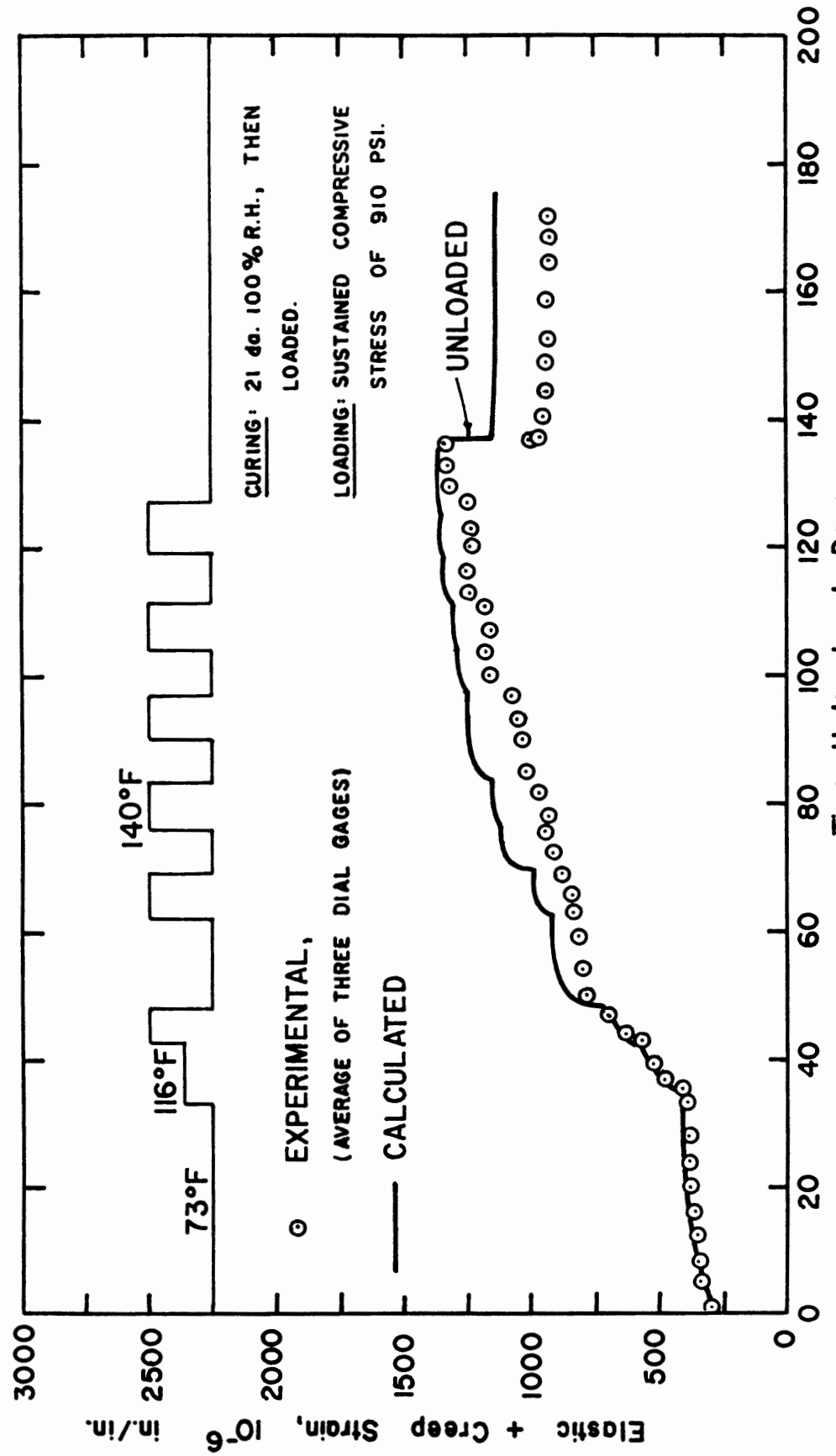

FIG. 39 COMPARISON OF CALCULATED AND EXPERIMENTAL CREEP IN COMPRESSION AT CYCLIC TEMPERATURE AND 100 PERCENT RELATIVE HUMIDITY

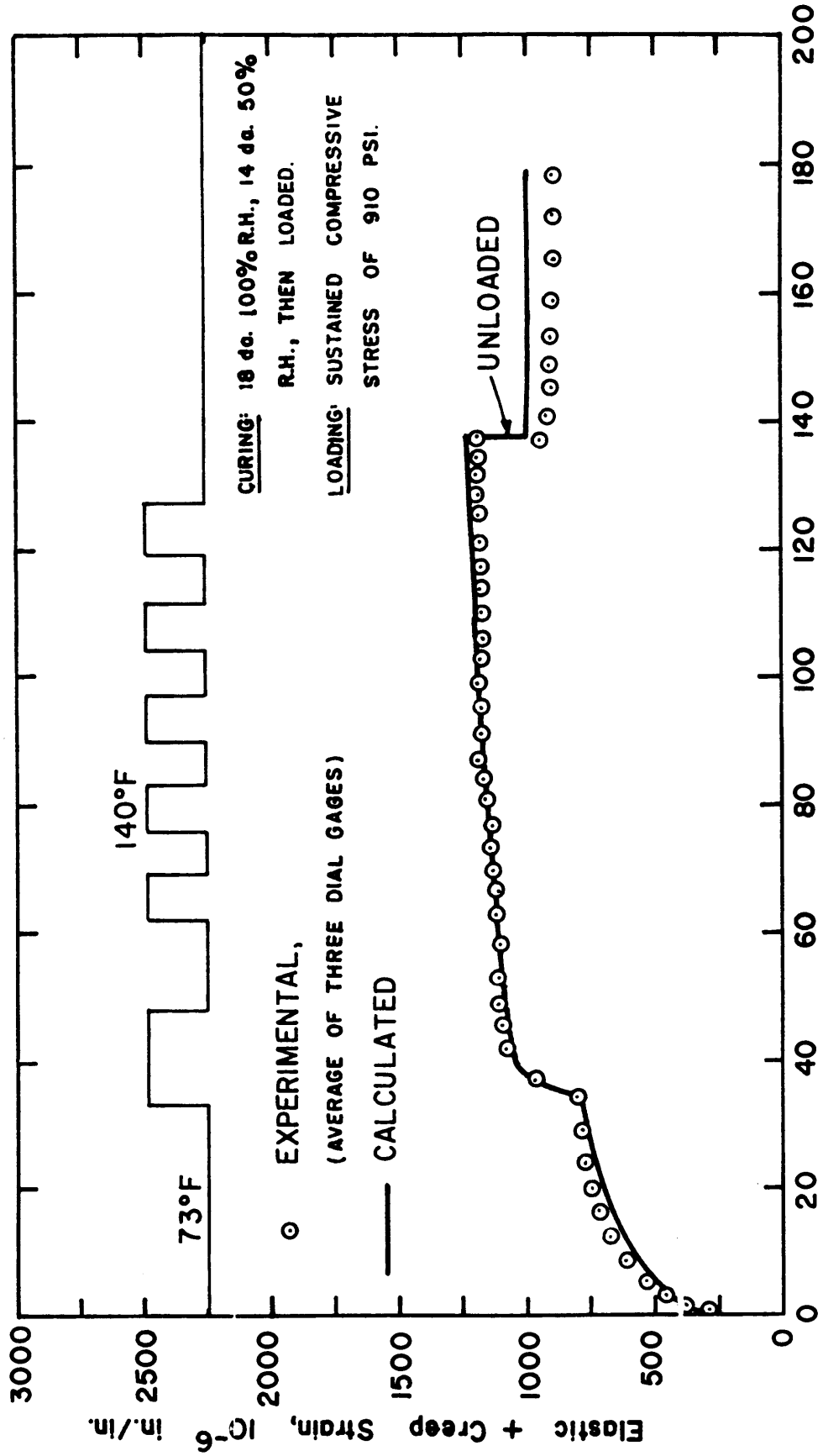

FIG. 40 COMPARISON OF CALCULATED AND EXPERIMENTAL CREEP IN COMPRESSION AT CYCLIC TEMPERATURE AND 50 PERCENT RELATIVE HUMIDITY

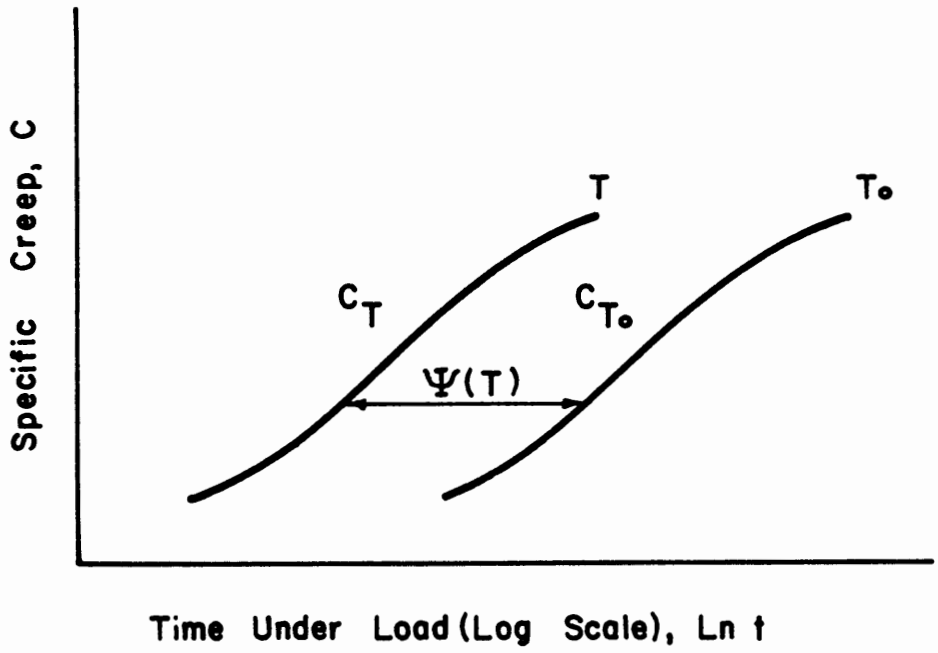

FIG. 41 TIME-SHIFT PRINCIPLE

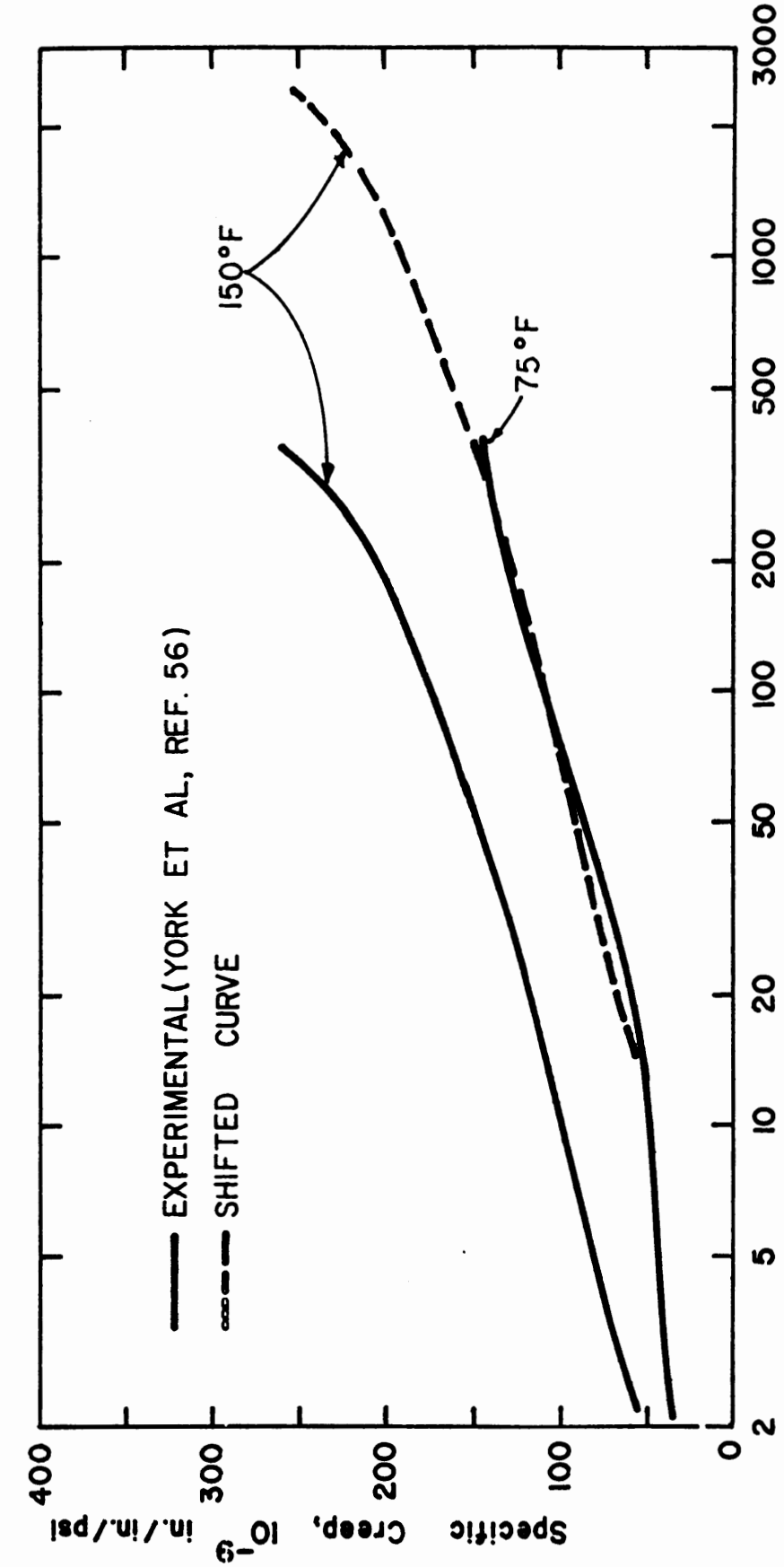

(a)

FIG. 42 CREEP RESULTS AT DIFEERENT TEMPERATURES

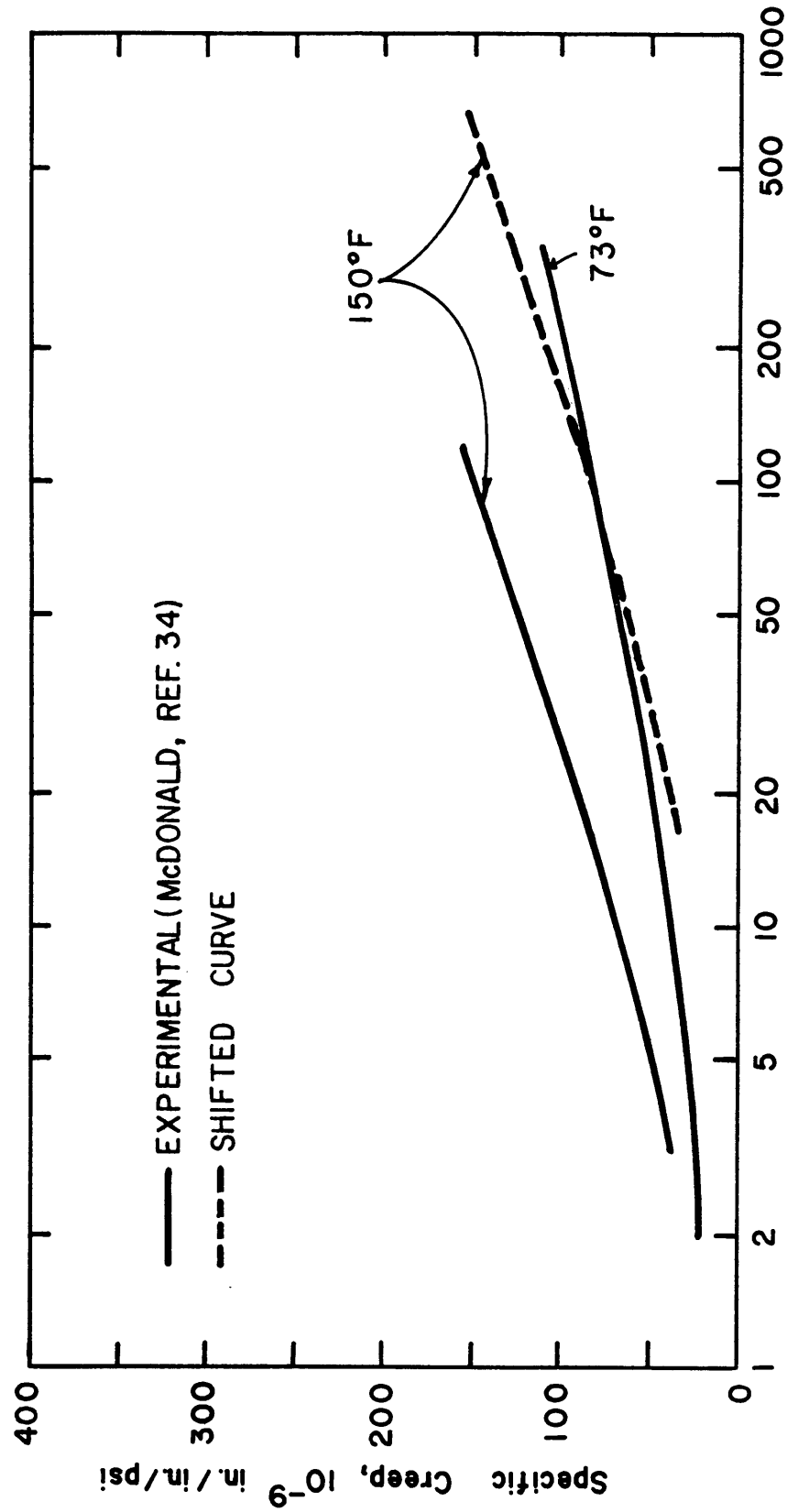

(b)

FIG. 42 (CONTINUED)

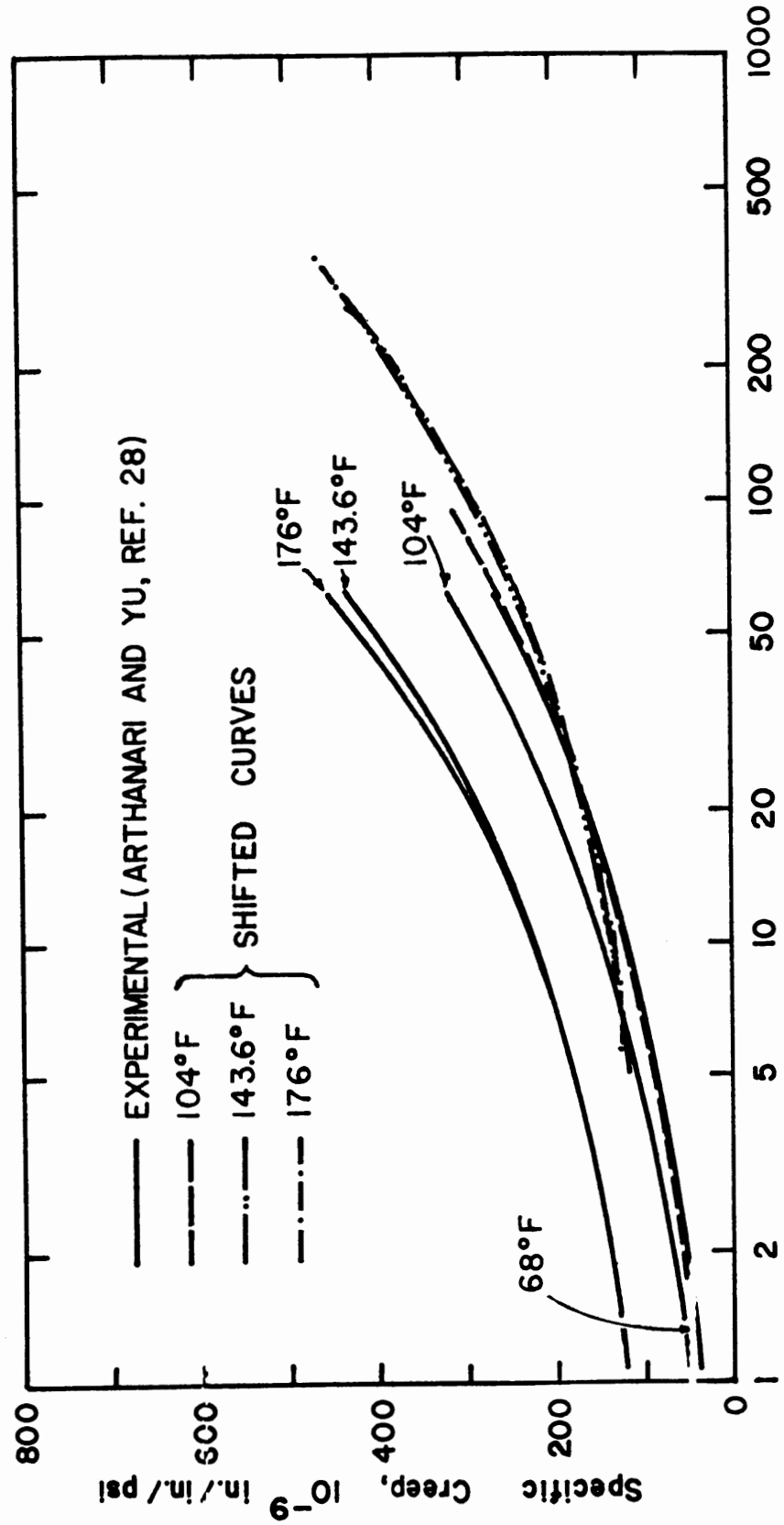

(c)

FIG. 42 (CONTINUED)

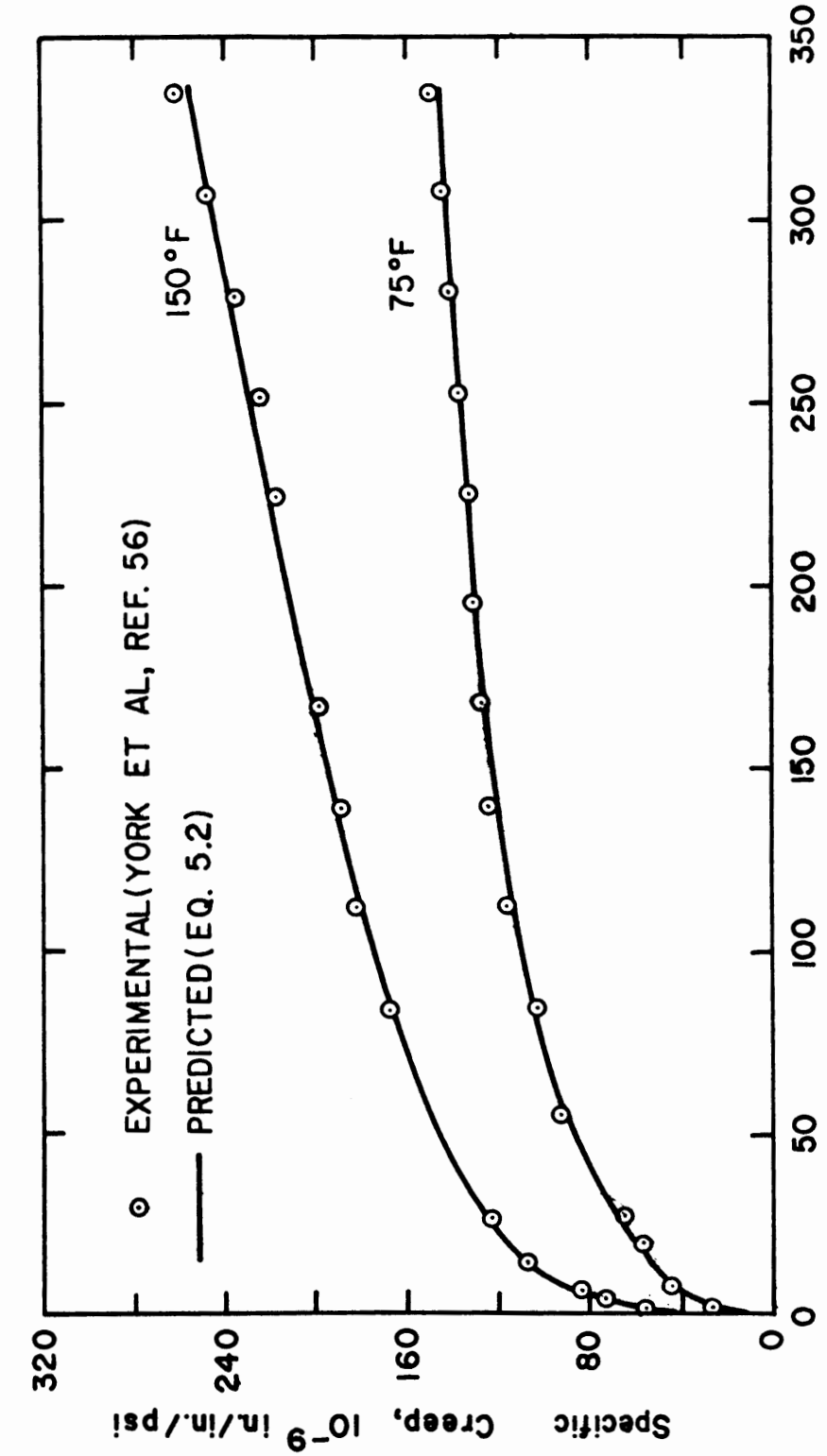

(a)

FIG. 43 COMPARISON OF PREDICTED AND EXPERIMENTAL CREEP STRAINS AT CONSTANT TEMPERATURES

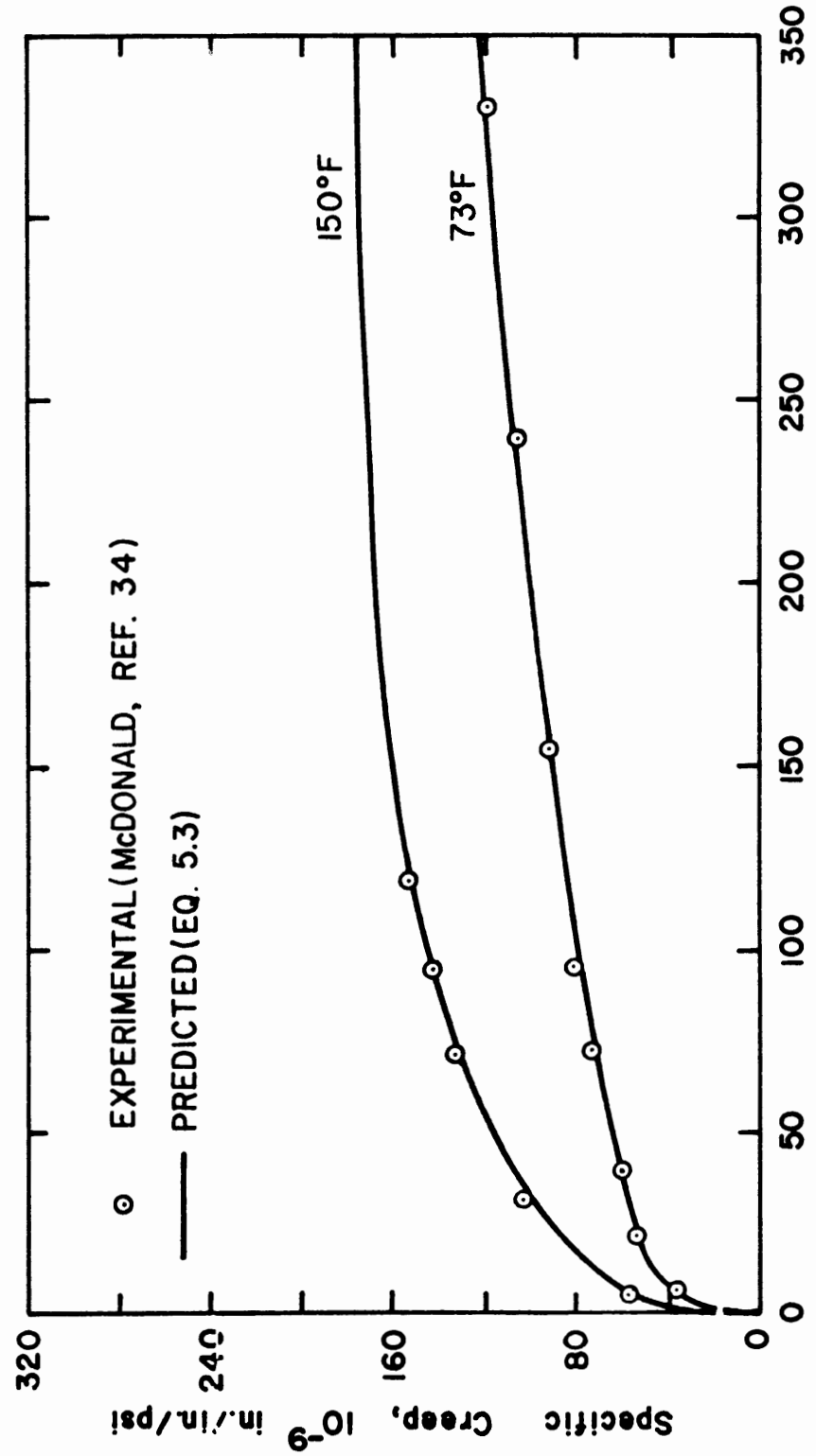

(b)

FIG. 43 (CONTINUED)

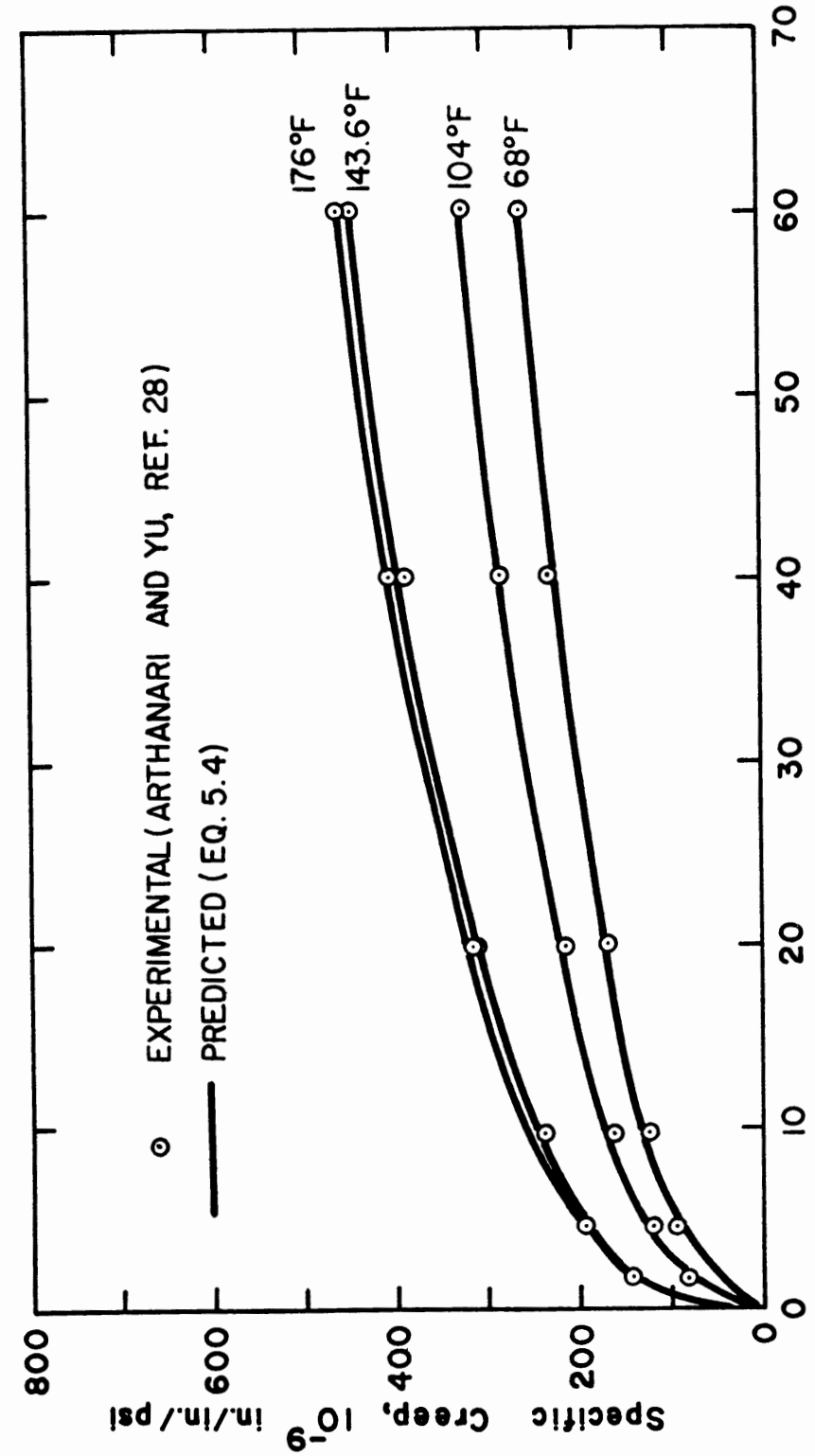

(c)

FIG. 43 (CONTINUED)

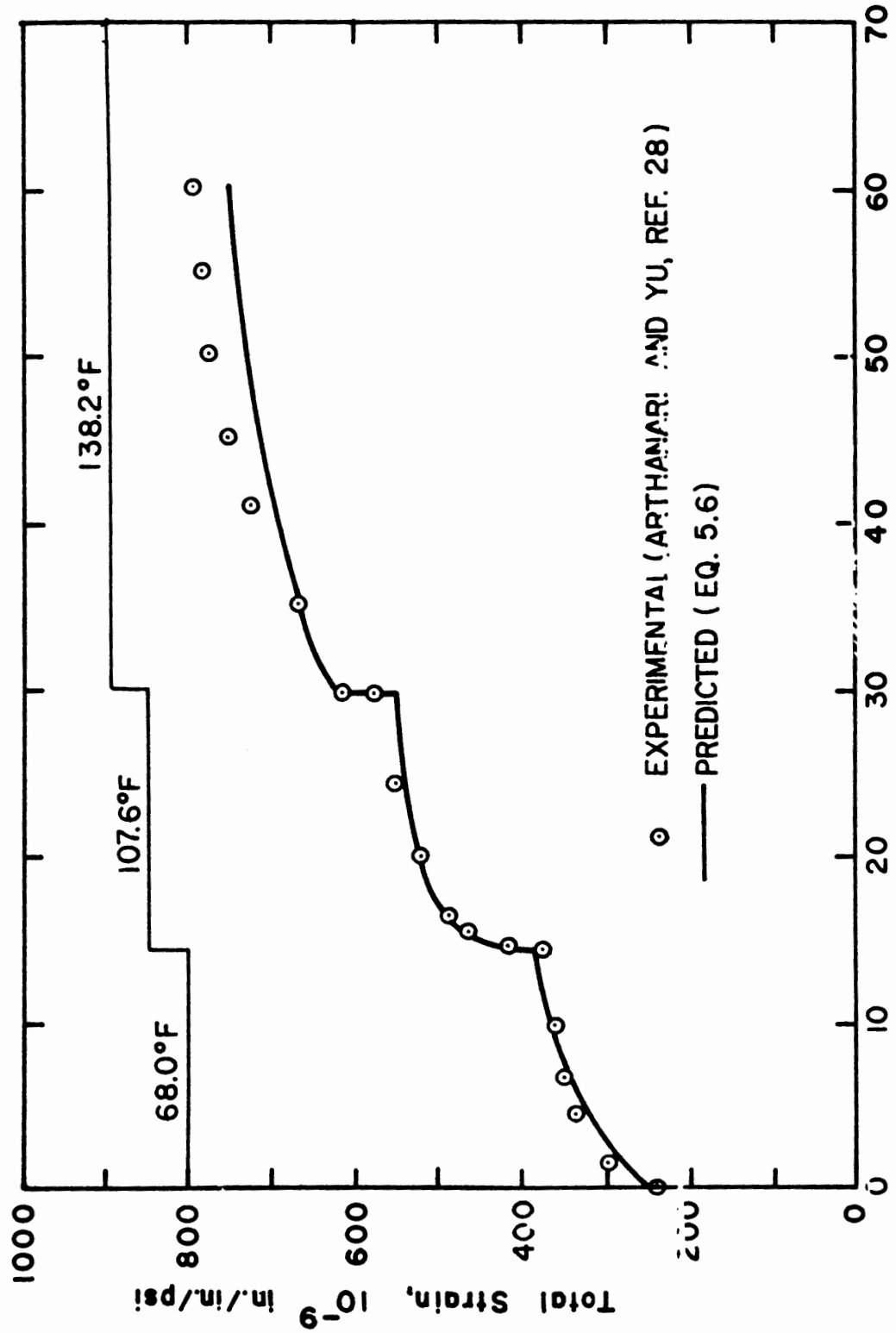

FIG. 44 COMPARISON OF PREDICTED AND EXPERIMENTAL TOTAL STRAINS OF SEALED CONCRETE AT VARIABLE TEMPERATURE

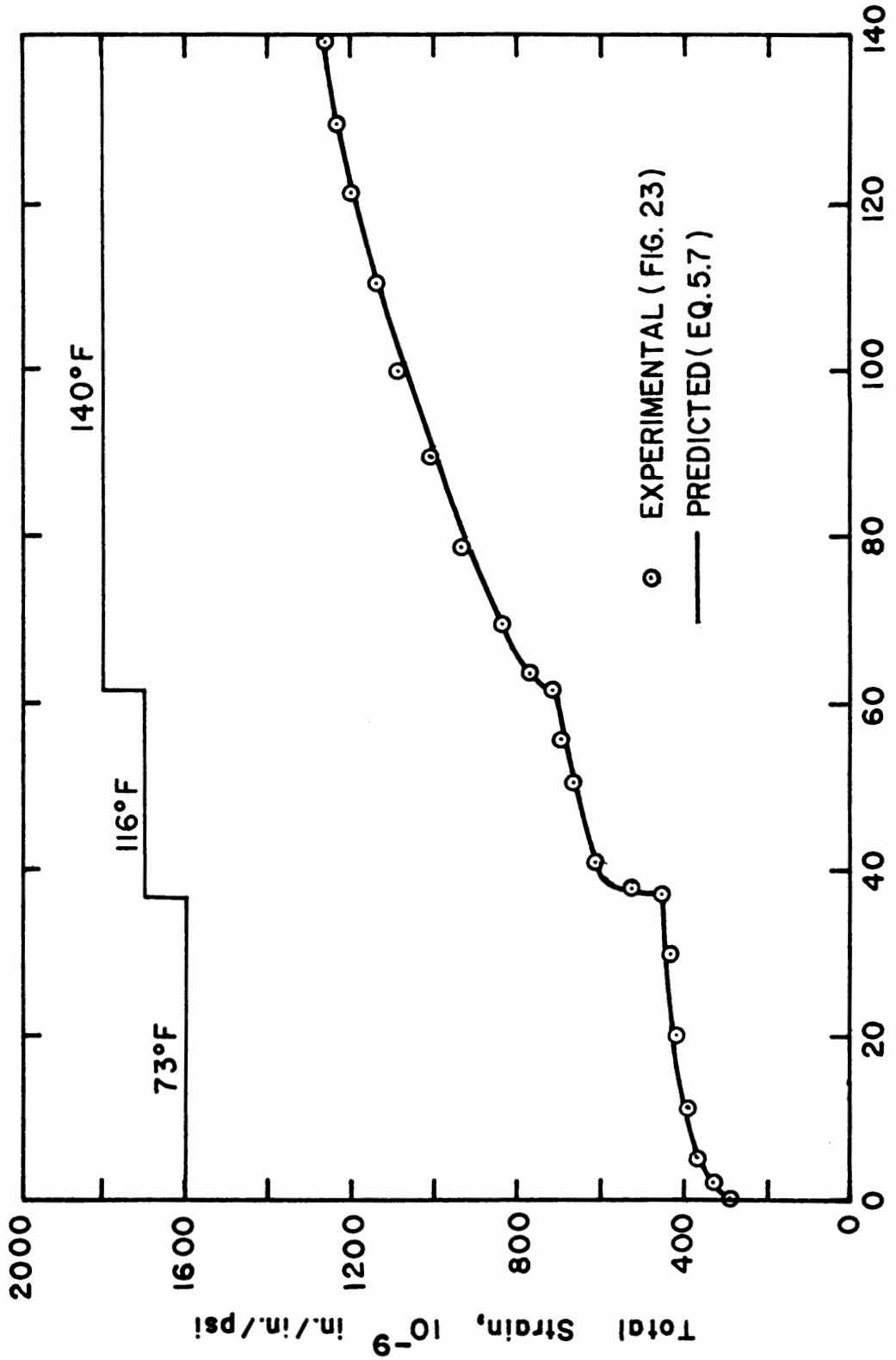

FIG. 45 COMPARISON OF PREDICTED AND EXPERIMENTAL TOTAL STRAINS AT VARIABLE TEMPERATURE AND 100 PERCENT RELATIVE HUMIDITY

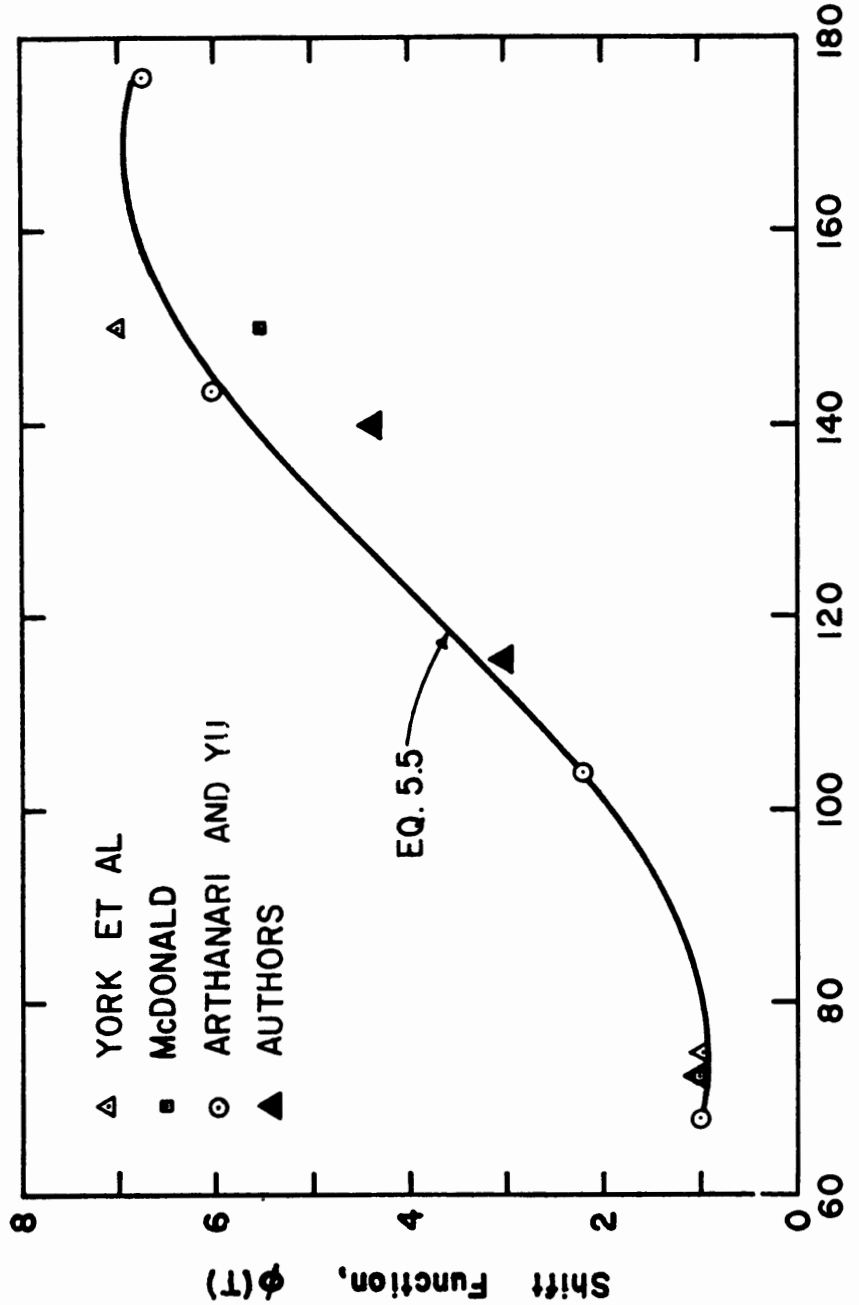

FIG. 46 EFFECT OF TEMPERATURE ON SHIFT FUNCTION

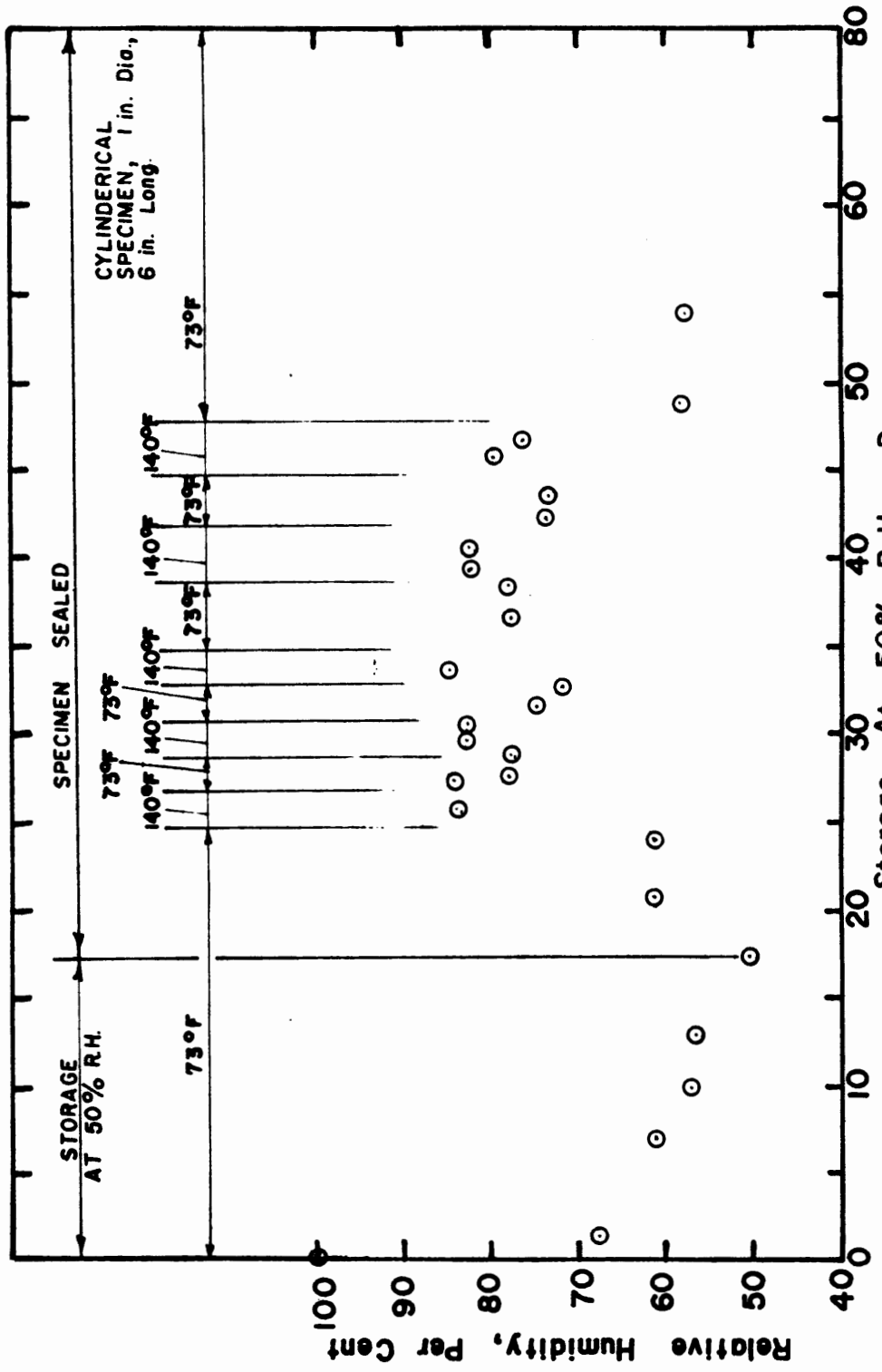

FIG. 47 CHANGE OF HUMIDITY WITH TEMPERATURE FOR CYLINDERICAL CONCRETE SPECIMEN

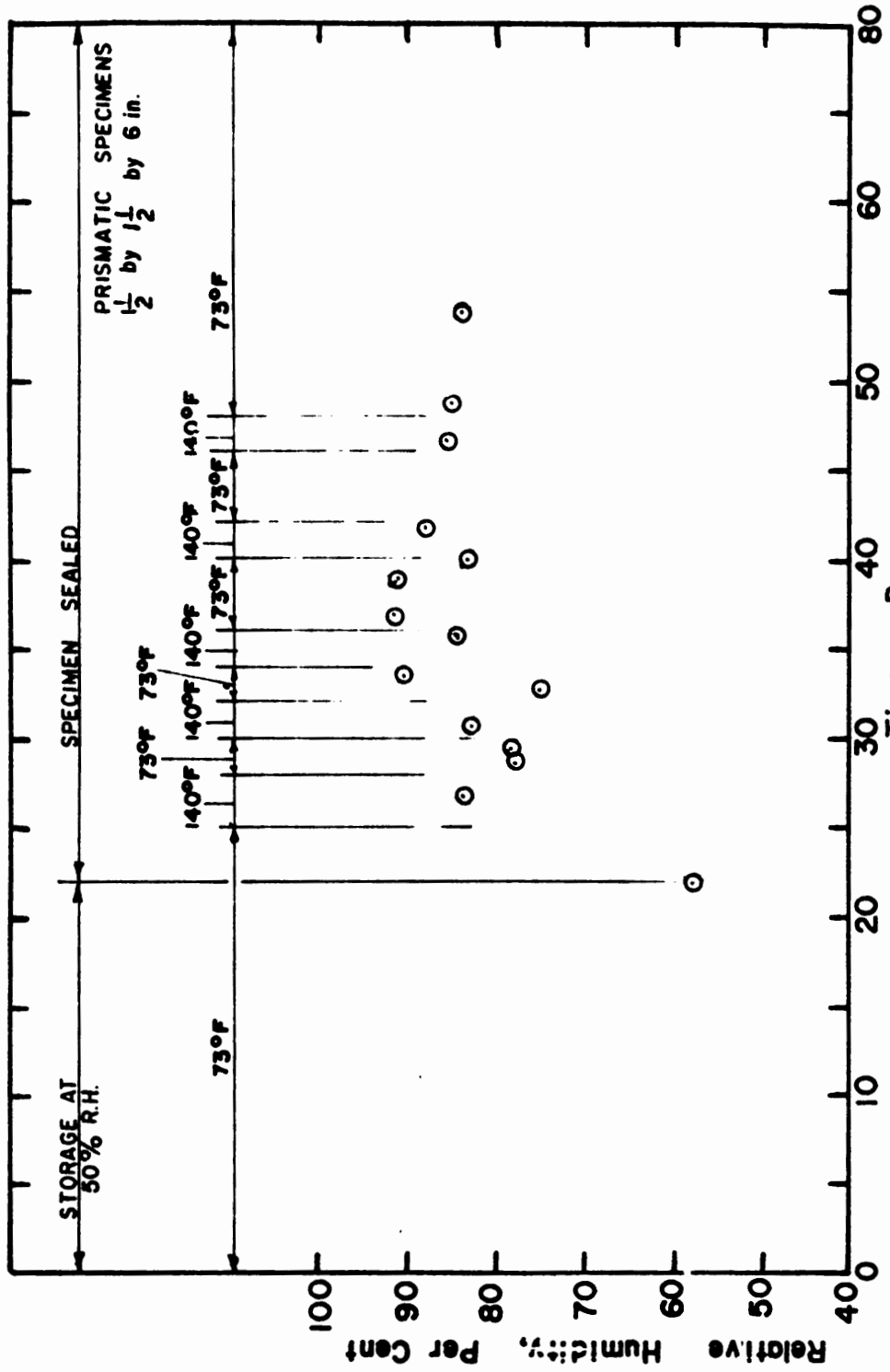

FIG. 48 CHANGE OF HUMIDITY WITH TEMPERATURE FOR PRISMATIC CONCRETE SPECIMEN

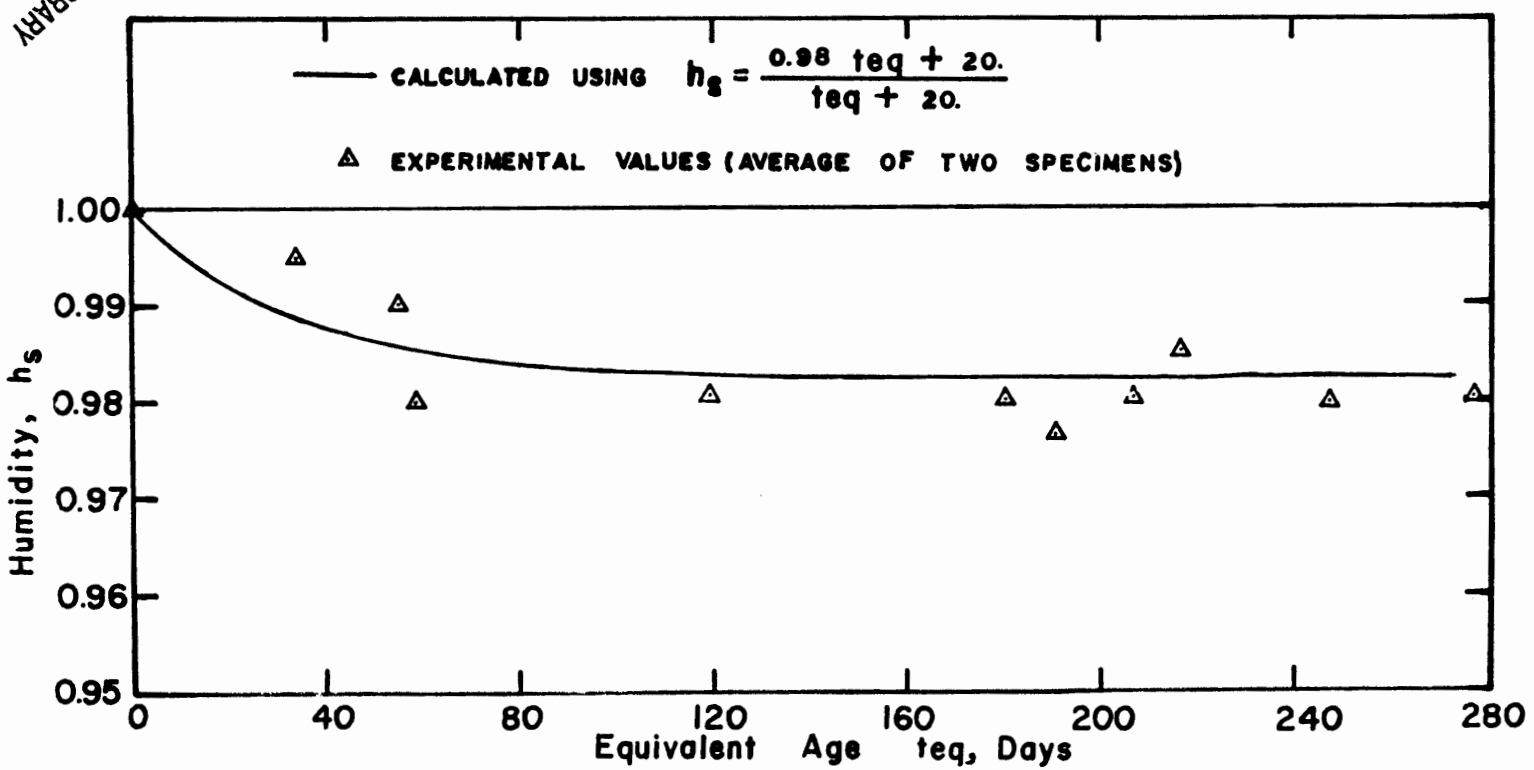

FIG. 49 EFFECT OF MATURITY ON HUMIDITY AT SELF-DESICCATION OF CONCRETE SPECIMEN